BENZO(A)PYRENE AND BENZO(A)PYRENE-INDUCED PROTEIN ADDUCTS IN HAIR AS BIOMARKERS OF TOXIC BENZO(A)PYRENE EXPOSURES

by

Sarah Colleen Campbell

A dissertation submitted to the faculty of
The University of Utah
in partial fulfillment of the requirements for the degree of

Doctor of Philosophy

Department of Pharmacology and Toxicology

University of Utah

August 2011

The University of Utah Graduate School

STATEMENT OF DISSERTATION APPROVAL

The dissertation of **Sarah Colleen Campbell**

has been approved by the following supervisory committee members:

Diana G. Wilkins	, Chair	**5/27/11** Date Approved
Douglas E. Rollins	, Member	**5/27/11** Date Approved
Lawrence D. McGill	, Member	**5/27/11** Date Approved
Garold S. Yost	, Member	**5/27/11** Date Approved
Stephen T. Tiffany	, Member	**5/27/11** Date Approved

and by **William R. Crowley**, Chair of

the Department of **Pharmacology and Toxicology**

and by Charles A. Wight, Dean of The Graduate School.

ABSTRACT

Cigarette smoking is the leading cause of preventable death in the United States. While there are more than 4,000 chemicals found in tobacco smoke, the polycyclic aromatic hydrocarbons (PAHs) have been clearly demonstrated to contribute to smoking-related cancers. Of this group of compounds, benzo(a)pyrene (B(a)P) is concidered to be the most carcinogenic and its ability to cause lung tumors is well documented.

Many conventional biomarker assays conducted today use the measurement of nicotine (and its metabolite cotinine) in blood, urine, or oral fluids for assessment of tobacco smoke exposure. However, these conventional assays do not measure exposure to carcinogenic compounds and are sensitive only to recent smoke exposures. Due to the ease of hair sampling and its extended detection window of substances incorporated into its matrix, this dissertational research proposes a promising new tool for the assessment of toxic tobacco smoke exposure.

We investigated the disposition of B(a)P and its electrophilic reactive metabolite, trans-7,8-dihydroxy-anti-9,10-epoxy-7,8,9,10-tetrahydro-benzo(a)pyrene (BPDE), in rat and human hair. BPDE is one of the most potent mutagens and carcinogens known, and forms protein and DNA adducts in

multiple tissues. Our overarching hypothesis was that *B(a)P and BPDE-protein adducts in hair can be used as biomarkers of toxic B(a)P exposure.*

The data presented in this dissertation demonstrate that B(a)P and BPDE-protein adducts are incorporated into rat hair in a dose-dependent manner. While B(a)P incorporation into rat hair is not dependent upon pigment content, BPDE-protein adducts concentrations are significantly greater in pigmented vs. nonpigmented hair.

Gross histopathological changes in rat lung tissue, such as alveolar wall thickening, decreased air space, and macrophage hyperplasia were visually evident in rats 14 days after B(a)P administration. Immunohistochemistry staining for myeloperoxide content (a marker for neutrophils) in the lung tissue of B(a)P-dosed rats was also significantly greater than vehicle control rats.

B(a)P can be detected in human hair, but BPDE-protein adducts could not be detected, despite evidence of active smoking status via plasma cotinine concentrations.

The results of this dissertational research demonstrate that hair may serve as an easily accessible surrogate tissue for the detection of a biomarker of toxic tobacco smoke exposure.

TABLE OF CONTENTS

LIST OF FIGURES

Figure Page

LIST OF TABLES

LIST OF ABBREVIATIONS

ANOVA – Analysis of Variance
B(a)P – Benzo(a)pyrene
BPDE – *trans*-7,8-dihydroxy-*anti*-9,10-epoxy-7,8,9,10-tetrahydro-benzo(a)pyrene
BPT – *R*-7,*T*-8,9,*C*-10-tetrahydroxy-7,8,9,10-tetra-hydrobenzo(a)pyrene
CV – Coefficient of variation
CYP450 – Cytochrome P450 enzymes
ETS – Environmental tobacco smoke
GC/MS – Gas chromatography / mass spectrometry
GC-MS/MS – Gas chromatography- tandem mass spectrometry
Hb - hemoglobin
HPLC – High performance liquid chromatography
IS – Internal standard
LC – Liquid chromatography
LC-MS/MS – Liquid chromatography- tandem mass spectrometry
PAH – Polycyclic Aromatic Hydrocarbon
PTS – Particulate tobacco smoke
LLOQ – Lower limit of quantitation
LOD – Limit of detection
r_S- Spearman correlation coefficient
SEM – Standard mean error
SPE – Solid phase extraction
ULOD – Upper limit of detection
ULOQ – Upper limit of quantitation

ACKNOWLEDGEMENTS

I would like to thank my advisor Dr. Diana Wilkins and my co-advisor Dr. Douglas Rollins, for their commitment and support of this dissertational research, and for taking time out of their busy schedules for our “Friday Meetings.” I know I was truly lucky to have two such wonderful mentors for my journey through graduate school.

I would also like to thank my dissertational committee members: Dr. Lawrence McGill, Dr. Stephen Tiffany, and Dr. Garold Yost, each of whom contributed to the success of this project. I would like to thank Dr. McGill for his guidance and training in histopathology and for sharing my enthusiasm for this project. I would like to thank Dr. Tiffany for his involvement in recruiting heavy smoking subjects and for taking the time to come to Salt Lake to support this project. I would like to thank Dr. Yost for sending me relEvanst literature and his overall guidance, as well as helping me obtain a very costly internal standard that greatly improved the quantitative analysis for BPT.

There are a number of other individuals who helped make this dissertational research possible. I would like to thank Dr. Kristen Keefe for access to her lab’s microscope and camera, as well as the Anticonvulsant Drug Discovery lab for the use of their light microscope. Additionally, I would like to extend my thanks to the personnel of the ARUP Animal Pathology Lab for their

assistance and training in preparation and staining of lung tissues. I would also like to thank to the professors and students in the Department of Pharmacology and Toxicology for their insights and support throughout the years, and the entire staff at the Center for Human Toxicology for providing such an enjoyable and supportive academic and professional work environment. Particularly, am very grateful that Drs. David Andrenyak, Eleanor Miller, and Gordon Murray were working at the CHT during my training, and were always willing to listen to my ideas and offer suggestions.

I would like to extend my thanks to my science professors at Westminster College who sparked my interest in the life sciences and for their dedication in to making passionate young scientists! Specifically, I would like to thank Dr. William Pool for recognizing me as an enthusiastic student and for giving me my first research project.

Additionally, I would like to thank my former colleagues at DataChem Laboratories who for seven years gave me a wonderful place to learn and expand my knowledge of analytical techniques.

I am very grateful to the National Cancer Institute, the National Children's Study Innovative Research Grant Program, and the Society of Toxicology for their financial support of my graduate education.

Additionally, I would like to thank my friends and family for their love, support and understanding throughout my graduate education. To my parents, Kent and Linda Campbell, I would especially like to thank them for supporting me though the private liberal arts college of my choice, for that is where I developed

my love for learning and my intense interest in the sciences which directly contributed to my desire in pursuing graduate school. Their love and support throughout my life has been incredible.

Last, but ABSOLUTELY not least, I would like to thank my fabulous husband of twelve years, Travis Winter, who has always been very supportive of my education and took on many extra challenges during my time though graduate school. I know I am very lucky to have such a wonderful, thoughtful, and caring person as my husband, and I will never forget all the sacrifices you have made on my behalf.

CHAPTER 1

OVERVIEW

Introduction

This chapter provides an introduction to the anatomy and physiology of hair, the history and science of hair testing, the role of biomarkers in toxicology, and a brief background on benzo(a)pyrene (B(a)P). This overview concludes with the objectives of this dissertational research and the experiments designed to test the overarching hypothesis.

Anatomy and Physiology of Hair

While hair may appear to be a simple structure, it is actually very complex, and to this day is only partially understood. A great deal still remains to be learned about hair growth and its anatomy.

Mammalian hair consists of proteins (65-95%), lipids (1-9%), pigment (0.1-5%), minerals (0.25-0.95%), and small quantities of water [2-9] and grows from follicles found in the epidermal epithelium. Hair has two distinct structures: 1) the ***hair follicle*** (portion below the skin) and; 2) the ***hair shaft*** (portion above the skin).

The only biologically active portion of hair is the ***hair follicle*** itself. The follicle contains the cells responsible for the production of the hair shaft and lies

3-4 mm below the skin's surface. The follicle also contains oil-producing sebaceous glands (which lubricate the hair) and arrector pili muscles (which can erect the hair) (see Figure 1.1). The follicle is the only organ in mammals that undergoes life-long cycles of rapid growth (anagen), regression and transition (catagen), and resting periods (telogen)(see Figure 1.2). The exact molecular mechanisms that drive this oscillating system remain unclear. However, it is recognized that the transformations in hair follicle cycling are controlled by the expression and activity of hormones, neurotransmitters, transcription factors, cytokines, enzymes, and cognate receptors [10]. These factors can also contribute to the typical growth rate of hair seen in mammals. For scalp hair in humans, the average growth rate is generally assumed to be 1 cm/month (or 0.45 mm/day for women / 0.44 mm/day for men) [11]. However, a wide range of growth rates from 0.6 cm/month (0.2 mm/day) to 3.36 cm/month (1.12 mm/day) have been reported [11-13]. Growth rates can also change with age, pregnancy, and nutritional status [9, 14]. Additionally, these rates are dependent upon anatomical location, gender, and race. In the rat, the average growth rate is faster (about 1 mm/day), however, the anagen phase is much shorter (about 16-20 days) [15] compared to that of humans (2- 6 yrs)[1].

In contrast to the hair follicle, mature ***hair shafts*** are nonliving biological fibers, whose cells are void of nuclei. The cells that make up the hair shaft become cornified during the process of epithelial differentiation. This cornification occurs when keratin protein is incorporated into longer keratin-intermediate filaments. Eventually the shaft looses water and cytoplasmic organelles and the

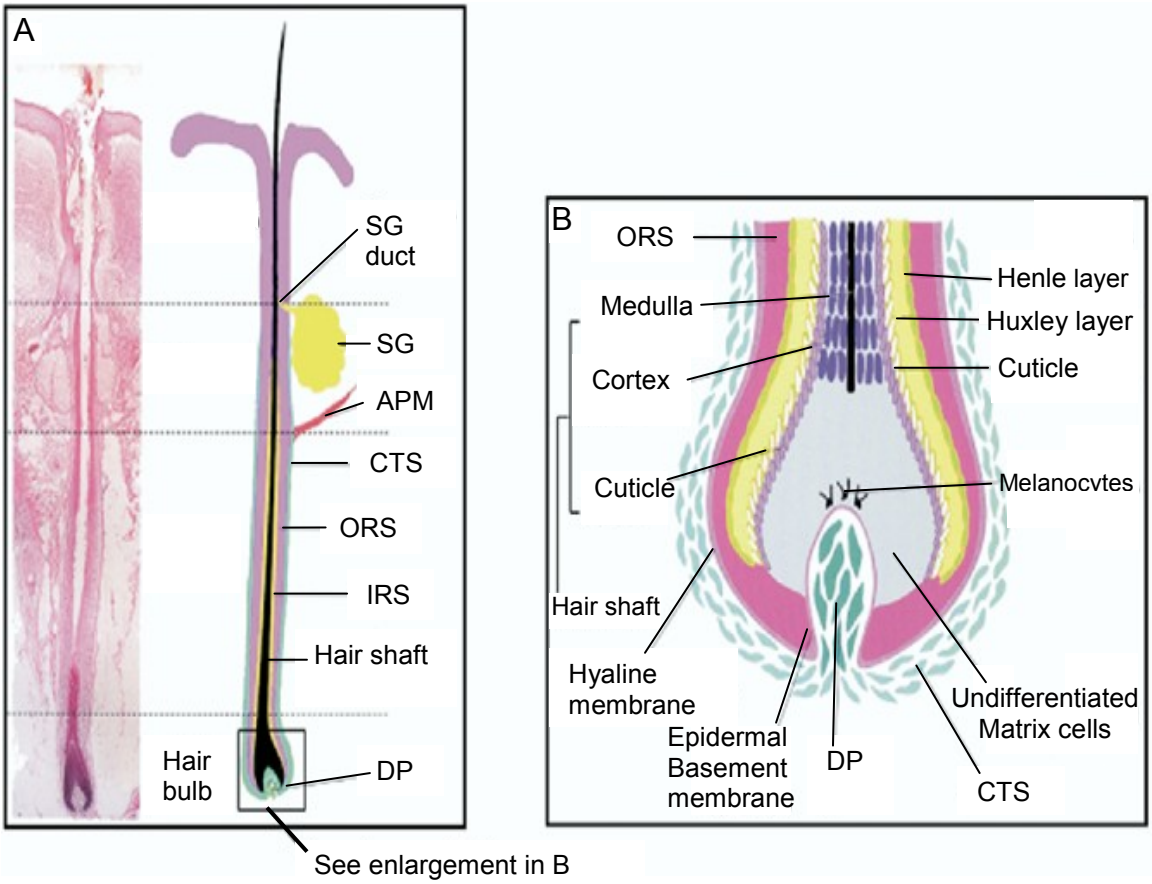

Figure 1.1 *Follicle anatomy.* A) Histologic longitudinal section of follicle on the left hand side; Schematic drawing of follicle with anatomical details on the right hand side. **B**, Hair bulb in detail (enlargement of schematic drawing in A).

APM, arrector pili muscle; **CTS**, connective tissue sheath; **DP**, dermal papilla; **IRS**, inner root sheath; **ORS**, outer root sheath; **SG**, sebaceous gland (modified after [16])

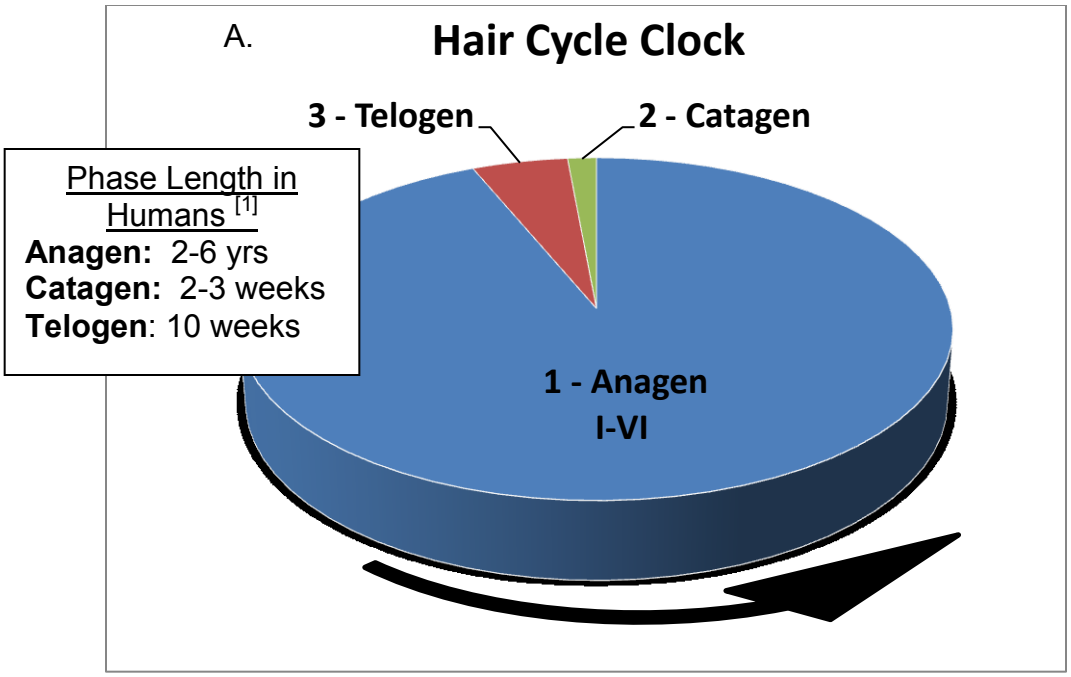

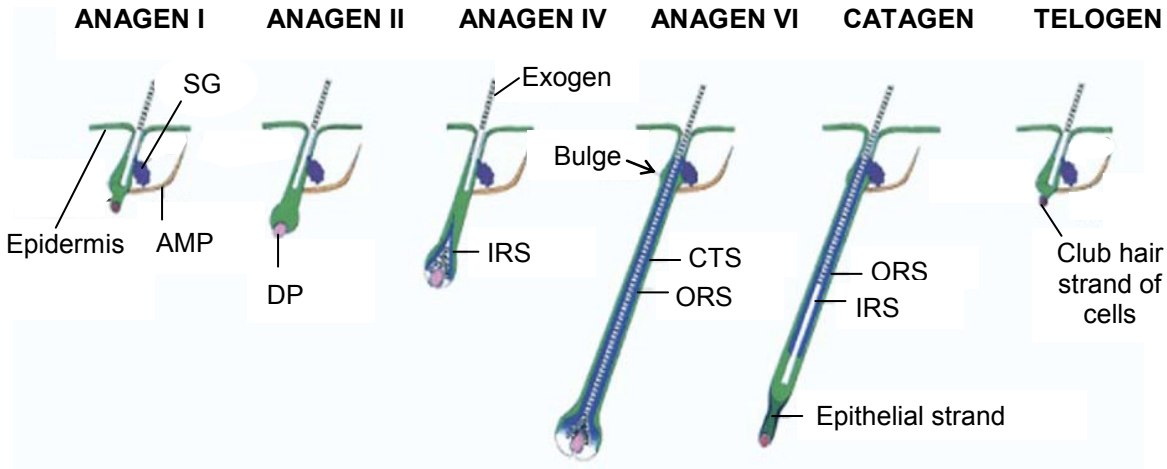

Figure 1.2 *Hair cycle phases.* A) The hair cycle clock showing average length of each phase. B) Representative drawings showing each phase of the hair cycle [10].

APM, arrector pili muscle; **CTS**, connective tissue sheath; **DP**, dermal papilla; **IRS**, inner root sheath; **ORS**, outer root sheath; **SG**, sebaceous gland (modified after [16])

cell nucleus disappears. Cell metabolism also ceases, and the cell undergoes apoptosis once completely keratinized. This feature of hair (i.e. non-living tissue) contributes to the stability of xenobiotics in hair; if metabolic activity ceases, then xenobiotics are not being metabolized or broken down and excreted.

The hair shaft can be divided into three zones (see Figure 1.3): 1) The ***cuticle***, or outer layer, consists of six to ten organized layers of thin flat cells that overlap like shingles; 2) The ***cortex***, which contains keratin rod-like bundles and constitutes the bulk of the hair shaft. The cortex also contains melanin granules, which depending on the type, number, and distribution determines the hair shaft's color; 3) And last, the ***medulla***, an open unstructured region in the fiber's center (gray hair can be void of a medulla where beard hair can possess a double medulla) [2, 17]. This region constitutes only a small percent of the overall mass of the hair fiber.

The predominant protein that makes up the hair shaft is keratin. This protein assembles into monomers, then subsequently into bundles to form rope-like intermediate filaments which provide strength and durability to the hair fiber. The biochemical feature that contributes to this physical strength of the fiber is disulfide bonding between keratin and other high sulfur proteins [18]. Some of the major amino acids that make up the keratin protein are glycine, threonine, aspartic acid, glutamic acid, lysine and very importantly cysteine [1]. Human hair is made up of approximately 14% cysteine, which contributes to the high sulfur content in hair [19]. The sulfhydryl group on cysteine is a potential binding site for xenobiotics in hair and other biological tissues [20, 21]. Other binding sites in

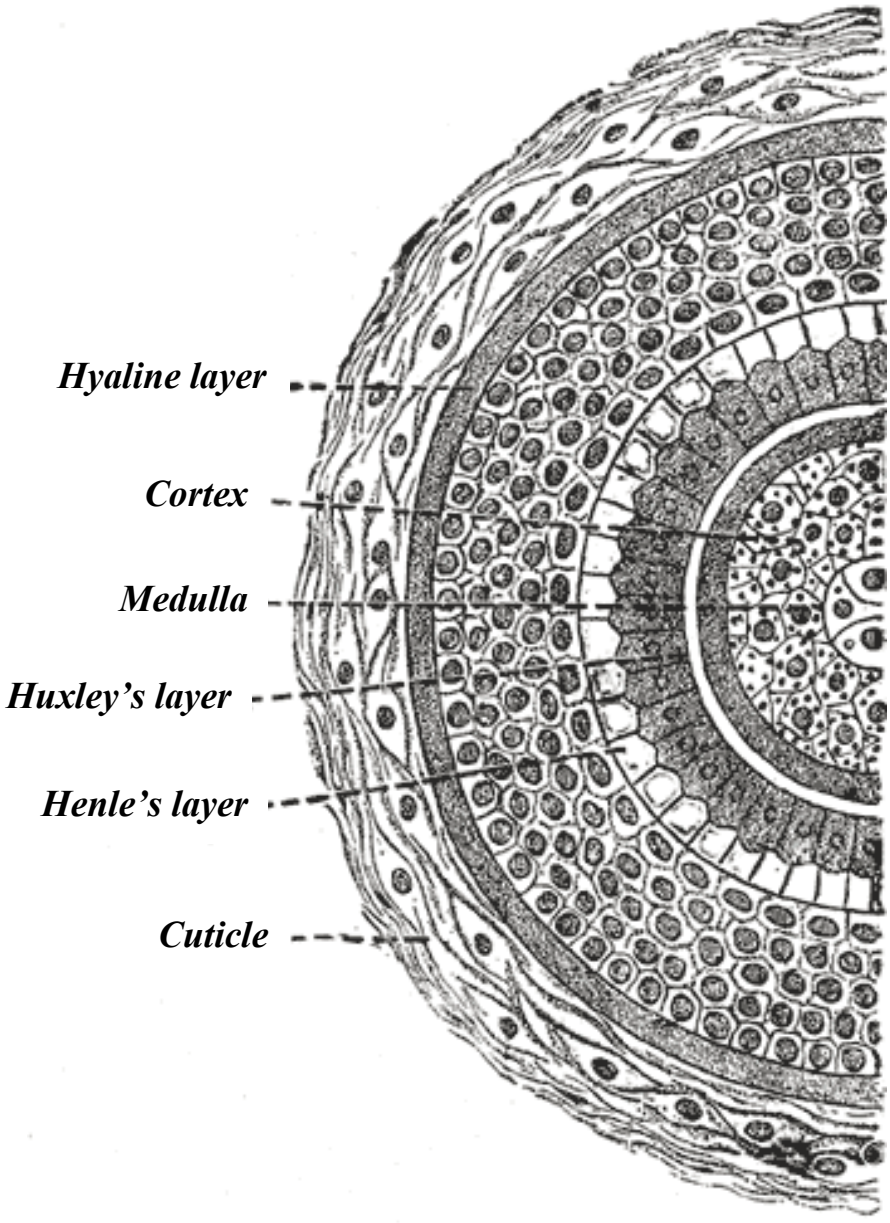

Figure 1.3 *Cross-sectional drawing of hair showing cuticle, cortex and medulla zone in hair.* (Modified from Gray's Anatomy [22].)

hair include the hydrocarbon side chains in glycine, the hydroxyl side chains in threonine, and the primary amide in aspartic and glutamic acid [23].

Hair Color and Its Importance in Drug Disposition

Certain drugs have been demonstrated to bind to darker hair to a greater extent than lighter colored hair [24-36]. Hubbard et al. demonstrated that cocaine, a basic drug, was incorporated into pigmented rat hair two orders of magnitude greater than nonpigmented rat hair [37]. This observation can be explained, in part, by the greater quantity of melanin present in pigmented hair compared to nonpigmented hair.

Melanin is a polyanionic polymer that can be found in hair, skin, the substantia nigra of the brain, the inner ear, and the uveal tract of the eye. In hair, melanin is produced by melanocytes and transferred to melanosomes in differentiating cortical and medullar cells. During the growth of a hair strand, these melanin-containing cells move upward from the hair follicle to the hair shaft and reside in the cortex and medulla layers (see Figure 1.1 B) [17]. The outer cuticle cell layer contains little to no melanin [38]. In addition, the quantity of melanin in hair can vary over one's lifespan, and from follicle to follicle.

Melanin is a derivative of the amino acid tyrosine (see Figure 1.4 A) and has multiple negatively charged carboxyl groups and *o*-semiquinones [39-41] binding sites for cationic xenobiotics (e.g., metals and compounds containing amine groups) [42] that are positively charged at physiological pH [41, 43]. B(a)P, an uncharged, lipophilic molecule, has also been demonstrated to bind melanin in *in vitro* settings [44, 45].

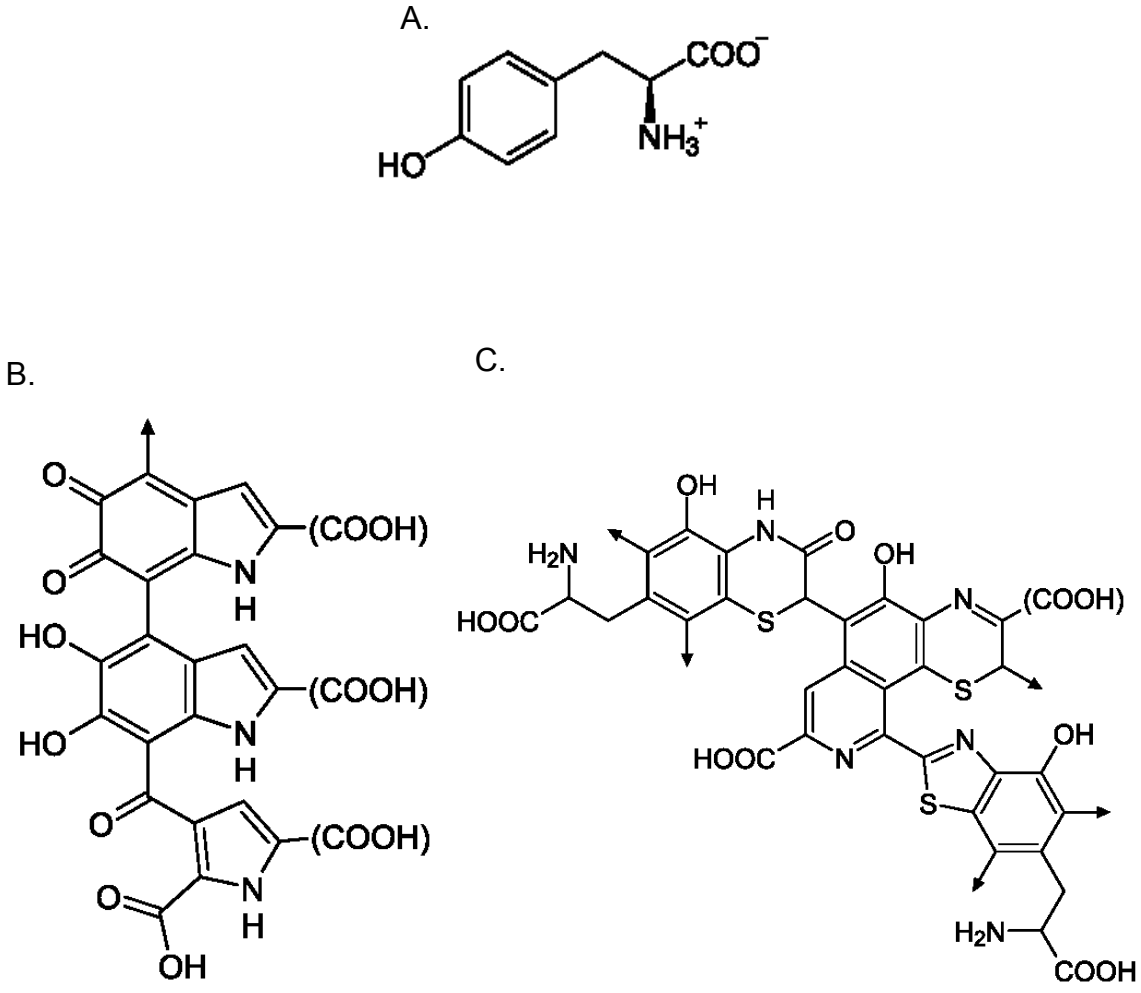

Figure 1.4. *Chemical structures of L-tyrosine, eumelanin, and pheomelanin.* A) L-Tyrosine structure, B) Proposed chemical structure of eumelanin* C) Proposed chemical structure of pheomelanin* (-COOH can also be H or other substituents (rare). Lines indicate where the polymer continues. (*with permission ©Clinuvel Pharmaceuticals Ltd 2011)

In general, the more melanin that is present in the hair shaft, the darker the hair color (e.g., brown and black hair). If less melanin is present, the hair color will be lighter (e.g blond hair). The specific color of the hair shaft results from two types of hair melanin: 1) *eumelanin*, the dominant pigment in brown and black hair (see Figure 1.4 B); 2) and *pheomelanin*, the dominant pigment in red hair (see Figure1. 4 C). Gray hair color results when melanin concentrations are extremely low to nonexistent.

The History and Science of Hair Testing

Hair analysis was used in the 1960s and 1970s to evaluate exposure to toxic heavy metals by atomic absorption spectroscopy. Starting in the early 1980s, researchers in the U.S. and Germany determined the presence of various organic drugs in hair by means of radioimmunoassay (RIA). Gas chromatography coupled with mass spectrometry (GC/MS) is the current method of choice for hair analyses due to high selectivity, sensitivity and specificity. However, other methods such as liquid chromatography coupled to tandem mass spectrometry (LC/MS-MS) are increasingly being used for hair testing.

Hair testing has been applied to a wide range of chemicals, and used in multiple settings from occupational to environmental to alternative medicine. Although controversial, hair mineral analyses have been used to diagnose and treat mineral deficiencies for over 20 years in alternative medicine practices. Although researchers have generally used hair testing as a way to monitor chronic environmental exposures to heavy metals [46-48] and pesticides

[49-51]), much of the focus has been directed towards the detection and quantification of drugs of abuse, particularly in forensic and clinical toxicology.

There are many advantages in testing for analytes in hair compared to plasma, urine, or oral fluids. First, there is a longer detection window with hair testing compared to the testing of blood, oral fluid, or urine [52]. In general, the detection window for urine and blood analyses is up to 3 days, while hair testing can be from weeks to months, or even years with certain chemicals [52]. Furthermore, when segmental hair analysis is employed, it may be possible to provide a xenobiotic exposure history [53-55]. Second, analyses of biomarkers in hair can more accurately account for chronic exposure [1, 56, 57]. Third, concentrations of biomarkers measured in hair are cumulative, therefore are less affected by daily fluctuations in intake/exposure; Specifically, in the case of tobacco use, concentrations of nicotine and cotinine measured can adjust for different tobacco products used over time and the different manners in which humans smoke cigarettes [1, 56, 57]. Fourth, hair samples are less susceptible to tampering than urine, and do not decompose like other body fluids or tissues. Fifth, using hair has the advantage of being easily collected with minimal discomfort, and does not require the specialized personnel that blood draws necessitate. Last, with regard to smoking, hair testing has been demonstrated to better correlate with self-reported tobacco exposures, compared to conventional testing [1, 56].

While hair testing does provide some major advantages, it is not without its limitations. Many of these limitations stem from gaps in our knowledge of

incorporation and stability of drugs/xenobiotics in hair, as well as general influences on hair growth (i.e. nutritional status, pharmaceuticals, ethnicity, gender, hormones, etc.). There are still many important questions that remain concerning the mechanisms of drug/xenobiotic incorporation into hair, as well as the effects of external contamination and the stability of the xenobiotics in hair through daily hygiene and cosmetic procedures. Confounding these issues are possible individual factors, which still remain largely unidentified.

Role of Biomarkers

Currently, intensive work is taking place on the discovery and development of innovative biomarkers of cancer risk. Optimally, these biomarkers would serve to determine if there is an increased risk of cancer for an individual, and therefore specific countermeasures could be put in place and the individual could be closely monitored.

In the case of tobacco-related biomarkers, the main focus has been on nicotine specific metabolites. Yuan et al. (2009), conducted a nested case controlled study involving 246 cases of lung cancer in which they determined urinary levels of cotinine and 4-(methylnitrosamino)-1-(3-pyridyl)-1-butanol (NNAL) a metabolite of 4-(methylnitrosamino)-1-(3-pyridyl)-1-butanone (NNK), a nicotine specific carcinogen. Their study suggested that urinary levels of cotinine and NNAL can be used as biomarkers of increased lung cancer risk [58].

To our knowledge, research to assess increased cancer risk via hair analysis of any tobacco-related chemical has not been performed. Several advantages of testing hair for biomarkers of tobacco smoke exposure over

conventional methods have been previously discussed, but whether testing hair for chemicals found in tobacco smoke can be used as a biomarker of cancer risk remains to be elucidated. The detection of the carcinogen B(a)P in human hair has only been reported in one small study involving 20 subjects [59]. None of B(a)P's metabolites, including benzo(a)pyrene diol epoxide (BPDE) or BPDE-protein adducts, have been reported in human hair to our knowledge. BPDE adducts to hemoglobin and albumin, as well as BPDE-DNA adducts, have been studied extensively [60], but the collection of these samples is invasive, and often are not detected (>60% for DNA adducts and about 40% for protein adducts) [60]. It is important to identify individuals with higher cancer susceptibility, and determining individuals who metabolically activate B(a)P to BPDE more extensively, and/or detoxify BPDE less, are presumed to have a higher cancer risk. Therefore, the BPDE-protein adduct biomarker in hair could help to facilitate many ongoing studies regarding activity-affecting polymorphisms in high-risk individuals with variations in B(a)P metabolizing enzymes such specific cytochrome P450s isoforms, epoxide hydrolase, as well as B(a)P detoxifying enzymes such as glutathione S-transferase. These biomarkers could also be applied in the testing of chemoprevention agents in B(a)P exposed animals. Lastly, this research can facilitate and address exposure and risk reduction not only for tobacco smoke exposure in multiple settings, but also for occupational exposuress to B(a)P.

B(a)P Background

Benzo(a)pyrene is a member of the chemical class polycyclic aromatic

hydrocarbons (PAHs) (formerly called polynuclear aromatic hydrocarbons) and is found in virtually all PAH mixtures. These compounds are formed by the incomplete combustion of organic matter and are commonly found in tobacco smoke, polluted air, water, and broiled/smoked foods [61-66]. B(a)P is also found in diesel exhaust and certain occupational settings, such as coking plants and graphite electrode producing plants [67-69]. Many of the PAHs are carcinogens, but B(a)P is considered the most potent.

B(a)P can enter the body through the lung, gastrointestinal tract, and skin. Conclusive evidence has demonstrated that B(a)P can readily induce tumors in laboratory animals in various tissues at relatively low doses [62, 70-73]. Independent of the route of exposure, one of the target tissues for B(a)P is considered to be the lung, and accumulation of B(a)P in the lungs of rats has been demonstrated [74, 75]. While, B(a)P is classified as a human carcinogen by the International Agency for Research on Cancer [73], animal studies have also suggested adverse developmental and reproductive outcomes with long-term B(a)P exposure [76]. Moreover, B(a)P is known to be an endocrine disruptor and is arthrogenic, in addition to being genotoxic and carcinogenic [77-81].

The U.S. Environmental Protection Agency (EPA) estimates the exposure to B(a)P is 1-3 ug/day for nonsmokers [76]. The amount of B(a)P exposure can vary widely in smokers (due to the different products on the market, and individual variations in smoking behavior), but are estimated at 1-30 ug/pack/day [63, 82-85]. B(a)P itself is considered a procarcinogen, and requires metabolism to elicit its toxic effects. The metabolism of B(a)P is very complex and produces

multiple metabolites of varying toxicity. The metabolism to the ultimate carcinogen BPDE is depicted in Figure 1.5. BPDE has been thoroughly demonstrated to be the most mutagenic and carcinogenic of the B(a)P metabolites [86-90]. BPDE is electrophilic, and binds covalently to nucleophilic groups on DNA (predominately the amino group of deoxyguanosine by the *trans* addition to carbon 10 of BPDE) and vital proteins in a highly stereospecific manner [91-95]. The Bay Region (see Figure 1.5) of the B(a)P molecule forms an angular ring area of steric hinderance and impedes detoxification of BPDE by glutathione conjugation, glucuronidation, and sulfation [70, 78, 88, 96], which contributes to its toxicity.

Rodent and human subcellular fractions have thoroughly demonstrated that the *trans, anti*- enantiomer of BPDE (B(a)P-*r*-7,*t*-8-dihydrodiol-*t*-9,10 epoxide) is the major product of epoxidation of *trans* B(a)P 7,8 diol (B(a)P *r*-7,*r*-8-diol) [70, 87, 97] (see Figure 1.5), although other minor enantiomers are also formed. The majority of BDPE-induced adducts are produced by the reaction with this enantiomer [70, 94]. Analysis of BPDE-induced adducts from B(a)P-treated animals and from humans exposed to B(a)P reveal that B(a)P-*r*-7,*t*-8,t-9,*c*-10-tetrahydrotetrol (BPT) is the predominant compound released upon hydrolysis of these adducts [70, 97, 98]. Like most research on BPDE-induced adducts, our research focuses on the detection of this major product from the hydrolysis of trans*, anti*-BPDE-induced adducts. The measurement of BPT therefore serves as evidence of a BPDE-induced adduct. Recently, Ragin *et al.* have reported the concentrations of the other enantiomers of benzo(a)pyrene

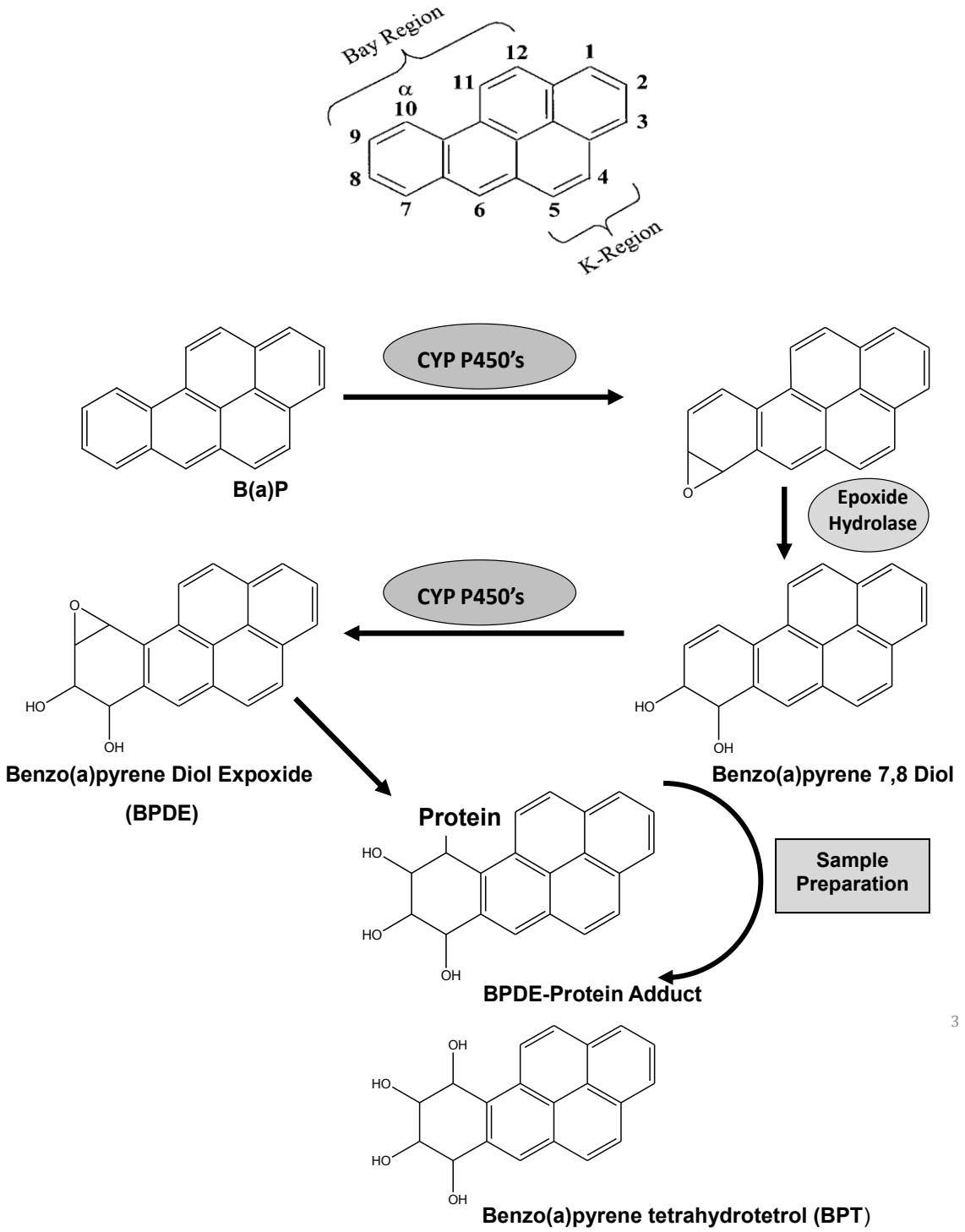

Figure 1.5. Metabolic activation scheme *of the activation of the B(a)P to the reactive electrophilic intermediate trans, anti-BPDE*. This reaction is completed by specific CYP450s (predominately CYP1A1 and CYP1A2 and CYP1B1 to a lesser extent) and epoxide hydrolase to eventually form the BPDE-protein adduct [88, 96, 99, 100]. During preparation of samples, the BPDE-protein adduct is hydrolyzed to BPT.

tetrahydrotetrol released from BPDE-Hb adducts in a small group of human participants [93]. Enzyme-linked immunosorbent assays (ELISA) have been used for whole protein adduct detection [101, 102], but require custom BPDE-specific antibodies. These antibodies are expensive, may not always be available, and the potential exists for non-specific binding to other PAH adducts.

Research Objectives

The objective of this research was to investigate whether B(a)P and/or BPDE-protein adducts measured in hair can be used as novel biomarkers of toxic exposure to B(a)P. The overarching hypothesis for this research was that ***B(a)P and BPDE-protein adducts in hair can be used as biomarkers of toxic exposures to B(a)P.*** To address this hypothesis the following specific aims were proposed:

1. Develop sensitive and specific mass spectrometry methods to detect and quantify low concentrations of B(a)P and BPDE-protein adducts in biological matrices.
2. Determine the concentrations of B(a)P and/or BPDE-protein adduct concentrations in hair and whether these concentrations are related to lung tissue damage in rats exposed to increasing amounts of B(a)P.
3. Determine the differences of B(a)P and BPDE-protein adducts in the hair of active smokers (those exposed to particulate tobacco smoke (PTS)) and nonsmokers (those with no exposure to PTS or environmental tobacco smoke (ETS)).

CHAPTER 2

QUANTIFICATION OF THE BIOMARKERS B(A)P AND BPDE-ADDUCTS IN PIGMENTED AND NONPIGMENTED RAT HAIR

Introduction

Mechanisms of xenobiotic incorporation in hair

B(a)P and BPDE-protein adduct concentrations, in an easily accessible surrogate tissue like hair, may reflect concentrations in a target tissue such as the lung. There have been a number of studies that show a positive correlation between the amount of drug found in hair and the dose administered [103-107]. However, this is not always the case [108]. There are several proposed models for the mechanisms of drug/ xenobiotic incorporation into hair [1, 52, 108, 109]. There are also many factors that influence drug/xenobiotic incorporation in hair, such as the physiochemical properties of the drug/xenobiotic (melanin affinity, basicity, lipophilicity, pKa, etc.) and its bioavailability, volume of distribution, and plasma elimination half-life [28, 110-115]. With these factors in mind, the following is a brief discussion of xenobiotic incorporation into hair.

The ***passive diffusion model*** is the simplest model proposed, and involves the passive diffusion of chemicals (from the vascular system that supplies the hair follicle) through the cell membranes of the keratinocytes at the

base of the hair follicle. These chemical then ultimately become tightly bound in the interior of the hair shaft following keratogenesis.

Since not all the data from studies of drug incorporation into hair fits the *passive diffusion model*, a second, more complex ***multicompartment model*** has been proposed. This model unites the theory of chemical incorporation via the blood during keratogenesis with additional incorporation of chemicals from sweat and sebum secretions after the hair has formed (but before the hair has emerged from the skin's surface). This model also accounts for the transfer of chemicals to the growing hair from the other compartments that surround the hair follicle, and the contribution of chemicals incorporating from the external environment after the hair has emerged from the skin (i.e., from smoke or vapors).

A third model, the ***deep compartment model***, has been proposed as a way to explain the unusual elimination of drugs such as cocaine and its metabolites from hair, as well as for very lipophilic compounds such as tetrahydocannbinol (THC) [108]. This model accounts for chemicals entering the hair via intradermal transfer from the accumulation of certain drugs into skin layers and other compartments such as erocrine (or eccrine) and apocrine glands.

The last model, the ***melanin-binding model***, includes the binding of xenobiotics to melanin. In this model, differences observed in xenobiotic incorporation into hair would be dependent on the amount of melanin present in hair, and the inter-individual differences of the types of melanin that are present in the hair shaft. Support for this model has been demonstrated for nitrogen

containing basic compounds, such as cocaine, nicotine, amphetamines, and morphine [28, 104, 112, 116, 117]. Several investigators have been able to demonstrate that these drugs are incorporated to the greatest extent in black hair compared to brown or blond hair [36, 118, 119]. Since melanin becomes incorporated into the hair shaft as the hair grows, the higher the melanin content (i.e. the darker the hair color), the higher the expected concentration of the drug/xenobiotic. For example, black hair would represent the highest concentration of the drug/xenobiotic compared to lighter hair colors regardless of the same dose being given.

Several different animal models have been used to study the incorporation of drugs/xenobiotics into hair, but the Long-Evans (LE) rat has a distinct advantage over the other models. This strain of rat has both pigmented and nonpigmented hair, thus eliminating the need to use two different strains to obtain both hair types. This allows the investigator the ability to study the effects that pigmentation may have on the incorporation of xenobiotics into hair. In addition, the use of only one strain of rat eliminates the need to consider the metabolic and pharmacokinetic differences of xenobiotic handling amongst different strains of rats.

The experiments presented in this chapter were designed to address the following objectives: 1) Develop sensitive and specific GC/MS methods (operated in electron ionization mode with selective ion monitoring, GC/MS-EI-SIM) methods to detect B(a)P in hair, lung, and plasma. 2) Develop sensitive and specific GC/MS (operated in negative ionization mode with SIM, GC/MS-

NCI-SIM) to detect BPT released from BPDE-protein adducts from hair and hemoglobin. 3) Using these developed methods, determine if B(a)P incorporates into rat hair in a dose-dependent manner. 4) Determine if B(a)P concentrations are greater in pigmented vs.nonpigmented rat hair. 5) Determine if BPT, released from BPDE-protein adducts, can be detected in rat hair, and whether concentrations are dose-dependent. 6) Determine whether concentrations of BPT released from BPDE-protein adducts in pigmented and nonpigmented hair statistically differ. 7) Determine if the concentration of B(a)P and/or BPT in hair correlate to formation of the BPDE-Hb adduct (the positive control). 8) Determine if B(a)P concentrations in hair reflect concentrations in a target tissue (lung) and plasma.

Materials and Methods

Chemicals and reagents

Benzo(a)pyrene (1 mg/mL) was purchased from SPEX Certiprep® Inc. (Metuchen, NJ), Restek (Austin, TX), and AccuStandards® (2 mg/mL)(New Haven, CT) for the preparation of calibration curves and quality control samples. The internal standard B(a)P-d_{12} (1 mg/mL), was purchased from SPEX Certiprep®, Inc.(Metuchen, NJ). For the dosing solutions, neat B(a)P ($\geq$96% purity) was purchased from Sigma-Aldrich® (St. Louis, MO). The vehicle for dosing solutions was corn oil (Mazola®, ACH Food Companies; Summit, IL). BPT (5 mg) was purchased from the National Cancer Institutes Chemical Repository (Midwest Research Institute, Kansas City, MO). The internal standard

[$^{13}C_6$]-BPT (1 mg), was purchased from Cambridge Isotopes Laboratories, Inc. (Andover, MA) by Dr. Stephen Hecht of Masonic Cancer Center (University of Minnesota), and a generous gift of a 1200 ng/mL [$^{13}C_6$]-BPT solution (1mL in DMSO) was provided for this dissertational research. Hexane, dichloromethane (DCM), methanol, acetonitrile, ethyl acetate were all GC/MS or high performance liquid chromatography grade and purchased from Burdick & Jackson® (Muskegon, MI). Acetone (GC/MS grade) was purchased from EMD (Gibbstown, NJ), and anhydrous tetrahydrofuran (THF) was purchased from Sigma-Aldrich® (Milwaukee, WI). The derivatization agent (*N*-Methyl-*N*-(trimethylsilyl) trifluoro-acetamide activated II, MSFTA II) was purchased from Fluka (Castle Hill, New South Wales, Australia). Proteinase K (from *Tritirachium album*, activity $\geq$30 units/mg) was purchased from Sigma-Aldrich®. Sep-Pak C18, 3cc solid phase extraction (SPE) cartridges were purchased from Waters Corporation (Milford, Massachusetts). All other reagent grade chemicals were purchased from Fisher Scientific (Pitsburg, PA), Sigma-Aldrich® and Fluka. Water used was either house-prepared Milli-Q water or NANOpure™ water obtained from ARUP Laboratories (Salt Lake City, Utah). Helium and ammonia gases used for GC/MS analysis were purchased from Airgas, Inc.® (Salt Lake City, UT). Whole blood from LE rats was obtained from Innovative Research (Novi, MI) for preparation of plasma and hemoglobin standards and quality control samples. RBC lysis buffer was purchased from Roche (Branford, CT) and phosphate buffered saline solution from Teknova (Hollister, CA). Sodium heparin Vacutainers® were purchased from BD (Franklin Lakes, NJ). Sodium heparin (5000 USP

units/mL) and sterile saline were purchased from the University of Utah's Outpatient Pharmacy (50 North Medical Drive, Room 1400, Salt Lake City, UT. 84132). Procter and Gambler Company's (Cincinnati, OH) Herbal Essences® shampoo was obtained from local retail store.

Stocks and solutions

Intermediate stock solutions of B(a)P were prepared in 1:1 (v/v) acetone/DCM at a concentration of 500 and 5000 ng/mL. Intermediate stock solutions for BPT were prepared in fresh anhydrous THF at a concentration of 100 ng/mL. Since B(a)P and BPT are light and air sensitive, all solutions were made in amber vials with septum screw caps to avoid over exposure to light and air and stored at -20°C. Matrix fortified calibration curves and quality control samples were prepared daily. The quality control samples for B(a)P (that were prepared with each batch of samples and for determination of assay imprecision and accuracy) were fortified with a reference material from a different manufacturer than the reference material used for the calibration curve. Since no other commercial source was available for BPT, a separate stock and intermediate solution for fortification of quality control samples were prepared by the quality control officer or other Center for Human Toxicology personnel.

Animals

Male Long-Evans rats (200-225g) were individually housed in cages with wire mesh bottoms to eliminate the potential for external contamination of the hair from social grooming and/or bedding. Rats were maintained under controlled

temperature and lighting conditions (12 hr light/dark cycle) and provided with food and water ad libitum. All procedures were in compliance with the National Institutes of Health *Guide for the Care and Use of Laboratory Animals* [120].

Multiple-dose hair experiments

Prior to exposure, an approximate 2 inch medial dorsal square of pigmented and nonpigmented hair was shaved with an electric shaver (hair sample used for baseline measurements). The rats were then administered B(a)P (in corn oil) intraperitoneal (i.p.) at 40 mg/kg (n=10), 80 mg/kg (n=10), or 160 mg/kg (n=10) once daily for seven days. (Solutions of B(a)P in corn oil were prepared at 25, 50, and 100 mg/mL for the 40, 80, and 160 mg/kg doses respectively. This was done in order to maintain a consistent volume of B(a)P in corn oil between the doses and groups). Control rats (n=10 total) were administered corn oil (i.p.), once per day for 7 days. Fourteen days after the first dose, the animals were anesthetized with chloral hydrate (450 mg/kg) and approximately a 1.5 inch medial dorsal square (inside the original 2 inch area) was shaved to collect newly grown pigmented and nonpigmented hair. These hair samples were then stored in air tight containers in the dark at 4°C (see dosing paradigm in Figure 2.1). While still under deep anesthesia, an abdominal aorta blood draw was performed with a sodium heparin-lined 10 mL syringe equipped with a 21 gauge needle. Blood was then transferred to a sodium heparin BD Vacutainer® tube. The animal's diaphragm on each side was then carefully pierced to allow the lungs to collapse. The lungs were then carefully

A.

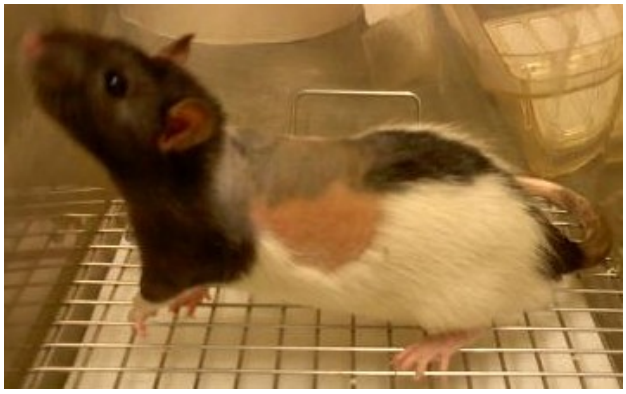

B.

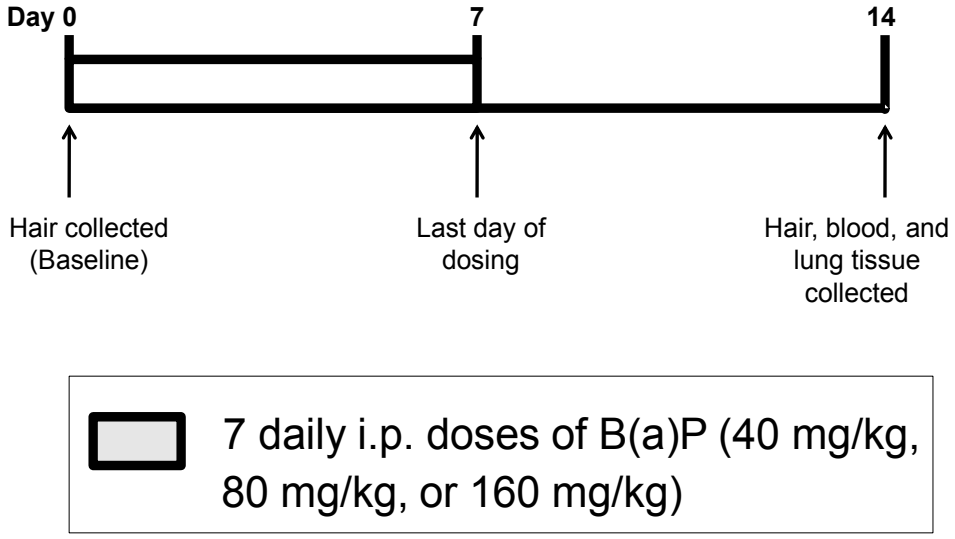

Figure 2.1. *Dosing paradigm for Long-Evans rats.* A) *Picture of Long-Evans rat showing area of shaved hair*. B) *Dosing paradigm for B(a)P and time points of hair collection.* Prior to exposure, a medial dorsal ~2 inch square of pigmented and nonpigmented hair was shaved (hair sample used for baseline measurements). Rats were then administered B(a)P (in corn oil) i.p. at 40 mg/kg (n=10), 80 mg/kg (n=10), or 160 mg/kg (n=10) daily for seven days. Control rats (n=10) were dosed i.p. with corn oil for seven days. Fourteen days after the first dose, a ~1.5 inch medial dorsal (inside the original 2 inch square) area was shaved to collect newly grown hair. Hair samples were then stored in air tight containers in the dark at 4°C until analysis. This dosing paradigm was based on literature searches for commonly used B(a)P dosing protocols, to ensure BPDE-Hb adduct formation would be adequate for detection, and to allow for the growth of new hair.

extracted by the trachea avoiding actual contact with the lung at all times. The left lobe was placed in 10% formalin (for histology). The right lobe was placed on tin foil on top of dry ice, then stored at -80°C until preparation for B(a)P analysis.

B(a)P assays

B(a)P: Hair preparation and extraction

Ten milligrams of hair (±10%) were weighed (Mettler Toledo, AG104) and B(a)P-d_{12} internal standard (IS) added. Calibrators were concurrently prepared by fortification of B(a)P and IS to analyte-free (blank) rat hair. After digestion of the hair (sonication in 1.5 mL of 2.5 N sodium hydroxide for 2 hrs) a liquid-liquid extraction was performed. Hexane (1.5 mL) was added to each hair sample digest, thoroughly vortexed, and then centrifuged at 3500 rpm for 4 mins to minimize the emulsification layer. This was performed a total of three times, then combined organic fractions were dried under a constant stream of nitrogen in a Zymark Turbovap® LV evaporator at 55°C. Residues were then reconstituted in 0.100 mL of 1:1(v/v) acetone/ dichloromethane and analyzed by GC/MS-EI-SIM (see *GC/MS-EI-SIM analysis for B(a)P* section for additional details).

B(a)P: Lung tissue preparation and extraction

A frozen 100 mg (±10%) posterior section of lung was weighed (Mettler Toledo, AG104) in a specimen vial. Ice-cold Milli-Q water (0.500 mL) was added o the frozen tissue in a cold room (4°C), and immediately sonicated (Sonics Vibracell, VC505) at 30% amplitude for 12 secs, a total of six times.

B(a)P-d_{12} IS was then added to the samples. Calibrators were concurrently prepared by fortification of B(a)P and IS to 0.500 mL aliquots of analyte-free (blank) lung homogenates (aliquots were one part lung tissue to five parts water, w/v). A liquid-liquid extraction was then performed. Hexane (1.5 mL) was added to lung homogenate, then thoroughly vortexed, and centrifuged at 3500 rpm for 4 mins. This was performed a total of three times, then combined organic fractions were dried under a constant stream of nitrogen in a Zymark Turbovap® LV evaporator at 55°C. Residues were then reconstituted in 0.050 mL of 1:1 acetone/dichloromethane, transferred to an autosampler vial, and analyzed by GC/MS-EI- SIM (see *GC/MS-NCI-SIM analysis for B(a)P* section for additional details).

B(a)P: Plasma preparation and extraction

To a 1 mL aliquot of plasma, B(a)P-d_{12} IS was added. Calibrators were concurrently prepared by fortification of B(a)P and IS to analyte-free (blank) rat plasma. A liquid-liquid extraction was then performed according to the following procedure. Hexane (1.5 mL) was added to each plasma sample, then thoroughly vortexed, and centrifuged at 3500 rpm for 4 mins. This was performed a total of three times, then combined organic fractions were dried under a constant stream of nitrogen in a Zymark Turbovap® LV evaporator at 55°C. Residues were then reconstituted in 0.050 mL of 1:1 acetone/dichloromethane, transferred to an autosampler vial for analysis by GC/MS-EI- SIM (see *GC/MS-EI-SIM analysis for B(a)P* section for additional details).

Assays for BPT released from BPDE-protein adducts

BPT: Hair preparation and extraction

Hair (100 mg (±10%)) was weighed out (Mettler Toledo, AG104) and [$^{13}C_6$]-BPT IS added. Calibrators were concurrently prepared by fortification of BPT and IS to analyte-free (blank) rat hair. To each hair sample, 2 mL of 200 ug/mL Proteinase K in incubation buffer (50 mM Tris buffer, 5 mM calcium chloride, pH 8.5) was added to digest hair. Samples were then placed in a sonicator for 1 hr (~37°C), transferred to a 37°C water bath and allowed to incubate overnight (total time ~20 hrs). After cooling, approximately 0.25 g of sodium chloride (NaCl) was added to each sample, and a liquid-liquid extraction was then performed. Ethyl acetate (6 mL) was added to each hair digestion solution, which was then thoroughly vortex-mixed followed by centrifugation at 3500 rpm for 4 mins. The liquid-liquid extraction was performed twice and then the combined organic fractions were placed in a Zymark Turbovap® LV evaporator at 55°C under a constant stream of N_2 until dry. The residues were then derivatized by adding 50 uL of MSTFA and allowing for 15 mins reaction time in a hot block at 80°C. Samples, in MSTFA, were then transferred to autosampler vials for analysis by GC/MS-NCI-SIM (see *GC/MS-NCI-SIM analysis for BPT* section for additional details).

BPT: Hemoglobin preparation from whole blood and extraction

Fresh whole blood from rats was centrifuged at 3500 rpm for 5 mins to separate plasma from red blood cells (RBCs). The plasma was removed and stored at -80°C for B(a)P analysis. The RBC portion remaining in the tube was

then washed twice with equivalent volumes of 0.9% sodium chloride solution in Milli-Q water to remove any free, unbound BPT (from metabolism by epoxide hydrolase and/or water). One volume of phosphate buffered saline (PBS) and two volumes of RBC lysis buffer were added to re-suspend the RBCs (e.g., 3 mL RBCs then 3 mL of PBS and 6 mL of RBC lysis buffer). This was done to keep volumes of reagents consistent between samples of differing volumes. The samples were then gently shaken for 10 mins for lysis of RBCs, followed by centrifugation at 2000 rpm to pellet ghost membranes. The supernatant was removed from each sample, and six volumes of ice-cold acetone (with 0.015% hydrochloric acid) was slowly added, dropwise, to precipitate Hb. After 5 mins the samples were centrifuged to pellet the precipitated Hb, and the excess fluid was decanted. The Hb pellet was then evaporated to dryness in a Zymark Turbovap® LV evaporator under a constant stream of nitrogen at 37°C and stored at -80°C until preparation for analysis. Hb (100 mg (±10%)) (prepared as described above) was weighed (Mettler Toledo, AG104) and IS added. Calibrators were concurrently prepared by fortification of BPT and IS to analyte-free (blank) rat Hb.

After Hb isolation, hydrolysis of the Hb samples was performed as follows: Two milliliters of NANOpure™ water and 30 µL of 6 N hydrochloric acid to each Hb sample, tightly capped, and incubation in a water bath at 90°C for 3 hrs. Samples were allowed to cool, then approximately 0.25 g of sodium chloride was added to each sample. A liquid-liquid extraction was then performed. Ethyl acetate (6 mL) was added to each Hb hydrosylate, then thoroughly vortex-mixed, and centrifuged at 3500 rpm for 4 mins. This was performed twice, and the

combined organic fractions were placed in a Zymark Turbovap® LV evaporator at 52°C under a constant stream of N_2 until dry. Samples were capped and stored at -20°C overnight, and extracted by SPE the following morning. Solid phase extraction (SPE) was performed by conditioning Waters C18 3cc columns with 2.5 mL of methanol followed by 2.5 mL of NANOpure™ water. The sample (reconstituted in a total volume of 2.5 mL of 50% aqueous methanol) was slowly loaded onto the column, and allowed to incubate for 5 mins. The column was washed with 2.5 mL of NANOpure™ water, then 50% aqueous methanol and then dried for 5 mins under a vacuum pressure around 5 psi. The samples were eluted from the column using two volumes of 2.5 mL 50:50 acetonitrile/methanol. The eluents were completely dried at 55°C in a Zymark Turbovap® LV evaporator under a constant stream of nitrogen. MSTFA (50 µL) was added to the residues and 15 min reaction time was allowed in a hot block at 80°C. Samples were then transferred to autosampler vials for analysis by GC/MS-NCI-SIM (see *GC/MS-NCI-SIM analysis for BPT* section for additional details).

Evaluation of wash procedure for rat hair

Two hundred mg of rat hair (from one individual 160 mg/kg B(a)P dosed rat) was separated into three groups: Group 1) Unwashed hair (n=2), Group 2) Shampoo washed hair (n=2), and 3) Dichloromethane wash hair (n=2). For Group one (unwashed hair), 10 mg $\pm$10% of hair were weighed (Mettler Toledo, AG104) for each sample, then digested and extracted as described in the "*B(a)P: Hair preparation and extraction"* section in *Materials and Methods* section. For Group 2 (shampoo washed hair), 0.1 mL of a 10% (v/v) shampoo aqueous

solution was added to each sample, quickly vortex-mixed, and liquid portion decanted from hair. Hair samples were then allowed to dry overnight at room temperature in the dark. The following day, 10 mg ±10% of hair were weighed for each sample, then digested and extracted as written above. For Group 3 (dichloromethane washed hair), 0.1 mL of dichlormethane was added to each sample, quickly vortex-mixed, and then decanted from hair. Hair samples were then allowed to dry overnight at room temperature in the dark. The following day, 10 mg ±10% of hair were weighed for each sample, then digested and extracted as previously described.

GC/MS-EI-SIM analysis for B(a)P

A Hewlett Packard (HP) GC 6890 was fitted with a Agilent DB-5UI-MS capillary column (part no. 122-5535UI, 30.0 m x 250 µm x 0.25 µm nominal). The injector was operated in the pulsed splitless mode (injection pulse 40 psi until 0.2 min, purge flow to split vent 30 mL/min at 0.75 min). The pressure of helium gas was programmed to 17.0 psi (total flow 33.8 mL/min). The inlet heater temperature was set at 300°C and the transfer line was set at 300°C. The injection volume was 1 µL. The solvent delay was set at 3 mins. The initial oven temperature was set at 120°C for 1 min, then ramped to 250°C at 25°C/min A 2nd ramp to 320°C at 10°C /min followed, and then oven was held at 320°C for 3.5 mins. The total run time equaled 16.7 mins. An HP MS 5973 was used to perform selective ion monitoring (SIM) was used to detect B(a)P at *m/z* 252 and its fragment at *m/z* 126. B(a)P-d_{12} was detected at *m/z* 264. To quantitate the results, ChemStation software (version: D.02.00.275) was used to generate

calibration curves from peak area ratios of target analyte and the corresponding internal standard over the concentration range.

GC/MS-NCI-SIM analysis for BPT

The same GC/MS system and column was used as stated in the GC/MS-EI-SIM analysis. The injector was operated in the pulsed splitless mode (injection pulse 17.6 psi until 1.33 min, purge flow to split vent 30 mL/min at 1.75 mins). The pressure of helium gas was programmed to 24.3 psi (flow 2.2 mL/min, total flow 34.5 mL/min). Ammonia reagent gas pressure was set at 17.0 mL/min The inlet heater temperature was set at 280°C. The transfer line was set at 300°C. The injection volume was 2 µL and the solvent delay was set at 9.0 mins. The initial oven temperature was set at 120°C for 1 min, then ramped to 250°C at 20°C/min A 2nd ramp to 300°C at 8°C /min followed. The total run time equaled 13.75 mins. SIM was used to detect the derivatized BPT at *m/z* 446. The derivatized ($^{13}C_6$)-BPT internal standard was detected at *m/z* 452. To quantitate the results, ChemStation software (version: D.02.00.275) was used to generate calibration graphs from peak area ratios of target analyte and the corresponding internal standard over the concentration range.

Statistical analysis

Graph Pad Prism® software (version 5.01) (La Jolla, CA) was used to compare results from 40, 80, and 160 mg/kg dosed rats using a one-way ANOVA and a Newman-Keuls posthoc test for: 1) B(a)P concentrations in hair of the 40, 80, and 160 mg/kg dosed rats, 2) BPT concentrations in hair of the 40, 80, and

160 mg/kg dosed rats, 3) BPT released from BPDE-Hb adducts in the 40, 80, and 160 mg/kg dosed rats, 4) B(a)P concentrations in rat lung of the 40, 80, and 160 mg/kg dosed rats, and 5) B(a)P concentrations in rat plasma of the 40, 80, and 160 mg/kg dosed rats. A Student's t-test was used to compare B(a)P and BPT concentrations between pigmented and nonpigmented rat hair. Spearman nonparametric correlation tests were used to measure the strength of the association between the following: 1) B(a)P concentrations in rat hair and the positive control (BPDE-Hb adducts), 2) BPT concentrations in rat hair and the positive control (BPDE-Hb adducts), 3) B(a)P concentrations in plasma and lung tissue. Differences were considered significant $\alpha \leq 0.05$.

Results

Validation of analytical methods for B(a)P

Hair

Figure 2.2 shows representative chromatograms for an extracted 0.25 ng/mg B(a)P calibration standard (lowest standard in curve) and an extracted blank rat hair sample. The assay was determined to be linear from 0.25 to 100 ng/mg. The lower limit of quantitation (LLOQ) and upper limit of quantitation (ULOQ) were 0.25 and 100 ng/mg, respectively. The coefficient of variation (CV) for the intra- and interassay accuracy and imprecision were less than or equal to 10% (Table 2.1).

The intra- and interaccuracy and imprecision data were determined by analysis of samples that were prepared with a stock solution from a different

Figure 2.2 *Representative ion chromatograms from (A) extracted analyte-free (blank) rat hair sample and (B) an extracted B(a)P-fortified (0.25 ng/mg, LLOQ) rat hair sample.* The small peak for B(a)P in extracted blank rat hair is due a small impurity present in the IS B(a)P-d_{12} (98.4% pure) (calculated concentration for this sample is below the LLOQ). There is no peak for B(a)P in blank rat hair without IS (data not shown). Analyte retention time (RT) is on the x-axis and signal intensity on the y-axis. B(a)P = 252 *m/z* and B(a)P-d_{12} = 264 *m/z*

A.

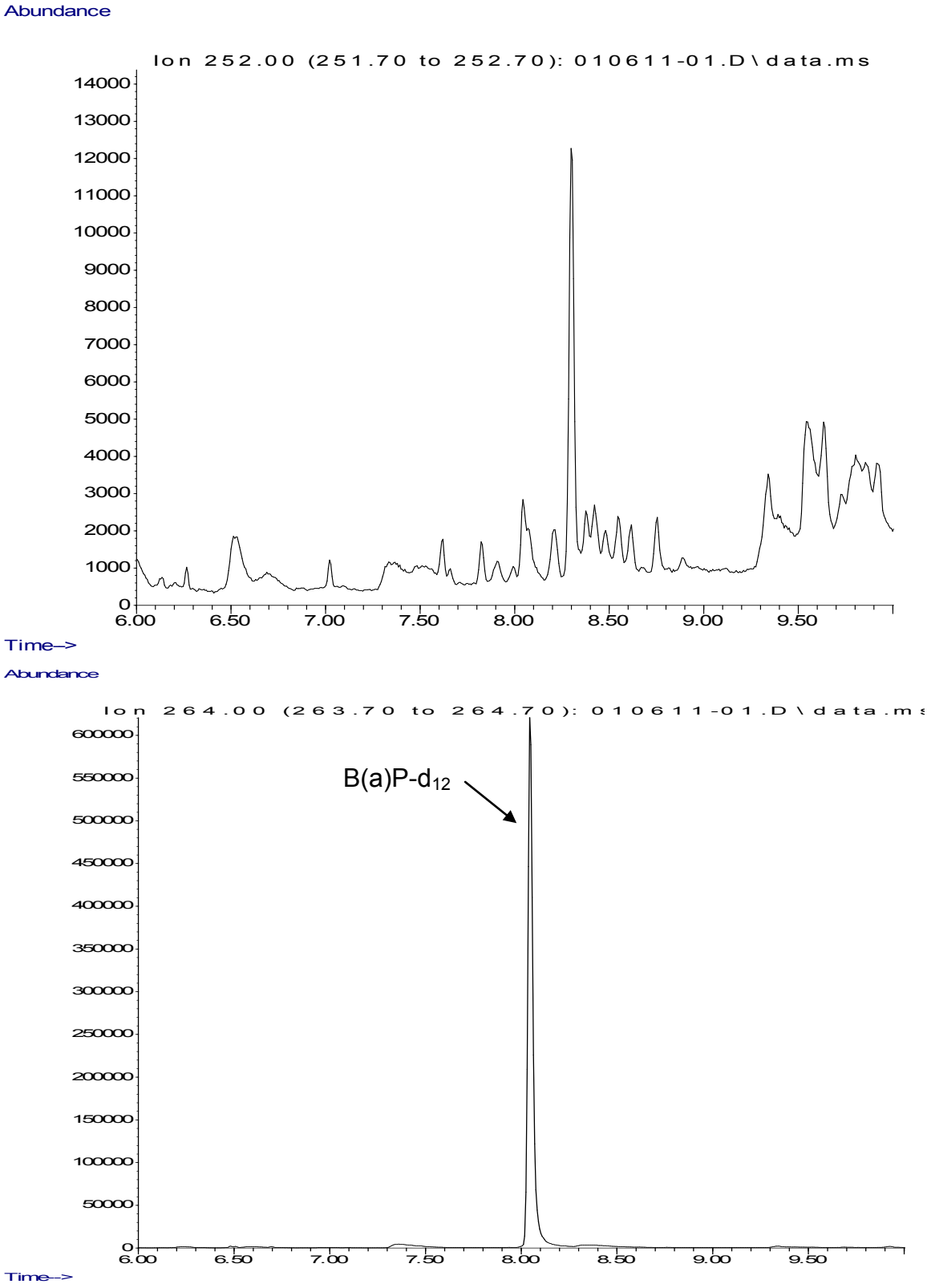
Abundance
Ion 252.00 (251.70 to 252.70): 010611-01.D\data.ms
14000
13000
12000
11000
10000
9000
8000
7000
6000
5000
4000
3000
2000
1000
0
6.00
6.50
7.00
7.50
8.00
8.50
9.00
9.50
Time-->
Abundance
Ion 264.00 (263.70 to 264.70): 010611-01.D\data.ms
600000
550000
500000
450000
400000
350000
300000
250000
200000
150000
100000
50000
0
B(a)P-d12
6.00
6.50
7.00
7.50
8.00
8.50
9.00
9.50
Time-->

B.

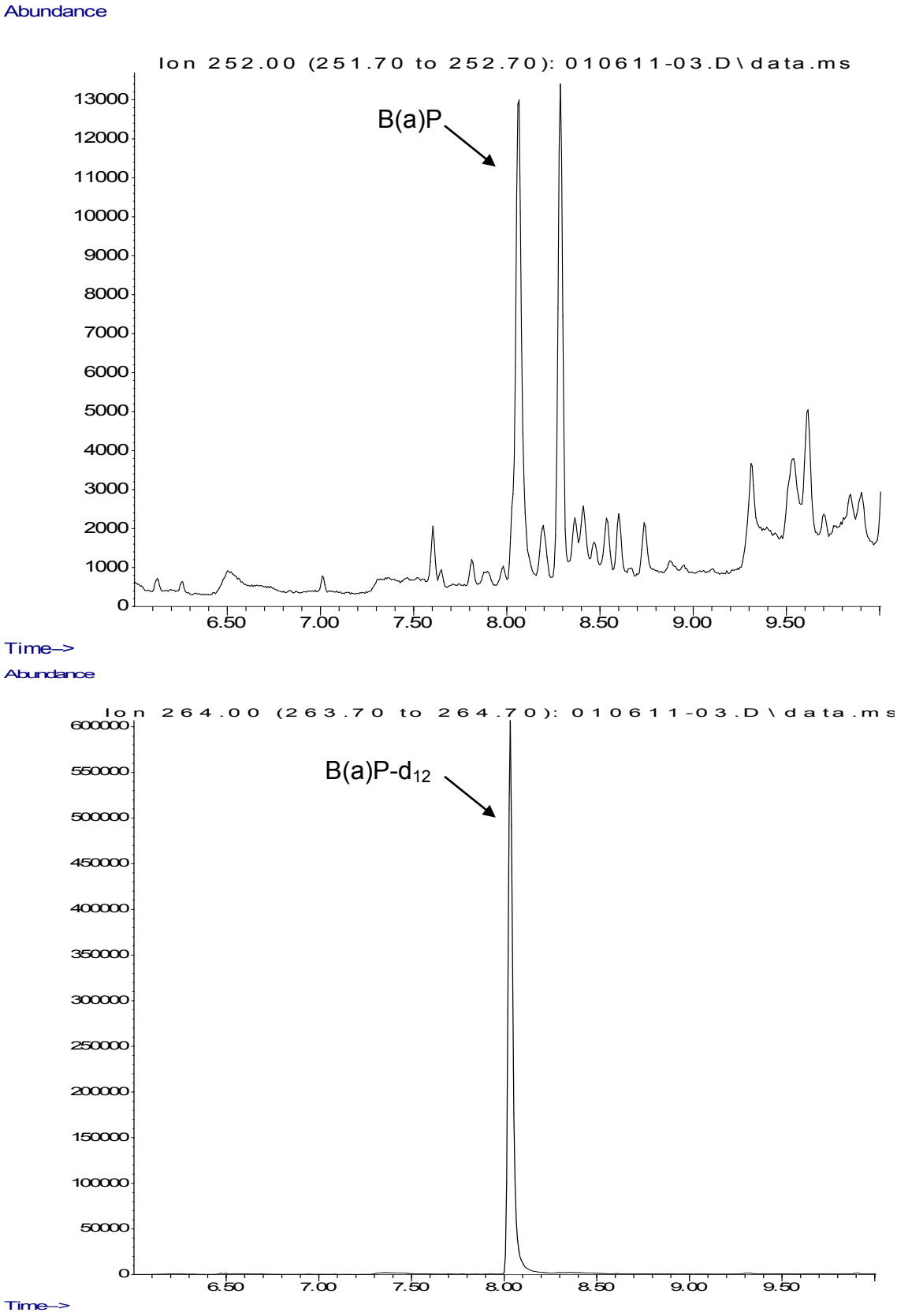
Abundance
Ion 252.00 (251.70 to 252.70): 010611-03.D\data.ms
B(a)P
13000
12000
11000
10000
9000
8000
7000
6000
5000
4000
3000
2000
1000
0
6.50
7.00
7.50
8.00
8.50
9.00
9.50
Time-->
Abundance
Ion 264.00 (263.70 to 264.70): 010611-03.D\data.ms
B(a)P-d12
600000
550000
500000
450000
400000
350000
300000
250000
200000
150000
100000
50000
0
6.50
7.00
7.50
8.00
8.50
9.00
9.50
Time-->

Table 2.1

Accuracy, imprecision, LLOQ, and ULOQ of B(a)P-fortified rat hair

	Target Concentration ng/mg	n[a]	Mean Concentration pg/mg	% of Target	%CV[b]
Intraassay					
	0.75	5	0.72	95.5	4.9
	40.00	5	42.14	105.4	1.2
	80.00	5	83.36	104.2	5.4
Interassay					
	0.75	15	0.71	95.2	10.2
	40.00	15	43.91	109.8	4.8
	80.00	15	88.32	110.4	6.8

	Target Concentration pg/mg	n[a]	Mean Concentration pg/mg	% of Target	%CV[b]
LLOQ					
	0.25	5	0.22	86.0	6.0
ULOQ					
	100.00	5	96.40	96.4	3.5

[a] Number of quality control replicate samples used
[b] CV= coefficient of variation

manufacturer from that used to make the calibration curve standards. Accuracy was calculated by dividing the observed concentration by the target concentration. This value was then multiplied by 100 to obtain a percentage. The percent CV was calculated by dividing the standard deviation of the group by the mean observed concentration of the group. This value was then multiplied by 100 to obtain a percentage. The percent CV calculated from the mean observed concentrations of samples tested is an estimate of imprecision of the assay.

The intraassay accuracy and imprecision were determined by analyzing five replicate samples of analyte-free rat hair fortified with known amounts of B(a)P (0.75, 40, and 80 ng/mg) within a single analytical batch on the same day. The intraassay accuracy ranged from 95.5-105.4% of the theoretical target concentrations. The intraassay imprecision ranged from 1.2-5.4%.

The accuracy and imprecision for the interassay were determined by comparing calculated concentrations from replicates (n=5 for each concentration, total n=15) of B(a)P-fortified rat hair samples at 0.75, 40, 80 ng/mg for three separate analytical batches on three separate days. The intraassay accuracy ranged from 95.2-110.4% of the theoretical target concentrations. The intraassay imprecision ranged from 4.8-10.2%.

The LLOQ was evaluated by the analysis of five replicates of B(a)P fortified analyte-free rat hair at 0.25 ng/mg. The average accuracy for these samples was 86.0%, and the imprecision was 6.0%.

The ULOQ was evaluated by the analysis of five replicates of B(a)P-fortified analyte-free rat hair at 100 ng/mg. The average accuracy for

these samples was 96.4%, and the imprecision was 3.5%.

Lung

Figure 2.3 shows representative chromatograms for an extracted 12.5 pg/mg B(a)P calibration standard (lowest standard in curve) and an extracted blank rat lung sample. The assay was determined to be linear from 12.5 to 1000 pg/mg. The LLOQ and ULOQ were 12.5 and 1000 pg/mg respectively. The coefficient of variation (CV) for the intra- and interassay accuracy and imprecision were less than or equal to 15% (Table 2.2).

The intra- and interaccuracy and imprecision data were determined by analysis of samples that were prepared with a stock solution from a different manufacturer from that used to make the calibration curve standards.
The intraassay accuracy and imprecision were determined as previously described. Analyte-free lung samples were fortified with B(a)P at 37.5, 400, and 750 pg/mg and analyzed within a single batch. The intraassay accuracy ranged from 100.7-114.8% of the theoretical target concentrations. The intra- assay imprecision ranged from 2.6-14.8%.

The accuracy and imprecision for the interassay were also determined as previously described. Analyte-free lung samples were fortified with B(a)P 37.5, 400, 750 pg/mg and analyzed in three separate analytical batches on three separate days. The intraassay accuracy ranged from 103.2-115.6% of the theoretical target concentrations. The intraassay imprecision ranged from 2.8-14.1%.

The LLOQ and ULOQ were also evaluated as described previously. The

Figure 2.3 *Representative ion chromatograms from (A) extracted analyte-free (blank) rat lung sample and (B) an extracted B(a)P-fortified (12.5 pg/mg, LLOQ) rat lung sample.* The small peak for B(a)P in extracted blank rat hair is due a small impurity present in the IS B(a)P-d_{12} (98.4% pure) (calculated concentration for this sample is below the LLOQ). There is no peak for B(a)P in blank rat lung without IS (data not shown). Analyte retention time (RT) is on the x-axis and signal intensity on the y-axis. B(a)P = 252 *m/z* and B(a)P-d_{12} = 264 *m/z*

A.

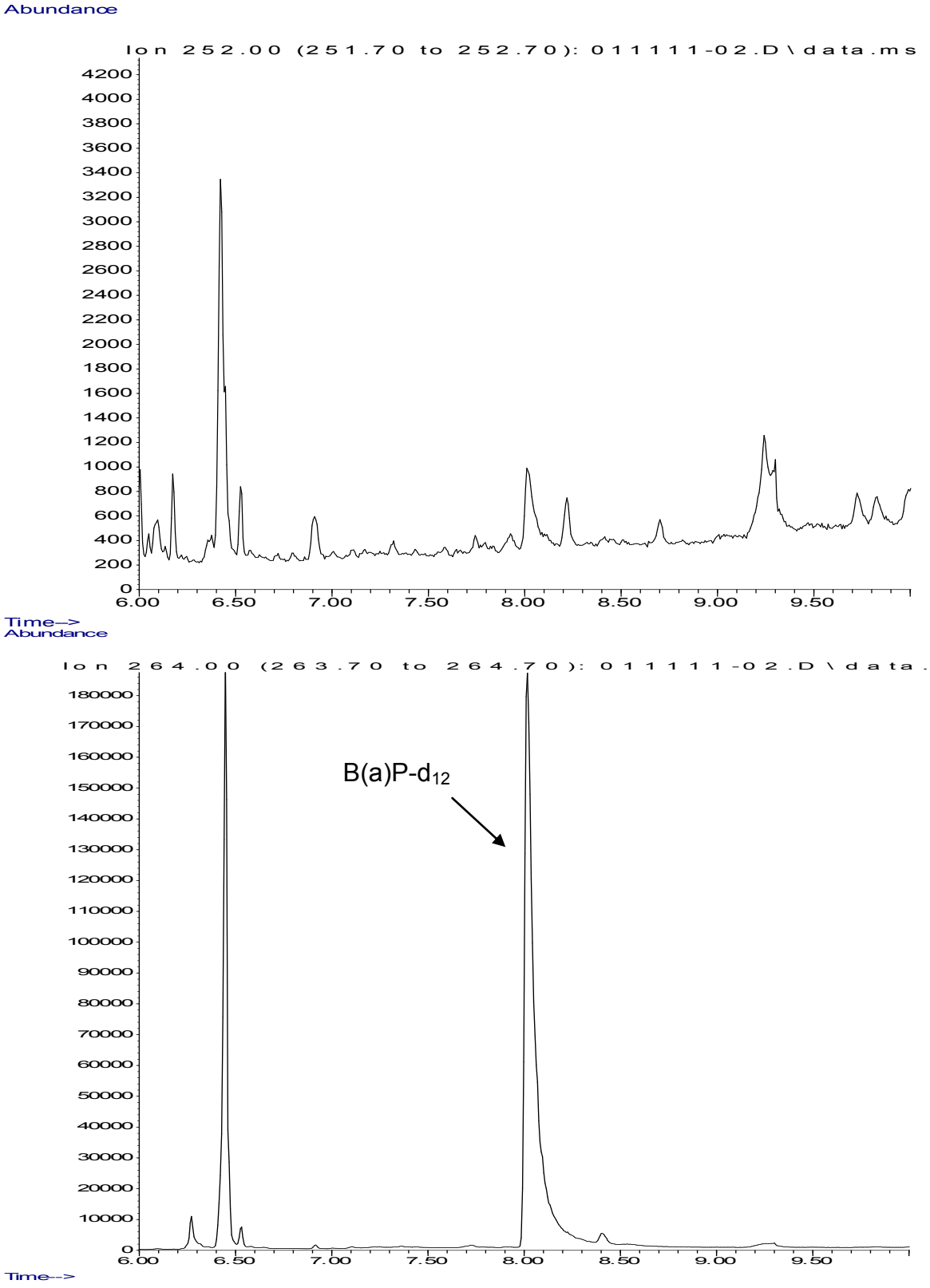
Abundance
Ion 252.00 (251.70 to 252.70): 011111-02.D\data.ms
Time-->
Abundance
Ion 264.00 (263.70 to 264.70): 011111-02.D\data.
B(a)P-d12
Time-->

B.

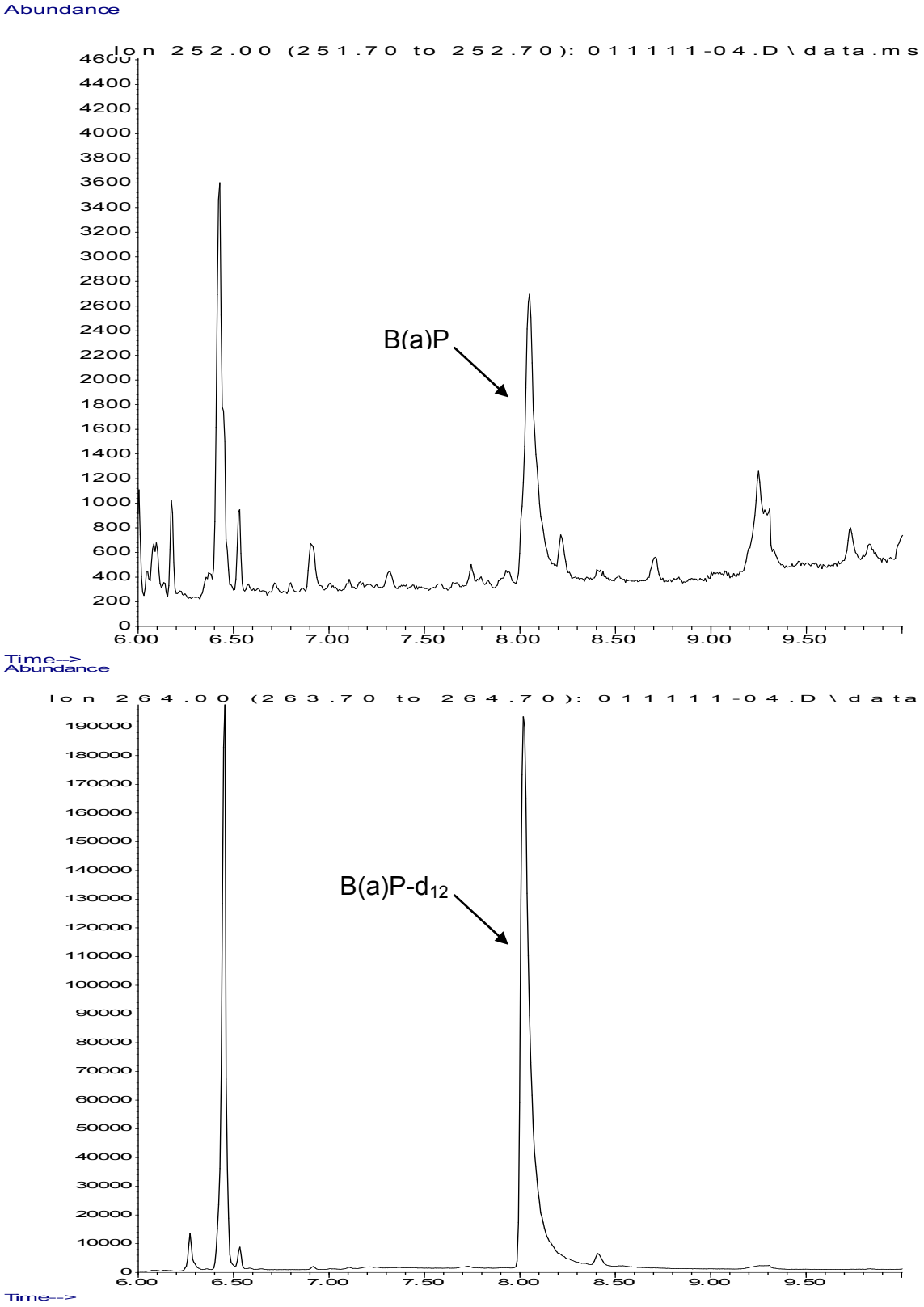
Abundance
Ion 252.00 (251.70 to 252.70): 011111-04.D\data.ms
B(a)P
Time-->
Abundance
Ion 264.00 (263.70 to 264.70): 011111-04.D\data
B(a)P-d12
Time-->

Table 2.2

Accuracy and imprecision of B(a)P-fortified rat lung tissue.

	Target Concentration pg/mg	n[a]	Mean Concentration pg/mg	% of Target	%CV[b]
Intraassay					
	37.5	5	43.1	114.8	4.2
	400.0	5	413.1	103.3	2.6
	750.0	5	805.8	100.7	14.8
Interassay					
	37.5	15	43.3	115.6	4.4
	400.0	15	412.6	103.2	2.8
	750.0	15	808.9	107.9	14.1

	Target Concentration pg/mg	n[a]	Mean Concentration pg/mg	% of Target	%CV[b]
LLOQ					
	12.5	5	14.6	117.0	1.9
ULOQ					
	1000.0	5	1031.4	103.1	2.6

[a] Number of quality control replicate samples used
[b] CV= coefficient of variation

mean average accuracy for the LLOQ was 117.0% with an imprecision of 1.9%. The average accuracy for the ULOQ was 103.1% with an imprecision of 2.6%.

Plasma

Figure 2.4 shows chromatograms for an extracted 25 ng/mL B(a)P calibration standard (lowest standard in curve) and an extracted blank rat plasma sample. The assay was determined to be linear from 25 to 3200 ng/mL. The LLOQ and ULOQ were 25 and 3200 ng/mL, respectively. The coefficient of variation (CV) for intra- and interassay accuracy and imprecision were less than 20% (Table 2.3).

The intra- and interaccuracy and imprecision data were determined by analysis of samples that were prepared with a stock solution from a different manufacturer from that used to make the calibration curve standards.

The intraassay accuracy and imprecision were determined as previously described. Analyte-free plasma samples were fortified with B(a)P at 75, 1500, and 2750 ng/mL and analyzed within a single batch. The intraassay accuracy ranged from 94.2-96.4% of the theoretical target concentrations. The intraassay imprecision ranged from 5.8-20.0%.

The accuracy and imprecision for the interassay were determined as previously described. Analyte-free plasma samples were fortified with B(a)P at 75, 1500, 2750 ng/mL and analyzed in three separate analytical batches on three separate days. The interassay accuracy ranged from 94.1 - 98.8% of the theoretical target concentrations. The intraassay imprecision ranged from 4.7 - 18.0%.

Figure 2.4 *Representative ion chromatograms from (A) extracted analyte-free (blank) rat plasma sample and (B) an extracted B(a)P-fortified (25 ng/mL, LLOQ) rat plasma sample.* The small peak for B(a)P in extracted blank rat hair is due a small impurity present in the IS B(a)P-d_{12} (98.4% pure) (calculated concentration for this sample is below the LLOQ). There is no peak for B(a)P in blank rat plasma without IS (data not shown). Analyte retention time (RT) is on the x-axis and signal intensity on the y-axis. B(a)P = 252 *m/z* and B(a)P-d_{12} = 264 *m/z*

A.

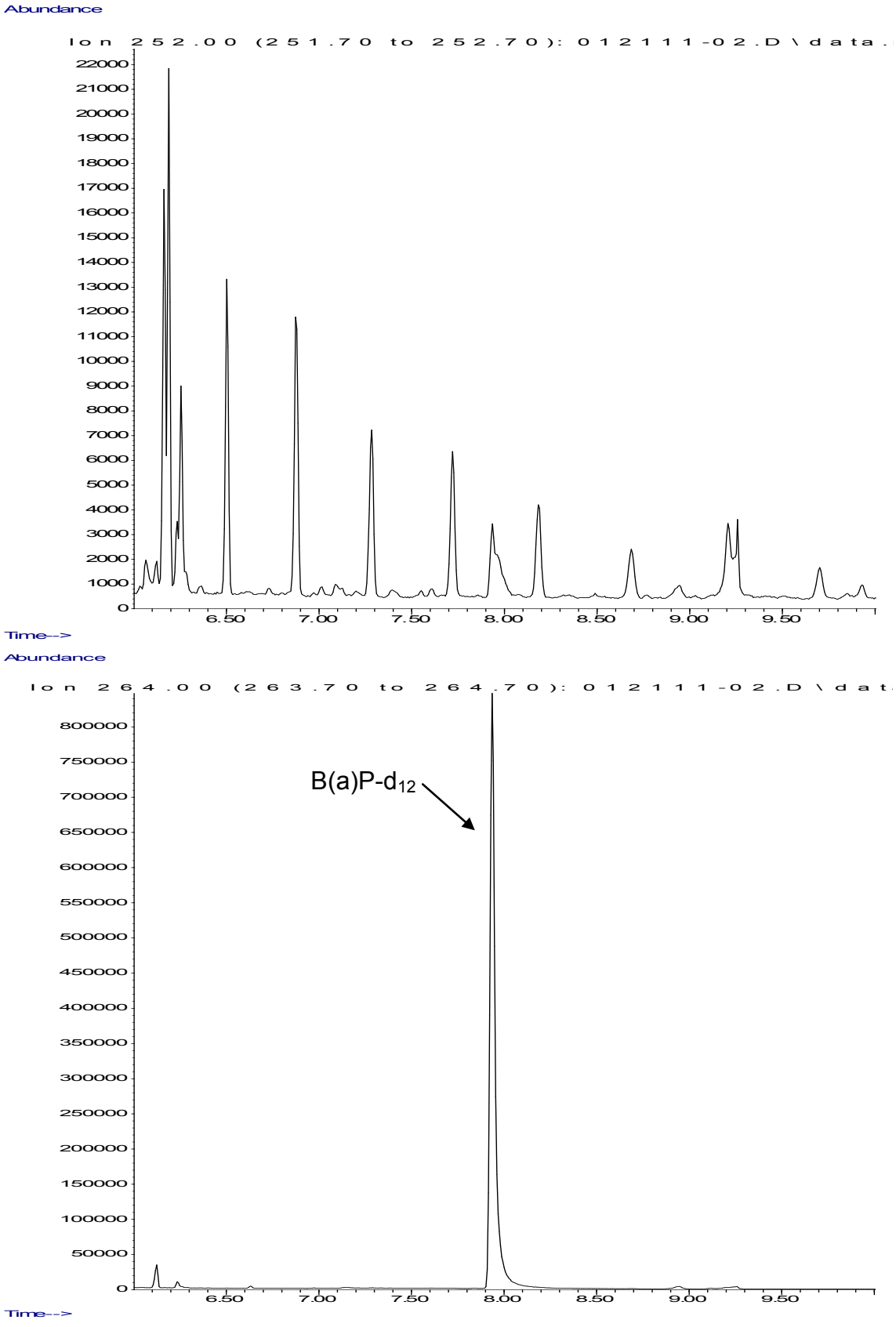
Abundance
Ion 252.00 (251.70 to 252.70): 012111-02.D \ data.
22000
21000
20000
19000
18000
17000
16000
15000
14000
13000
12000
11000
10000
9000
8000
7000
6000
5000
4000
3000
2000
1000
0
6.50
7.00
7.50
8.00
8.50
9.00
9.50
Time-->
Abundance
Ion 264.00 (263.70 to 264.70): 012111-02.D \ dat
800000
750000
700000
650000
600000
550000
500000
450000
400000
350000
300000
250000
200000
150000
100000
50000
0
B(a)P-d12
6.50
7.00
7.50
8.00
8.50
9.00
9.50
Time-->

B.

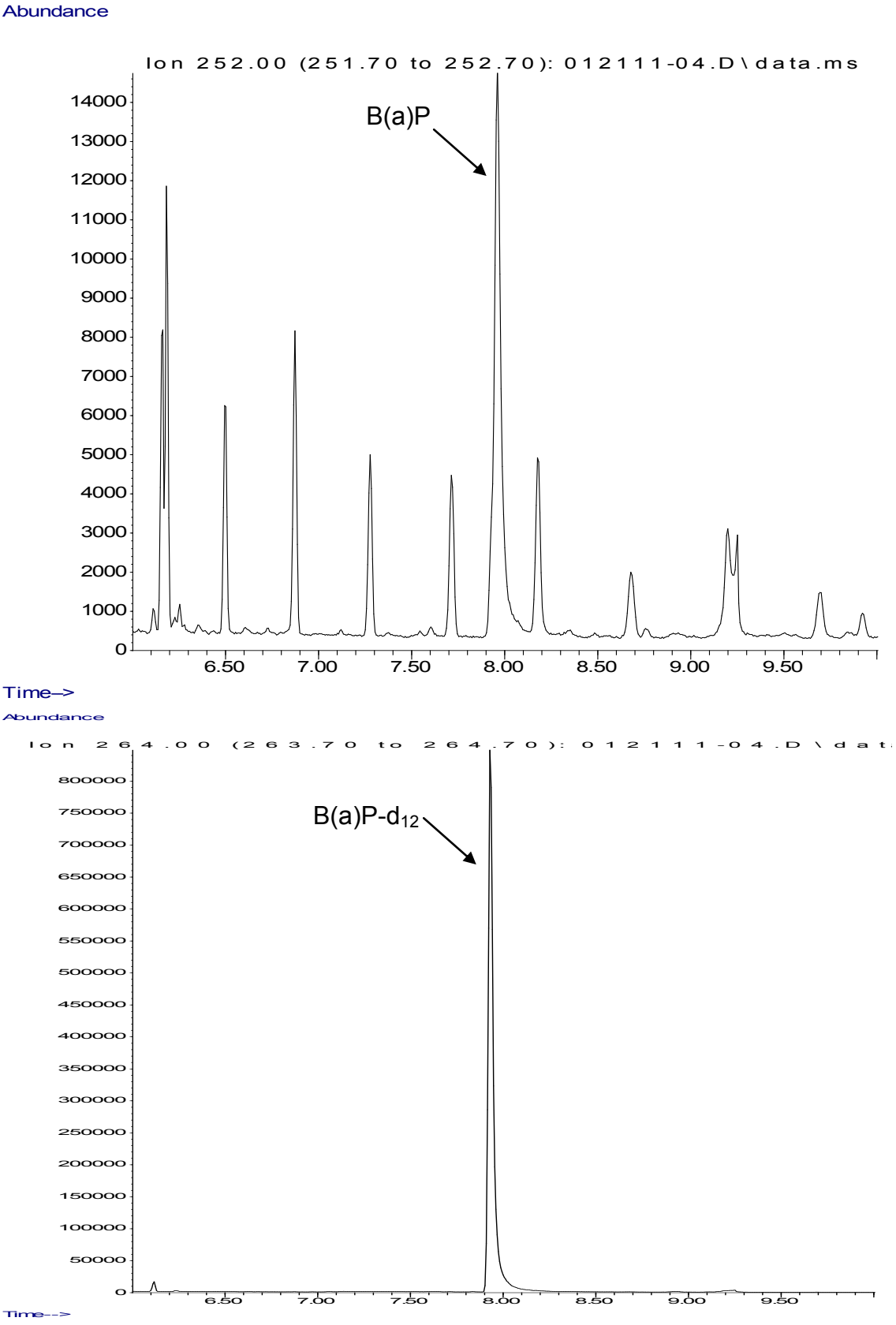
Abundance
Ion 252.00 (251.70 to 252.70): 012111-04.D\data.ms
B(a)P
14000
13000
12000
11000
10000
9000
8000
7000
6000
5000
4000
3000
2000
1000
0
6.50
7.00
7.50
8.00
8.50
9.00
9.50
Time-->
Abundance
Ion 264.00 (263.70 to 264.70): 012111-04.D\dat
B(a)P-d12
800000
750000
700000
650000
600000
550000
500000
450000
400000
350000
300000
250000
200000
150000
100000
50000
0
6.50
7.00
7.50
8.00
8.50
9.00
9.50
Time-->

Table 2.3

Accuracy and imprecision of B(a)P-fortified rat plasma.

	Target Concentration ng/mL	n[a]	Mean Concentration ng/mL	% of Target	%CV[b]
Intraassay					
	75	5	70.7	94.2	5.8
	1500	5	1450	96.4	5.2
	2750	4*	2600	94.4	20.0
Interassay					
	75	15	74.1	98.8	12.7
	1500	15	1415.2	94.3	4.7
	2750	12*	2588.3	94.1	18.0

	Target Concentration ng/mL	n[a]	Mean Concentration ng/mL	% of Target	%CV[b]
LLOQ					
	25	5	27.4	109.5.	10.4
ULOQ					
	3200	5	3184.3	99.5	3.0

[a] Number of quality control replicate samples used
[b] CV= coefficient of variation
*Sample(s) in set was considered an outlier and therefore not used in calculations (sample inadvertently double fortified with B(a)P)

The LLOQ and ULOQ were evaluated as described previously. The mean accuracy the LLOQ was 109.5% with a imprecision of 10.4%. The mean accuracy for the ULOQ was 99.5% with a imprecision of 3.0%.

Validation of analytical methods for BPT

Hair

Figure 2.5 shows chromatograms for an extracted 5 pg/mg BPT calibration standard (lowest standard in curve) and an extracted blank rat hair sample. The assay was determined to be linear from 5 to 40 pg/mg. The LLOQ and ULOQ were 5 and 40 pg/mg, respectively. The coefficient of variation (CV) for the intra- and interassay accuracy and imprecision were less than 10% (Table 2.4).

The stock and intermediate solutions for accuracy and imprecision for intra- and interassay samples were made by the quality control officer, or other Center for Human Toxicology personnel (since only one supplier existed for BPT at the time of this research). The stock and intermediate solutions used to make the calibration standards were prepared by Sarah Campbell. Accuracy and imprecision were calculated as previously described.

The intraassay accuracy and imprecision were determined as previously described. Analyte-free rat hair samples were fortified with BPT at 15, 25, and 30 pg/mg and analyzed within a single batch. The intraassay accuracy ranged from 95.4 - 98.0% of the theoretical target concentrations. The intraassay imprecision ranged from 5.9 - 9.7%.

The accuracy and imprecision for the interassay were also determined as

Figure 2.5 *Representative ion chromatograms from (A) extracted analyte-free (blank) rat hair sample and (B) an extracted BPT-fortified (5 pg/mg, LLOQ) rat hair sample.* Samples shown were also fortified with the internal standard ($^{13}C_6$)-BPT. Analyte retention time (RT) is on the x-axis and signal intensity on the y-axis. Derivatized BPT = 446 *m/z* and derivatized [$^{13}C_6$]-BPT = 452 *m/z*

A.

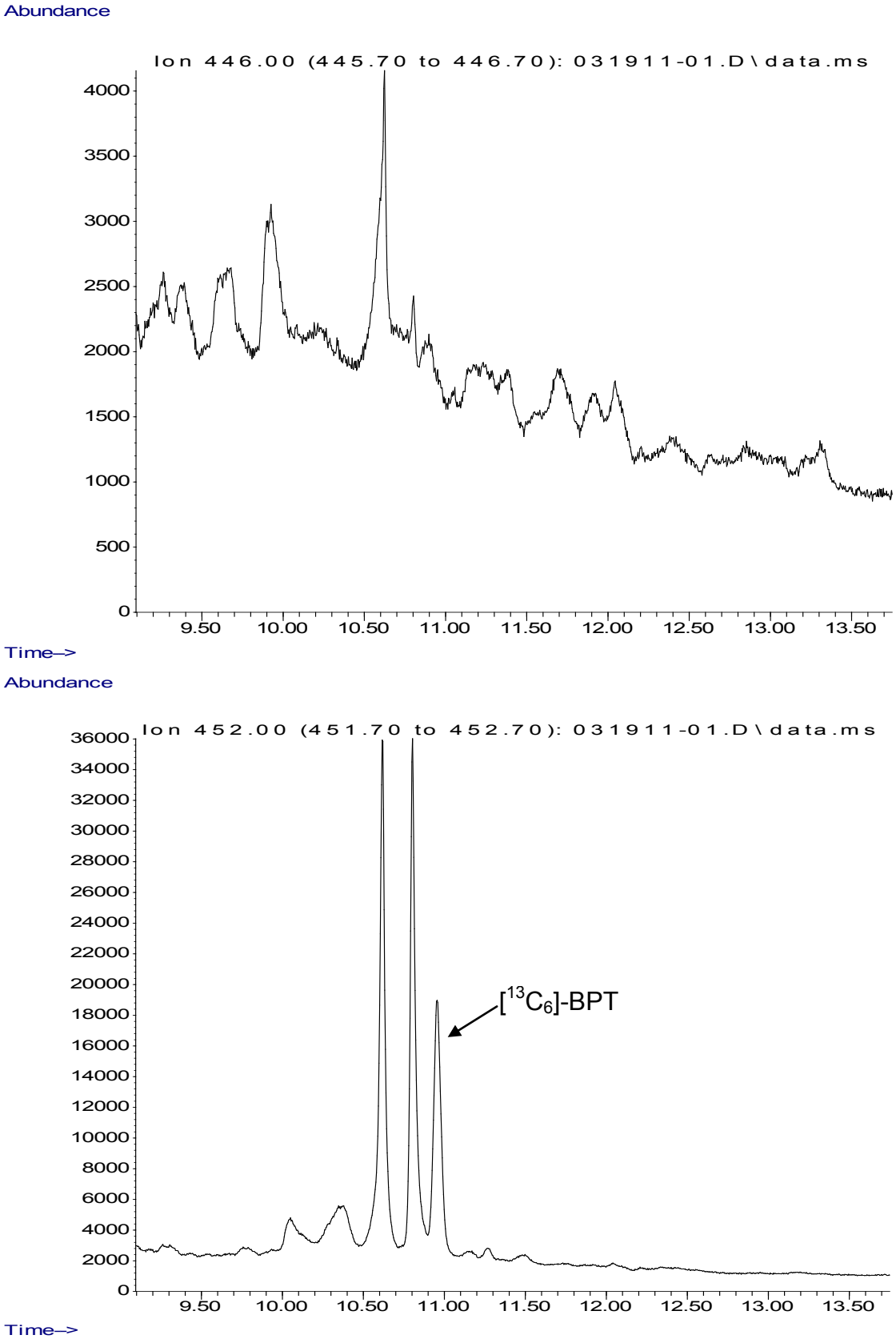
Abundance
Ion 446.00 (445.70 to 446.70): 031911-01.D\data.ms
4000
3500
3000
2500
2000
1500
1000
500
0
9.50
10.00
10.50
11.00
11.50
12.00
12.50
13.00
13.50
Time-->
Abundance
Ion 452.00 (451.70 to 452.70): 031911-01.D\data.ms
36000
34000
32000
30000
28000
26000
24000
22000
20000
18000
16000
14000
12000
10000
8000
6000
4000
2000
0
[13C6]-BPT
9.50
10.00
10.50
11.00
11.50
12.00
12.50
13.00
13.50
Time-->

B.

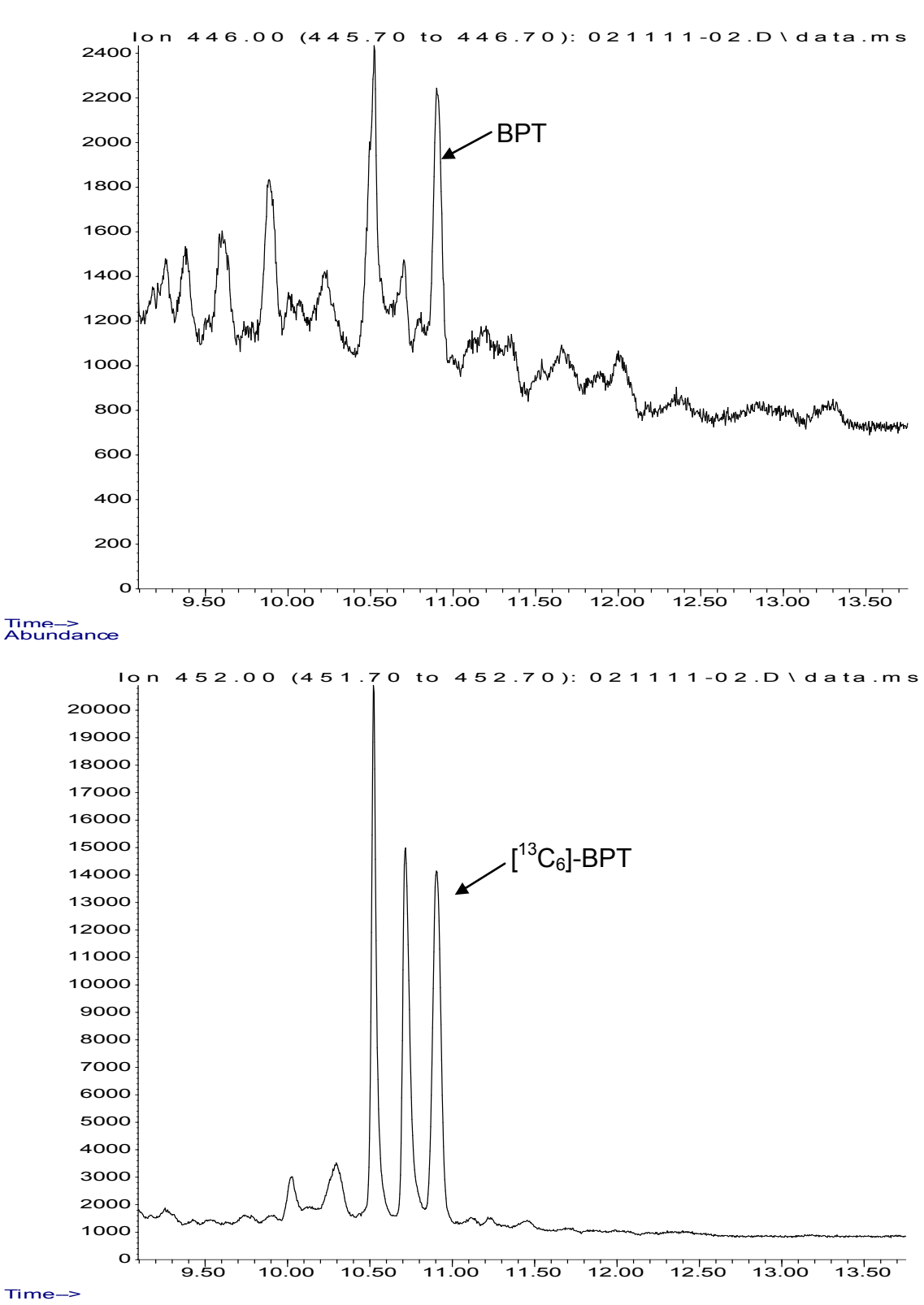
Abundance
Ion 446.00 (445.70 to 446.70): 021111-02.D\data.ms
BPT
Time-->
Abundance
Ion 452.00 (451.70 to 452.70): 021111-02.D\data.ms
[13C6]-BPT
Time-->

Table 2.4

Accuracy and imprecision of BPT-fortified rat hair.

	Target Concentration pg/mg	n[a]	Mean Concentration pg/mg	% of Target	%CV[b]
Intraassay					
	15	5	14.7	98.0	9.7
	25	5	24.3	97.2	6.3
	35	4*	33.4	95.4	5.9
Interassay					
	15	15	14.7	97.9	6.8
	25	15	24.0	95.9	5.2
	35	14*	34.0	97.3	4.7

	Target Concentration pg/mg	n[a]	Mean Concentration pg/mg	% of Target	%CV[b]
LLOQ					
	5	5	4.2	84.0	10.2
ULOQ					
	40	5	39.0	97.5	9.7

[a] Number of quality control replicate samples used
[b] CV= coefficient of variation
*Sample in set did not get injected

previously described. Analyte-free hair samples were fortified with BPT at 15, 25, 35 pg/mg and analyzed in three separate analytical batches on three separate days. The intraassay accuracy ranged from 95.9 - 97.9% of the theoretical target concentrations. The intraassay imprecision ranged from 4.7 - 6.8%.

The LLOQ and ULOQ were evaluated as described previously. The mean accuracy for the LLOQ was 84.0% with a imprecision of 10.2%. The mean accuracy for the ULOQ samples was 97.5% with a imprecision of 9.7%.

Hemoglobin

Figure 2.6 shows chromatograms for an extracted 2.5 pg/mg BPT calibration standard and an extracted blank rat Hb sample. The assay was determined to be linear from 2.5 to100 pg/mg. The LLOQ and ULOQ were 2.5 and 100 pg/mg, respectively. The coefficient of variation (CV) for the intra- and interassay accuracy and imprecision were less than 10% (Table 2.5).

The stock and intermediate solutions for accuracy and imprecision for intra- and interassay samples were made by the quality control, or other Center for Human Toxicology personnel (since only one supplier exists for BPT). The stock and intermediate solutions used to make the calibration standards were prepared by Sarah Campbell.

The intraassay accuracy and imprecision were determined as previously described. Analyte-free Hb samples were fortified with BPT at 7.5, 37.5, and 80 pg/mg and analyzed within a single batch. The intraassay accuracy ranged from 95.0 - 97.3% of the theoretical target concentrations. The intraassay

Figure 2.6 *Representative ion chromatograms from (A) extracted analyte-free (blank) rat Hb sample and (B) an extracted BPT-fortified (2.5 pg/mg, LLOQ) rat Hb sample.* Samples shown were also fortified with the internal standard ($^{13}C_6$)-BPT. Analyte retention time (RT) is on the x-axis and signal intensity on the y-axis. Derivatized BPT = 446 *m/z* and derivatized [$^{13}C_6$]-BPT = 452 *m/z*

A.

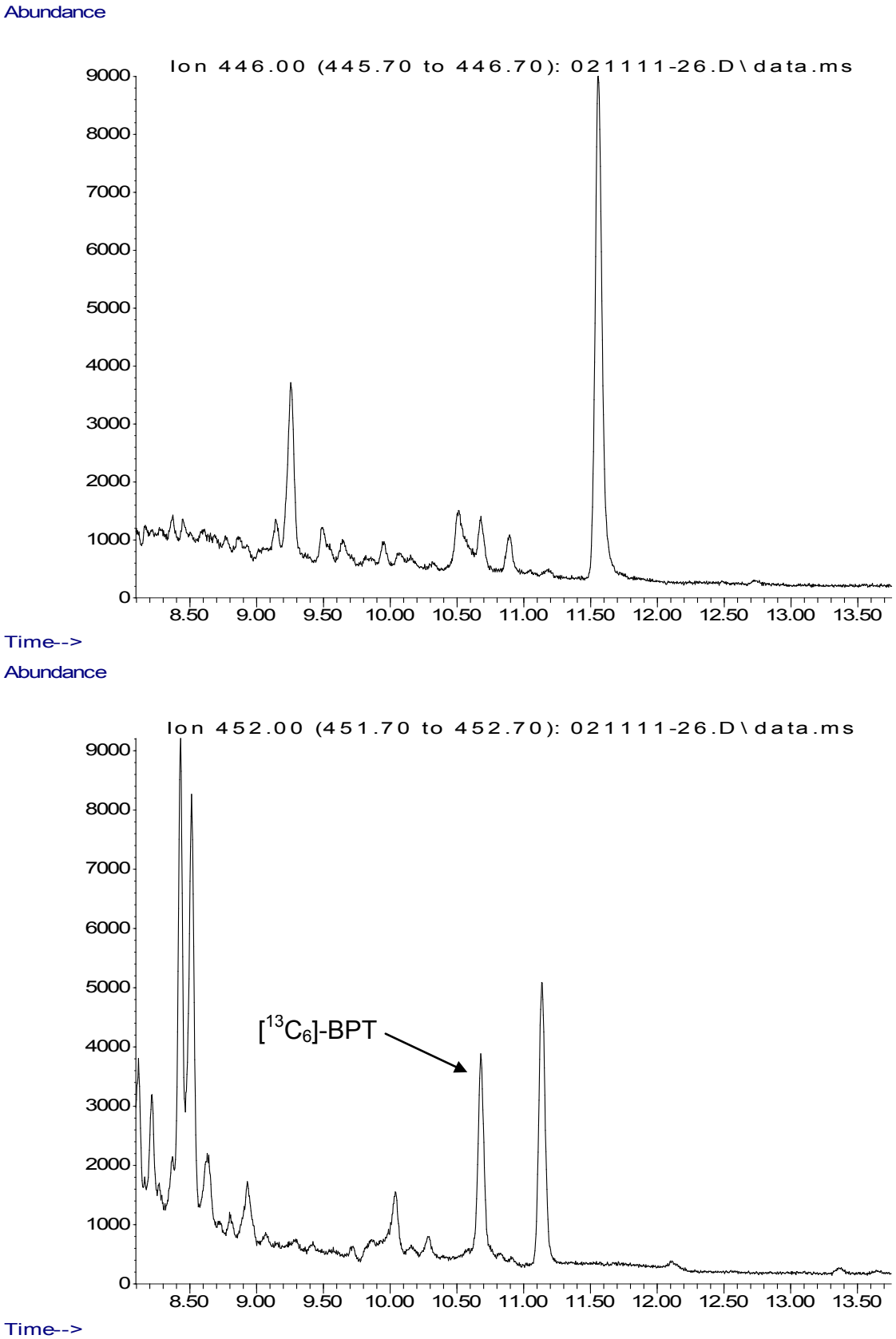
Abundance
Ion 446.00 (445.70 to 446.70): 021111-26.D\data.ms
9000
8000
7000
6000
5000
4000
3000
2000
1000
0
8.50
9.00
9.50
10.00
10.50
11.00
11.50
12.00
12.50
13.00
13.50
Time-->
Abundance
Ion 452.00 (451.70 to 452.70): 021111-26.D\data.ms
[13C6]-BPT
Time-->

B.

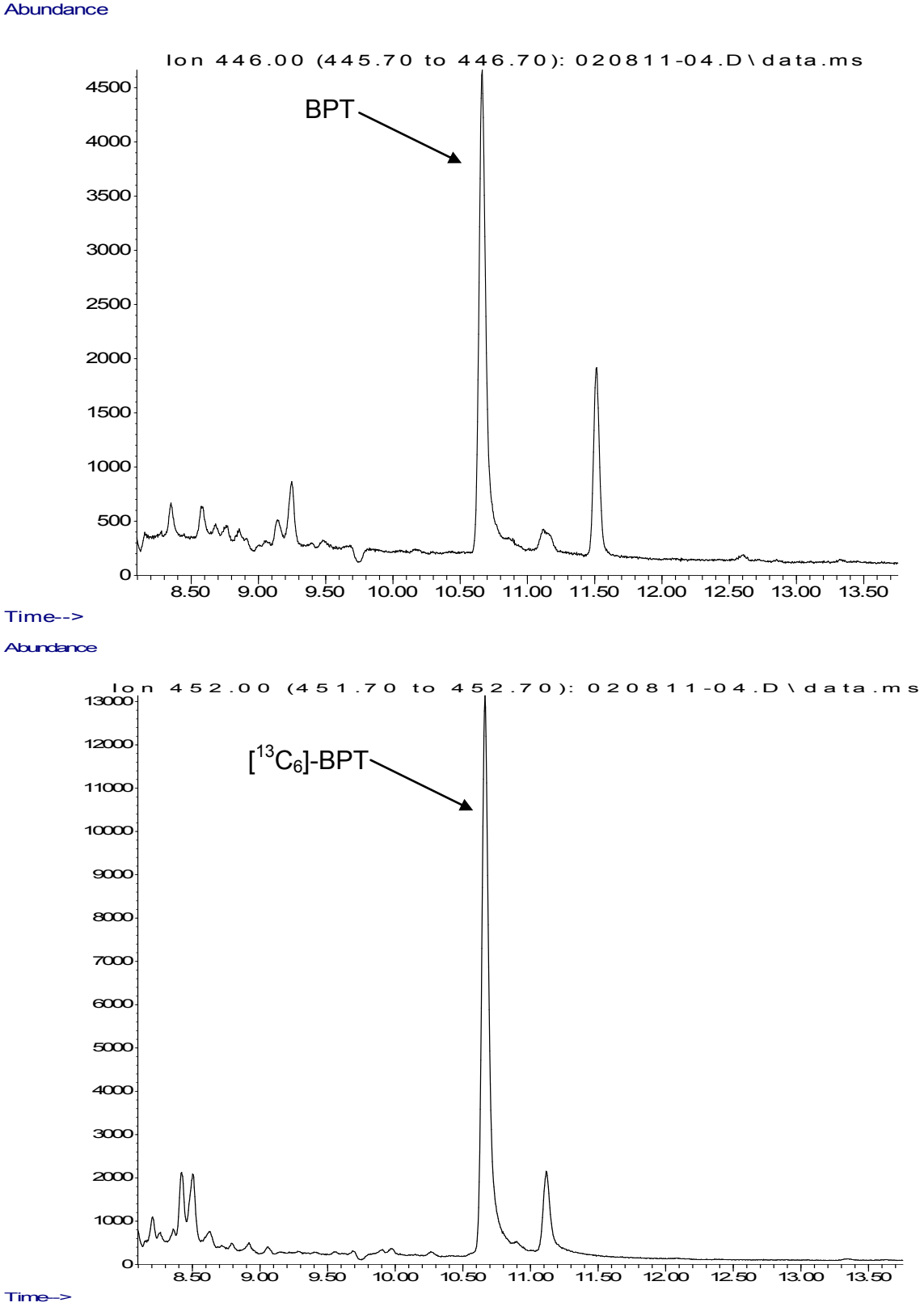
Abundance
Ion 446.00 (445.70 to 446.70): 020811-04.D\data.ms
BPT
4500
4000
3500
3000
2500
2000
1500
1000
500
0
8.50
9.00
9.50
10.00
10.50
11.00
11.50
12.00
12.50
13.00
13.50
Time-->
Abundance
Ion 452.00 (451.70 to 452.70): 020811-04.D\data.ms
[13C6]-BPT
13000
12000
11000
10000
9000
8000
7000
6000
5000
4000
3000
2000
1000
0
8.50
9.00
9.50
10.00
10.50
11.00
11.50
12.00
12.50
13.00
13.50
Time-->

Table 2.5

Accuracy and imprecision of BPT-fortified rat Hb.

	Target Concentration pg/mg	n[a]	Mean Concentration pg/mg	% of Target	%CV[b]
Intraassay					
	7.5	5	7.3	97.3	6.1
	37.5	5	35.6	95.0	0.9
	80.0	5	76.7	95.9	0.5
Interassay					
	7.5	15	7.3	97.9	5.5
	37.5	15	35.5	94.6	1.5
	80.0	13*	76.9	96.1	1.0

	Target Concentration pg/mg	n[a]	Mean Concentration pg/mg	% of Target	%CV[b]
LLOQ					
	2.5	4**	3.0	121.2	20.0
ULOQ					
	100.0	5	98.7	98.7	2.9

[a] Number of quality control replicate samples used
[b] CV= coefficient of variation
*Two samples in group did not get injected
**Sample in group was considered an outlier due to poor chromatography and not used in calculation

imprecision ranged from 0.5 - 6.1%.

The accuracy and imprecision for the interassay were determined as previously described. Analyte-free Hb samples were fortified with BPT at 7.5, 37.5, 80 pg/mg and analyzed in three separate analytical batches on three separate days. The intraassay accuracy ranged from 94.6 - 97.9% of the theoretical target concentrations. The intraassay imprecision ranged from 1.0 - 5.5%.

The LLOQ and ULOQ were evaluated as described previously. The mean accuracy for the LLOQ was 121.2% with a imprecision of 20.0%. The mean accuracy for the ULOQ was 98.7% with a imprecision of 2.9%.

Results from animal experiments

Incorporation of B(a)P into rat hair

Baseline (Day 0) rat hair samples, as well as Day 14 hair samples from control rats, both analyzed using the developed methods, were below the LLOQ for B(a)P (data not shown). Figure 2.7 shows the mean $\pm$ SEM (standard error of the mean) concentrations for B(a)P detected in pigmented hair from rat administered 40 mg/kg, 80mg/kg, or 160 mg/kg B(a)P.

The concentration of B(a)P detected in rat hair at Day 14 increases in a dose-dependent manner, ranging from nondetected to 3.3 ng/mg. Specifically, hair concentrations of B(a)P were 0.10 $\pm$ 0.06 ng/mg for 40 mg/kg dosed rats, 0.7 $\pm$ 0.2 ng/mg for the 80 mg/kg dosed rats, and 1.1 $\pm$ 0.3 ng/mg for 160 mg/kg dosed rats. We found no significant difference in the concentration of B(a)P in

Figure 2.7 *Concentrations of B(a)P in Rat Hair.* A) *Hair concentrations of B(a)P in the hair of B(a)P dosed rats.* B(a)P concentrations in rat hair increase in a dose-dependent manner . B) *B(a)P concentrations in pigmented and nonpigmented rat hair from 160 mg/kg dosed rats.* B(a)P concentrations in pigmented and nonpigmented rat hair do not statistically differ. Error bars represent the mean ± SEM.

A.

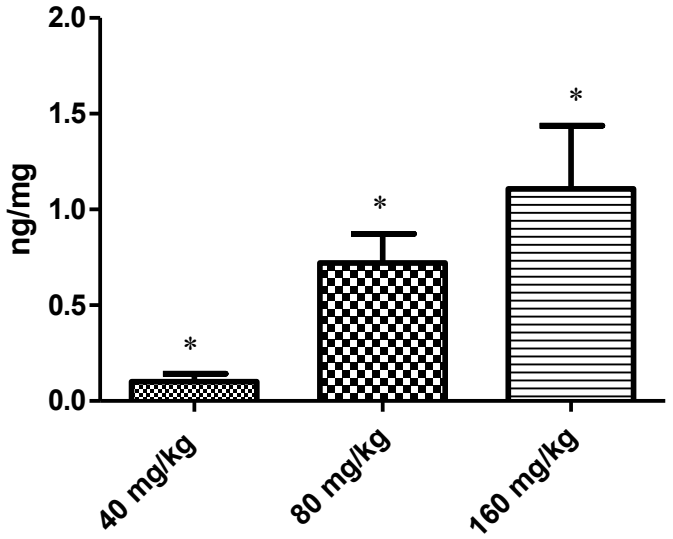
2.0
1.5
1.0
0.5
0.0
ng/mg
*
*
*
40 mg/kg
80 mg/kg
160 mg/kg

B.

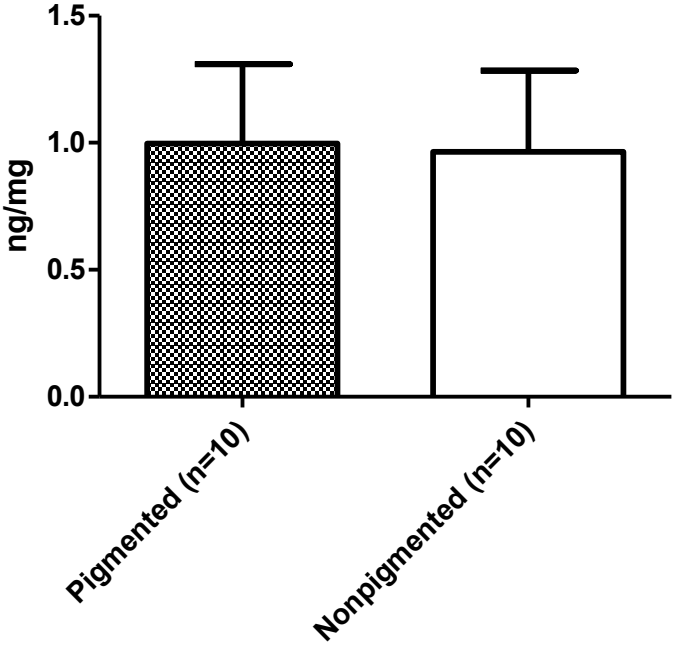
1.5
1.0
0.5
0.0
ng/mg
Pigmented (n=10)
Nonpigmented (n=10)

pigmented and nonpigmented rat hair from animals dosed at 160 mg/kg (Figure 2.7). At this dose the mean (± SEM) for B(a)P concentration for pigmented hair from 160 mg/kg dosed animals was 1.0 ± 0.3 ng/mg and 1.0 ± 0.3 ng/mg in nonpigmented.

Incorporation of BPT into rat hair

Baseline (Day 0) rat hair samples, as well as Day 14 hair samples from control rats, were all below the LLOQ for BPT (data not shown). Figure 2.8 shows the mean ± SEM (standard error of the mean) concentrations for BPT released from pigmented rat hair after the administration of 40 mg/kg, 80mg/kg, and 160 mg/kg B(a)P. The concentration of BPT detected in rat hair increases in a dose- dependent manner; The measured concentrations of BPT in the hair of B(a)P dosed rats at Day 14 ranged from 3.6 to 62.6 pg/mg. Hair concentrations of BPT released were 7.3 ± 0.6 pg/mg for 40 mg/kg dosed rats, 9.9 ± 0.7 pg/mg for the 80 mg/kg dosed rats, and 42.1 ± 4.1 pg/mg for 160 mg/kg dosed rats. There was a significant difference in the concentration of BPT released from pigmented and nonpigmented rat hair after administration of 160 mg/kg B(a)P (Figure 2.8). The mean (± SEM) for BPT concentrations released from hair from 160 mg/kg B(a)P-dosed animals was 41.5 ± 0.3 pg/mg and 26.3 ± 0.3 pg/mg in pigmented and nonpigmented hair, respectively.

Positive control results

BPDE-Hb adducts were selected as the positive control for these experiments, since they have been extensively studied and previously

Figure 2.8 *Concentrations of BPT in Rat Hair.* A) *BPT released from hair of B(a)P dosed rats.* BPT concentrations released from rat hair increase in a dose-dependent manner. However, results from 40 mg/kg and 80 mg/kg are not statistically different from each other, whereas results between 80 mg/kg and 160 mg/kg, and 40 mg/kg and 160 mg/kg statistically differ. B) *BPT released from pigmented and nonpigmented from 160mg/kg dosed rats.* BPT released from pigmented and nonpigmented are statistically different. Error bars represent the mean $\pm$ SEM.

A.

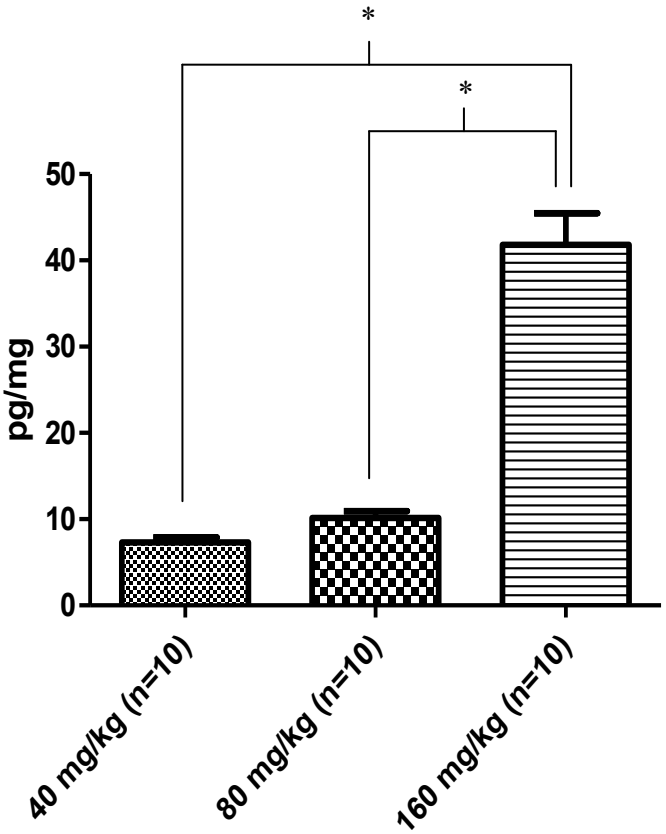
*
*
50
40
30
20
10
0
pg/mg
40 mg/kg (n=10)
80 mg/kg (n=10)
160 mg/kg (n=10)

B.

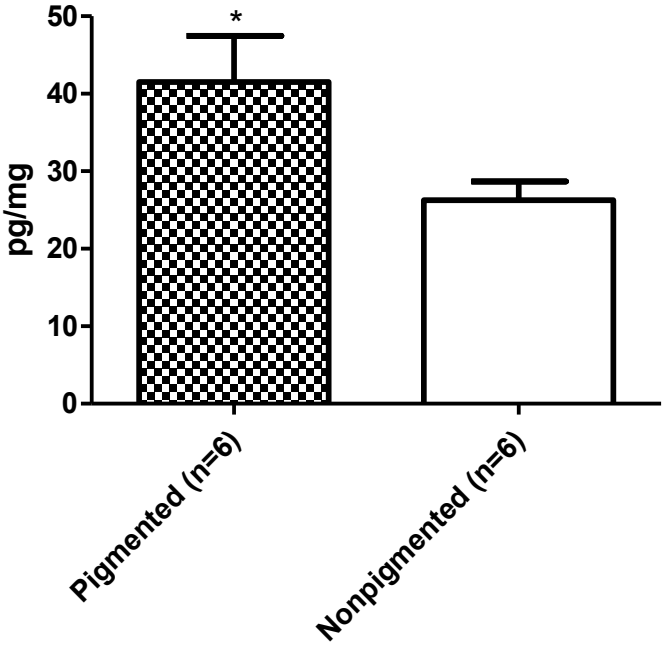
*
50
40
30
20
10
0
pg/mg
Pigmented (n=6)
Nonpigmented (n=6)

characterized as a biomarker of B(a)P exposure. These adducts are associated with toxicity, and account for cumulative exposures over the life-span of an erythrocyte (120 days). BPDE-protein adducts have been studied in blood proteins (e.g., Hb, albumin) [60, 121-124] and BPDE-DNA adducts in several different tissues [125-129]. While DNA adducts have provided useful information regarding carcinogenicity, major limitations exist: 1) BPDE-DNA adducts are subject to enzymatic repair by excision repair enzymes; 2) There is a high frequency (as much as 70%) of BPDE-DNA samples in which no adducts are found. To combat these issues, we chose the BPDE-Hb adduct, rather than the DNA adduct, as it is much more abundant and not subject to enzymatic repair. BPDE-Hb adducts are commonly used as surrogates for DNA adducts in order to assess diseases progression and cancer risk [60] .

As expected, we saw a dose-dependent increase in the BPDE-Hb adduct (measured by BPT released) (Figure 2.9) from the blood of B(a)P dosed rats. Hb samples from control rats were at or below the LLOQ for BPT, with the exception of one rat at about three times the LLOQ. However, the result for this rat was still below the concentrations observed in our lowest B(a)P dosed group.

The major source for B(a)P in nonsmokers is via the ingestion and inhalation of B(a)P from foods (especially charbroiled foods), water, and air [76]. Rats from this study may also be exposed to B(a)P from similar sources. We tested the corn oil used for making the dosing solutions and did not find detectable levels of B(a)P (data not shown). BPDE-Hb adducts can be detected in humans who are nonsmokers, so our findings of BPDE-Hb adducts in

Figure 2.9 *Positive control results for B(a)P dosed rats.* A) *BPDE-Hb adduct concentrations from B(a)P dosed rats.* BPDE-Hb adducts increase in a dose-dependent manner. B) *Spearman correlation test results for the comparison of B(a)P in rat hair and BPDE-Hb adducts.* Each dot represents a single rat. There is a significant correlation between concentrations of B(a)P detected in hair and our positive control. (Data from rats that were nondetected for B(a)P in hair are not included.) C) *Spearman correlation test results for the comparison of BPT released from rat hair and BPDE-Hb adducts.* There is a significant correlation between BPT released from hair and our positive control. D) *Spearman correlation test results for the comparison of B(a)P and BPT released from rat hair.* There is a significant correlation between B(a)P and BPT released from rat hair. (Data from rats that were nondetected for B(a)P in hair are not included.) Error bars represent $\pm$ SEM.

A.

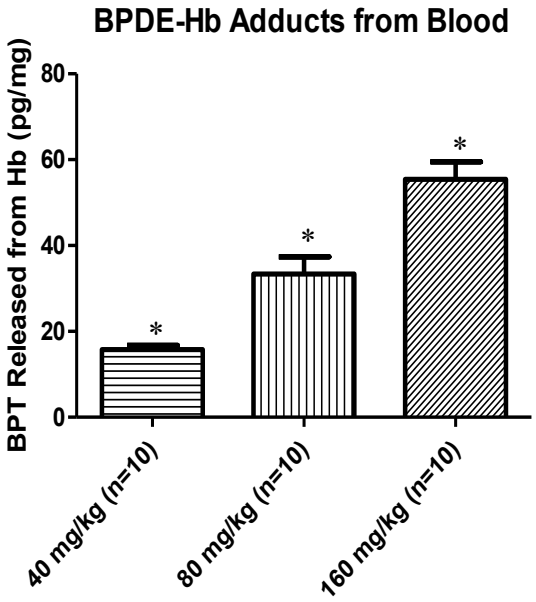

B.

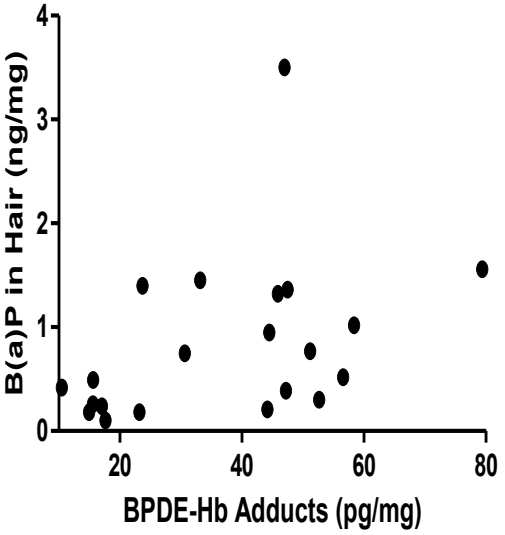

r_S=0.52
P=0.0147

C.

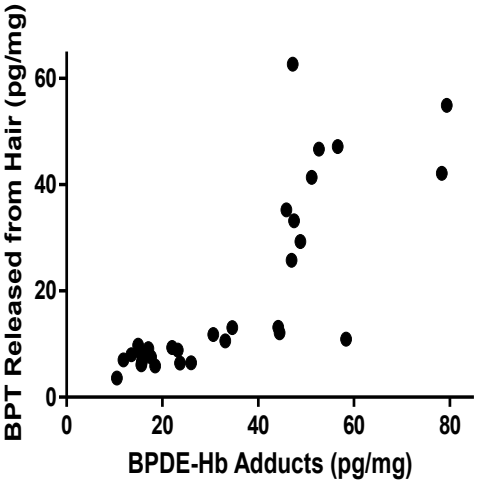

r_S =0.84
P<0.0001

D.

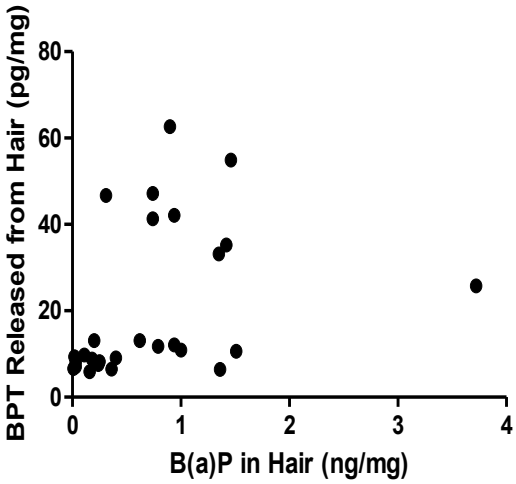

r_S =0.53
P=0.0046

unexposed control rats is not unusual. Figure 2.9 A shows the mean ± SEM concentrations for BPT released from the Hb of 40 mg/kg, 80mg/kg, and 160 mg/kg dosed rats. The measured concentrations of BPDE-Hb adducts in the B(a)P dosed rats ranged from 11.9 to 79.4 pg/mg. The mean ± SEM BPDE-Hb adduct concentrations were 15.7. ± 1.1 pg/mg for 40 mg/kg dosed rats, 33.4 ± 4.0 pg/mg for the 80 mg/kg dosed rats, and 55.4 ± 4.0 pg/mg for 160 mg/kg dosed rats.

We compared the concentrations of B(a)P and BPT released from rat hair with the results from our positive control (BPDE-Hb adducts) to determine whether there was a positive association between the measures (Figure 2.9, panels B and C). There was a significant correlation between concentrations of B(a)P detected in hair and the presence of BPDE-Hb adducts from blood (our positive control, $p<0.01$). There was a more robust significant correlation between BPT released from hair and our positive control ($p<0.0001$). We also determined there was a significant correlation between concentrations of B(a)P in rat hair and BPT released from rat hair (Figure 2.9, panel D).

B(a)P in lung tissues of dosed rats

The measured concentration of B(a)P in lung tissue from corn oil-treated control rats, were all below the LLOQ (data not shown). Figure 2.10 shows the mean ± SEM concentrations for B(a)P detected in lung tissue collected on Day 14 from 40 mg/kg, 80mg/kg, and 160 mg/kg B(a)P dosed rats. The results represented in Figure 2.10 are therefore due to the retention of B(a)P in the lung (all dosing in these animals was discontinued seven days prior to the sacrifice

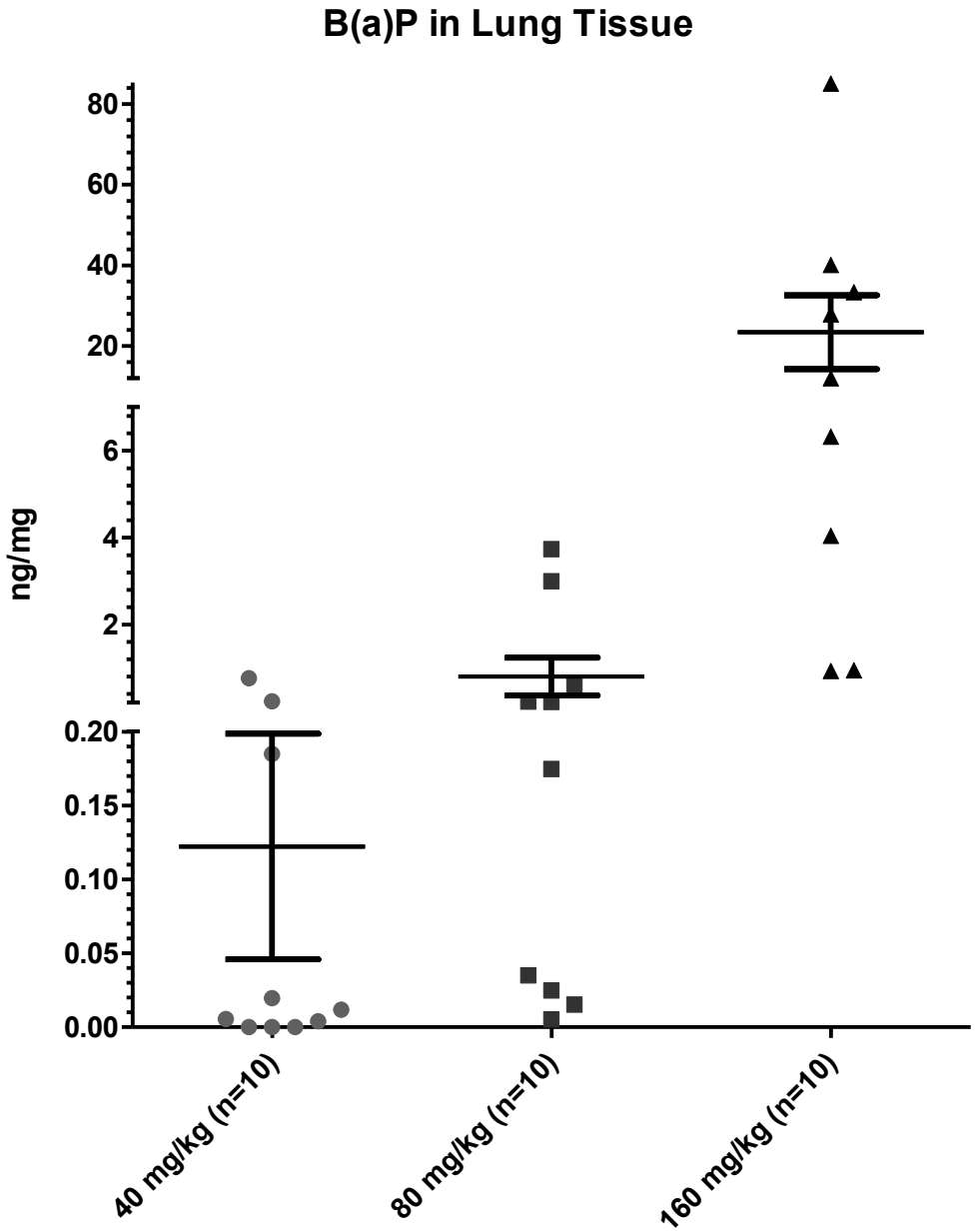

Figure 2.10 *B(a)P remaining in rat lung tissues at Day14.* The concentration of B(a)P detected in rat lung tissues increases in a dose-dependent manner, with a sharp increase in the concentration between the 80 mg/kg and 160 mg/kg doses animals. Solid horizontal bars represent the mean and the vertical error bars represent the ± SEM.

increases in a dose-dependent manner, with a sharp increase in the day). The mean concentration of B(a)P detected in rat lung tissues at Day 14 concentration between the 80 mg/kg and 160 mg/kg dosed animals. Specifically, the measured concentrations of B(a)P remaining in the lung ranged from nondetected to 85.1 ng/mg. Then mean ± SEM lung tissue concentrations of B(a)P were 0.1 ± 0.1 ng/mg for 40 mg/kg dosed rats, 0.8 ± 0.4 ng/mg for the 80 mg/kg dosed rats, and 23.4. ± 8.4 ng/mg for 160 mg/kg dosed rats, respectively.

B(a)P in the plasma of dosed rats

The measured concentration of B(a)P in plasma from corn oil control treated rats, were all below the LLOQ (data not shown). Figure 2.11 shows the mean ± SEM concentrations for B(a)P detected in plasma from 40 mg/kg, 80mg/kg, and 160 mg/kg dosed rats. The results in Figure 2.11 represent circulating B(a)P concentrations after dosing had been discontinued seven days earlier. The concentrations of circulating B(a)P at Day 14 increases in a dose-dependent manner, with a sharp increase in the concentration between the 80 mg/kg and 160 mg/kg dosed animals (as seen in B(a)P concentrations in the lung tissues, Figure 2.10). The measured concentrations of B(a)P remaining in the plasma ranged from nondetected to 33.2 ug/mL. The mean ± SEM plasma concentrations of B(a)P were 7.0 ± 5.3 ng/mL for 40 mg/kg dosed rats, 106.3 ± 53.1 ng/mL for the 80 mg/kg dosed rats, and 6926 ± 3400 ng/mL for 160 mg/kg dosed rats. There was no correlation between concentrations of B(a)P circulating the plasma at Day 14 and hair concentrations of B(a)P or BPT (data not shown).

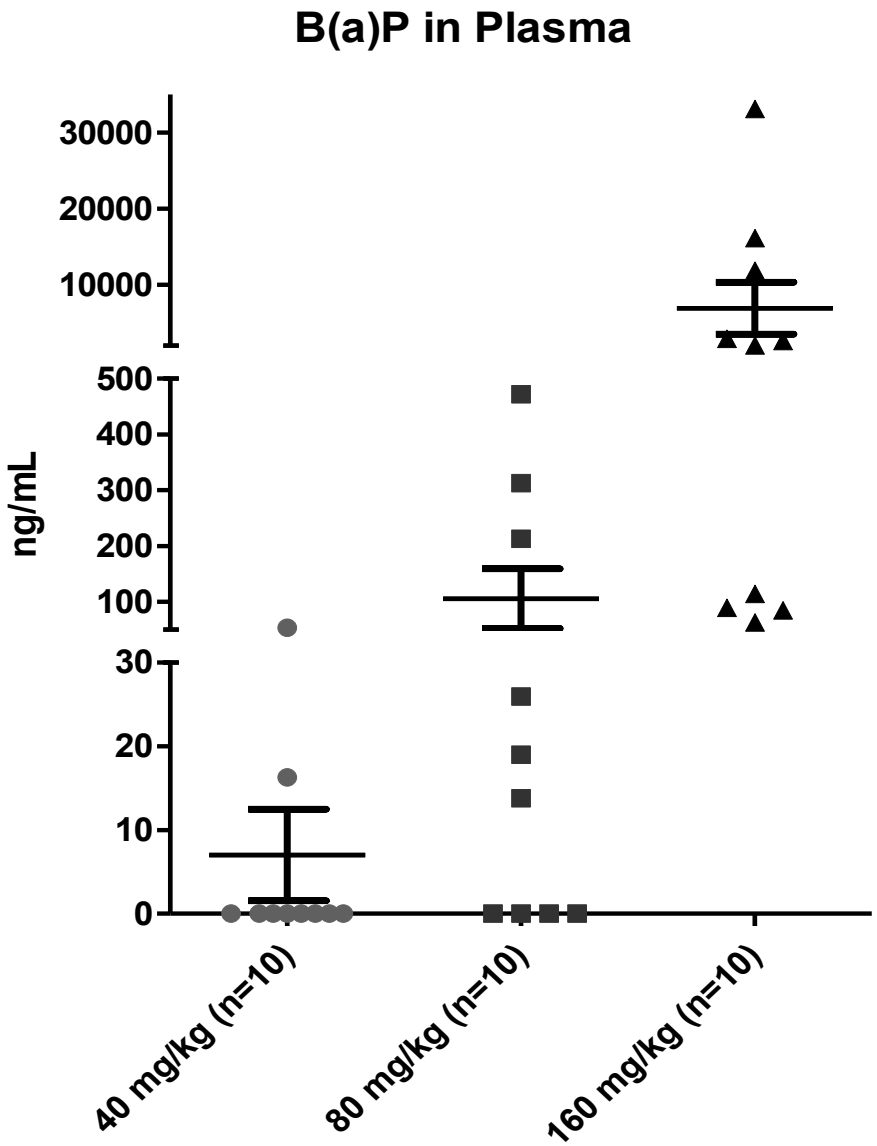

Figure 2.11 *B(a)P concentrations circulating in rat plasma at Day 14.* The circulating concentrations of B(a)P detected in rat plasma increases in a dose-dependent manner, with a sharp increase in the concentration between the 80 mg/kg and 160 mg/kg dosed animals (as seen in the rat lung tissue). Solid horizontal bars represent the mean and the vertical error bars represent the $\pm$ SEM.

There was a significant correlation between concentrations of B(a)P remaining in lung tissue and circulating B(a)P concentrations in the plasma (Figure 2.12).

Wash experiment on rat hair

The results from an initial wash experiment with B(a)P incorporated in rat hair using a shampoo solution and an organic solvent (dicloromethane) are shown in Figure 2.13. The mean ± SEM concentration for B(a)P in the unwashed hair hair sample was 0.49 ng/mg. In contrast, the mean ± SEM concentration for B(a)P in the hair washed with either shampoo or dichlormethane were 0.10 pg/mg and 0.13 pg/mg, respectively. Since performing a wash greatly reduced the concentration of B(a)P several fold from what had been incorporated into the rat hair shaft, we chose not to perform washes on any of the samples from this study.

Discussion

The described GC/MS methods in this chapter are sensitive and specific, and were developed 1) to detect B(a)P in hair, lung, and plasma, 2) BPDE-induced adducts from the hair, and 3) hemoglobin of B(a)P dosed rats. Using these methods, we determined that B(a)P and BPDE-protein adducts can be detected in rat hair and are incorporated into hair in a dose-dependent manner. To our knowledge, the detection of these compounds in rat hair is a novel finding. Whereas B(a)P concentrations in rat hair do not statistically differ between pigmented vs. nonpigmented rat hair, BPDE-protein adduct concentrations in pigmented hair are about 1.6 times greater than nonpigmented hair. Both B(a)P

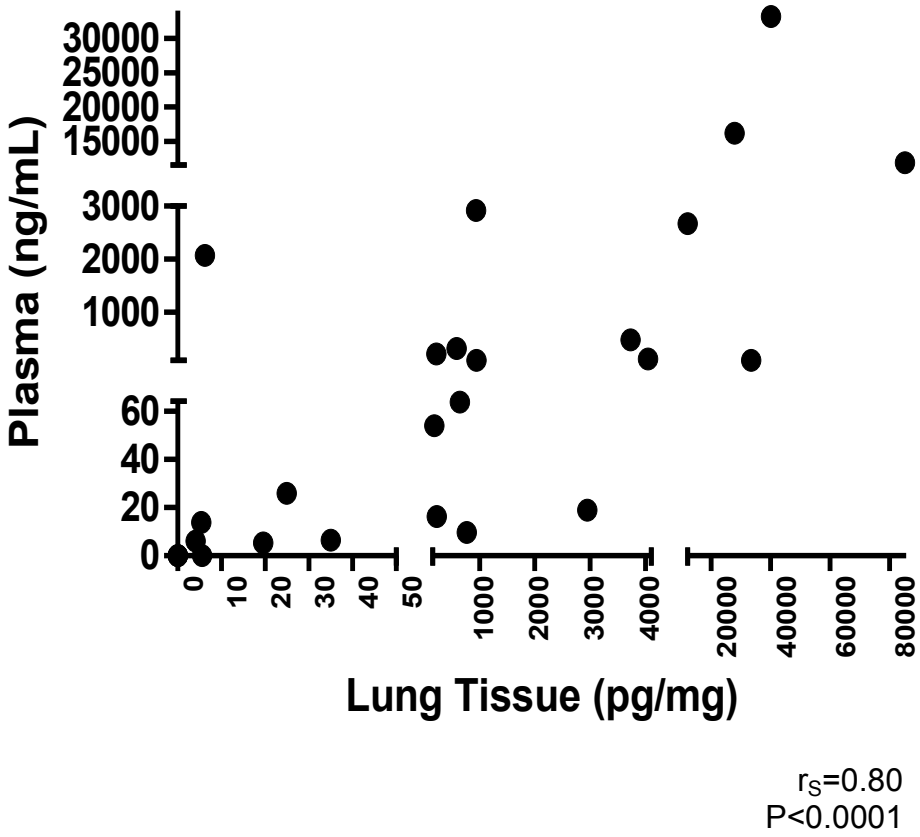

Figure 2.12 *Spearman correlation test results for the comparison of B(a)P in plasma and lung at Day 14.* Each dot represents a single rat. There is a significant correlation between concentrations of B(a)P in the plasma and lung. (Data from rats that were nondetected for B(a)P in plasma and lung were not included.)

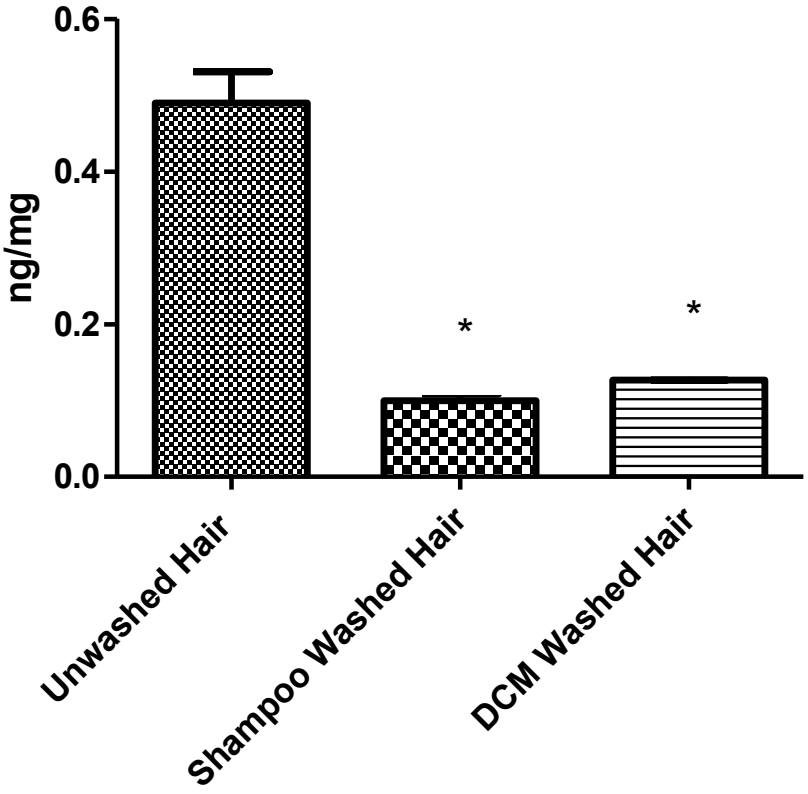

Figure 2.13 *Results from the washing of B(a)P incorporated rat hair.* These results demonstrate that washing hair with a 10% aqueous shampoo wash solution and dichloromethane (DCM) greatly reduce the detectable amount of B(a)P in the hair of dosed rats.

and BPDE-protein adduct hair concentrations correlate to concentrations of the positive control (the extensively studied and well-characterized BPDE-Hb adduct) using a Spearman's correlation test. This demonstrates that these novel hair biomarkers may provide a useful tool to monitor B(a)P exposure in many different settings. The studies presented in this chapter were used to support our research on the incorporation of B(a)P and BPDE-protein adducts into human hair (Chapter 4), and their use as biomarkers of B(a)P exposure in smokers and nonsmokers.

Possible mechanisms of B(a)P and BPDE-protein adduct incorporation in hair

No published data have previously been reported for the identification of B(a)P or BPDE-protein adducts in rat hair. The actual mechanisms whereby these novel biomarkers incorporate into hair remains to be elucidated, and although it was not the focus of this dissertational research, the results from our rat studies support a *passive diffusion model* of incorporation (detailed in the *Introduction* of this chapter). In conjunction this model, we hypothesize that B(a)P passively diffuses from the bloodstream at the base of the follicle to the hair forming cells, and then becomes incorporated into the growing hair shaft. Furthermore, we also hypothesized the electrophilic reactive intermediate BPDE is formed by the metabolism of B(a)P in the follicular cells of the hair bulb by CYP450's and epoxide hydrolase enzymes. (The metabolism of B(a)P in hair follicles has been previously described [130-132]). BPDE would then react to form adducts with surrounding proteins. Possible binding sites for BPDE could

involve the formation of a covalent bond between the epoxide of BPDE and the thiol group on the very abundant cysteine residue in hair. There is strong evidence that BPDE binds to cysteine residues in intracellular proteins, and thiol groups in general are known to covalently bind with epoxides [133]. Morrison *et al*. have demonstrated with *in vitro* studies that depletion of thiol groups in hepatocytes leads to an increase in BPDE-protein adduct concentrations [134]. Several studies have also addressed that the nucleophile glutathione, which contains a cysteine and is known to detoxify BPDE, plays a critical role in preventing the carcinogenesis of BPDE [135]. Also, it has been demonstrated that N-acetyl cysteine reduces, or eliminates, BPDE-adducts in the lung [136]. BPDE and reaction with acidic amino acids by ester linkage is also supported since upon proteolysis of adducted proteins tetrols are released. This has been previously described with BPDE's reaction mainly by alkylation of the amino acid aspartate number 47 (on its α side chain) in human Hb [98]. Other possible amino acid side chains in hair proteins that may participate in BPDE binding include: amines, carboxyaminde, carboxyl guandidine, hydroxyl, imidazole, indole, phenol, and sulfhydryl groups.

In the *deep compartment* and *multicompartment models*, other routes of entry contribute to xenobiotic incorporation into hair. These routes include exposure through sweat and sebum excretions, as well as from external environmental contaminants. However, since rats only have sweat glands on the digital, palmar, and plantar pads of their feet, sweat is not a likely route of B(a)P and BPDE-protein adduct incorporation in the hair from the back of the rat. In

contrast, secretions of these compounds via sebum cannot be ruled out as a possible route of incorporation. Like the hair follicle, sebaceous glands are nourished by a dense network of capillaries though which xenobiotic can diffuse. Due to its highly lipophilic nature, B(a)P would likely accumulate in the sebum excreted from these glands. Sebaceous glands in the rat have CYP450s and other enzymes that have also been demonstrated to metabolize B(a)P [137]. Whether BPDE-protein adducts are formed in the sebaceous gland and then discharged through its canal in connection with the hair follicle, or whether BPDE itself is transferred via the canal to react with proteins of the growing hair shaft remains to be elucidated.

For the melainin-binding model, pigment content is considered an important feature in the incorporation of xenobiotics into hair. Since certain drugs and xenobiotics have high affinities for melanin, the amount of melanin present in hair would have effects on the concentration found in different colors of hair. Since B(a)P is known to bind to melanin *in vitro* (including melanin in hair follicles) [44, 45, 138], we hypothesized that B(a)P would be incorporated to a greater extent in pigmented vs. nonpigmented rat hair. This, however, was not the case for the neutral B(a)P compound, but may be playing a role in the incorporation of BPDE-protein adducts. Concentrations of BPDE-protein adducts were about 1.6 times higher in pigmented vs. nonpigmented rat hair. The electrophilicity of BPDE and/or the functional groups present (i.e. epoxide and hydroxyl) on the BPDE molecule are most likely are contributing to the increased incorporation into pigmented hair.

As previously mentioned, there is general concern over hair analyses and confounding effects of external contamination, especially with smoked drugs. To limit potential sources of contamination in the present studies, rats were individually housed (to prevent social grooming) in hanging wire cages (to prevent contamination of the coat from bedding) and hair was only collected from areas where the animal would not be able to self-groom. Furthermore, since BPDE and BPT are metabolites of B(a)P and only synthesized in the body, contamination of hair with these compounds was unlikely to contribute to the findings in our studies. We did perform an initial wash experiment with B(a)P incorporated rat hair using dichloromethane and a 10% aqueous shampoo solution (results shown in Figure 2.13). Since performing a wash greatly reduced the concentration of B(a)P several fold from what had been incorporated into the rat hair shaft, we chose not to perform washes on any of the samples.

Limitations of analysis for BPDE-protein adducts in hair

One caveat of measuring BPT released from hair, as evidence of a BPDE bound protein adduct, is that the analysis may also be measuring BPT as a metabolite from the further metabolism of BPDE by epoxide hydrolase and/or water. Additionally, since enzymatic hydrolysis was used during the sample preparation, it is also possible that BPT may be released from BPDE conjugates such as BPDE-glutathione, BPDE-glucuronide and BPDE-sulfate conjugates. Given that hair is a solid structure comprised mostly of proteins, it would be difficult to isolate th intact protein (as done with Hb) without denaturing the

proteins themselves. Further research is needed to elucidate the percentage of free BPT vs. BPT released directly from BPDE-protein adducts in hair.

Positive correlation of hair biomarkers and BPDE-Hb adducts

We compared the concentrations of B(a)P and BPDE-protein adducts from rat hair with the results from our positive control (BPDE-Hb adducts) to determine whether there was a positive association between these measures (Figure 2.9, panel B). There was a significant correlation between the concentrations of B(a)P detected in the hair and our positive control ($p<0.0147$). There was an even more robust correlation between BPT released from hair and our positive control ($p<0.0001$). Since the BPDE-Hb adduct has been thoroughly investigated and characterized [121-123, 139-141], and demonstrates that known adduct formation has occurred, our novel hair biomarkers presented in this chapter show great promise for assessing toxic B(a)P exposure.

Plasma and lung B(a)P concentrations

These studies did not find a correlation between concentrations of B(a)P or BPDE-protein adducts in hair and the concentrations of B(a)P remaining in the lung or plasma at Day 14. However, hair concentrations are considered a cumulative marker of exposure, whereas concentrations in the plasma or lung would represent an acute exposure, so the lack of correlation was not completely unexpected. The concentrations of B(a)P that remained in the lung, and that were still in the circulation at Day 14, were high. These data illustrate the rat

lung's inability to clear the high doses of B(a)P that were given and the high volume of distribution of B(a)P itself. The accumulation of B(a)P in rat lung has been previously described even after lower doses [74, 75, 142], and may be due to the substantially lower abundance of CYP450s in the lung to metabolize B(a)P in comparison with the liver [142]. Lung-mediated elimination of xenobiotic compounds presents toxicological and pharmacological important aspects, and the accumulation of B(a)P we observed in the lungs may be closely related to its toxic effects. A future goal would be to elucidate whether concentrations of BPDE-protein adducts in the hair have a relationship to concentrations of BPDE-protein adducts formed in the lung of our B(a)P dosed rats.

In conclusion, the results presented in this chapter show great promise for biomonitoring of B(a)P exposure by means of these novel hair biomarkers. While the incorporation of B(a)P and BPDE-protein adducts may occur through multiple different mechanisms, and at various periods during hair growth, more research is needed to elucidate the mechanisms surrounding B(a)P and BPDE-protein adduct incorporation into hair.

CHAPTER 3

HISTOPATHOLOGY OF LUNG TISSUE FROM RATS EXPOSED TO BENZO(A)PYRENE

Introduction

Route of B(a)P administration

The pattern of pulmonary injury varies for inhaled toxicants compared to systemically and i.p administered toxicants. We chose to administer B(a)P by i.p. injection because it is simple, easily controlled, and provides an exact known dosage. It has also been demonstrated that i.p. administration of B(a)P is effective at inducing lung toxicities such as tumors and inflammation [143-146]. We did not use inhalation delivery for several reasons: 1) Volatile and semivolatile compounds, such as B(a)P, are poor candidates for inhalation toxicological dose-response studies due to their loss during the exposure process and poor reproducibility, which is prohibitory in the validation of fume concentrations [64, 73]; 2) High doses of B(a)P are not achievable by inhalation; 3) Rodents undergo avoidance reactions when exposed to an inhalant; 4) Given that rodents are obligatory nose breathers, and do not inhale the way humans do, this has differential effects in the dynamics of particle deposition in the rat's respiratory tract; and 5) Delivery by inhalation can cause irritation-induced

histological changes that are independent of the administered toxicant.

B(a)P and pulmonary toxicity

The mammalian lung consists of more than 40 distinctive cell types. In general however, pneumotoxins select only six of these cell types as targets: type I and type II alveolar epithelial cells, capillary endothelial cells, pulmonary alveolar macrophages, ciliated bronchiolar epithelial cells, and clara cells (nonciliated bronchiolar epithelial cells). It is thought that the patterns of toxicity seen in the lung after xenobiotic exposure reflect the differences in formation of toxic reactive intermediates from metabolism in these cell types. The specific CYP450 isoforms (i.e., CYP1A1, CYP1A2, and CYP1B1) that are responsible for the metabolism of B(a)P to the reactive BPDE metabolite are present in high abundance in several lung cell types [147], yet the exact histopathological events and mechanisms that take place in the lung after acute and early chronic B(a)P exposure are not completely known. In our pilot experimental dose studies (80 mg/kg), we set out to determine what histopathological events in the lung may be contributing to B(a)P's mechanism of pulmonary toxicity. In these preliminary pilot studies, we observed an increase in alveolar wall thickness, as well as an increase in the numbers of neutrophils and activated macrophages in rat lung tissue from 80 mg/kg dosed rats compared to normal untreated control rats. Thus, this dissertational research sought to provide insight into the biological and biochemical factors underlying B(a)P-mediated toxicity such as hyperplasia, hypertrophy, and increased inflammation.

Hyperplasia and hypertrophy in lung tissues

Hyperplasia and hypertrophy frequently occur together and may contribute to an increase in alveolar wall thickness. Where hypertrophy is an increase in the size of the cell (which can be seen in the skeletal muscle during weight training), hyperplasia is an increase in the number of cells. Hyperplasia can be a normal response (as seen in the glandular tissue of the breast during pregnancy), or an abnormal (atypical) response. Atypical hyperplasia can be a preneoplastic response to a stimulus or secondary to a pathological cause. It has even been demonstrated to be a precursor in some cancers [148]. The cause of atypical hyperplasia may also be due to a chronic inflammatory response.

Neutrophils and macrophages in the lung

An association between chronic inflammation and cancer has been recognized for a long time [149-151]. Experimental studies with rats, as well as molecular epidemiological studies in humans, have provided evidence that the influx of neutrophils into the airways is an important process that may link inflammation with carcinogenesis. Neutrophils (or polymorphonuclear neutrophils, PMNs) are the most abundant type of white blood cells, and are a critical part of the innate immune system. Neutrophils can be identified in tissues by their unique nucleus which is divided into two to five lobes. Neutrophils are normally found in the blood stream, but during the acute phase of inflammation they migrate from the vessels towards the site of tissue inflammation. Neutrophils have been demonstrated to increase during some environmental exposures [152], and some cancers [153, 154]. Neutrophil attachment to the

endothelium has been demonstrated to be related to an increase in endothelial injury [155, 156]. This damage is accomplished by the release of reactive oxygen and nitrogen species from an enzyme called myeloperoxidase (MPO).

MPO enzymes are most abundant in neutrophils and are considered a marker of neutrophilic inflammation. The reactive species produced by this enzyme are cytotoxic and intended to kill bacteria and pathogens. However, MPO enzymes are nonselective in their targets, and therefore also induce cellular injury and necrosis in host tissue. Neutrophil infiltration itself then becomes an offender in the pathogenesis of disease. An association of MPO and the severity of coronary artery disease has been established [157]. However, the role of MPO in lung injury and disease is still being ascertained.

Like neutrophils, alveolar macrophages are white blood cells. Their role is to consume cellular debris and pathogens in the lungs to keep the lung's environment sterile. They also phagocytize neutrophils as they age [147]. They can stimulate lymphocytes and other immune cells, but unlike neutrophils, which are short-lived (about 2 days), macrophages can survive much longer in the body (up to several months) [158]. This may explain why the dominant inflammatory cells seen in chronic infections are macrophages [159]. Many agents that increase macrophage activity also increase the risk of inflammatory-related injury in the lung [160]. The disruption of the delicate balance of the macrophage population in the lung can have deleterious consequences [160]. Furthermore, macrophages have been demonstrated to promote cancer cell proliferation [161]. Macrophages are attracted to oxygen-starved tumor cells and promote tumor

necrosis factor (TNF-α) release, which in turn activates nuclear factor-kappa B (NF-κB). This arrests apoptosis and promotes cell proliferation and inflammation [162]. TNF-α release has also been demonstrated in a number of in vivo models of xenobiotic-induced lung injury [160].

Both the neutrophils and alveolar macrophages have been demonstrated to metabolize B(a)P, or B(a)P metabolites, to the ultimate carcinogen BPDE [163, 164]. The resultant BPDE-protein and DNA adducts may contribute to the histopathological events in the lung after B(a)P exposure as well as mutagenesis. Figure 3.1 provides a simplified overview of the pathways by which these cells may impact pulmonary toxicology, and demonstrates the rationale behind our research objectives.

Histopathology and staining techniques

Histopathology is the study of microscopic anatomical changes that are characteristic of disease. Since biological tissues have little inherent contrast using visible light microscopy, various staining techniques are employed to establish general relationships among cells in tissues. Before biological tissues are processed for staining, chemical fixatives are used to preserve tissue from degradation. The most common fixative for light microscopy is a 10% formalin solution. Permeation of tissues with this solution maintains the structure of the cell and sub-cellular components (mainly by irreversibly cross-linking proteins to formaldehyde), and prevents autolysis. The fixed tissue can then be sectioned and stained accordingly. The hematoxylin and eosin (H&E) stain that was employed for this dissertational research is one of the most commonly used

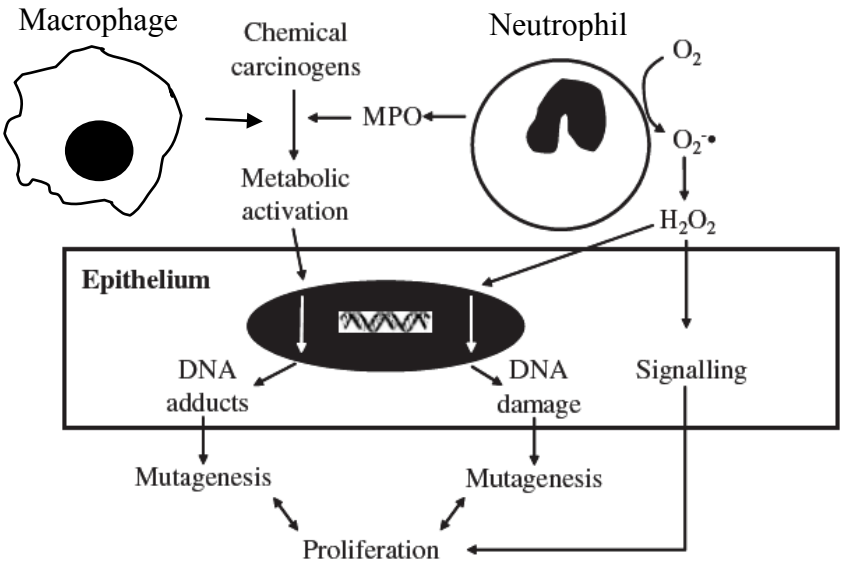

Figure 3.1 *Simplified overview of the pathways by which neutrophils and macrophages may impact pulmonary toxicity.* Neutrophils can cause not only oxidative DNA damage through generation of reactive species, but also are able to activate B(a)P metabolites to the ultimate carcinogen BPDE via metabolism by MPO [164-166]. Additionally, macrophages have been demonstrated to metabolize B(a)P to BPDE via P450-dependent and -independent pathways [163] (Figure adapted from [167])

stains used today. Hematoxylin is a basic dye that stains basophilic structures blue (i.e. nuclei and endoplasmic reticulum) and eosin is an acidic dye that stains eosinophilic structures pink (i.e., cytoplasm and red blood cells). H&E staining therefore allows for the general study and differentiation of cell nuclei and cytoplasms in all types of tissues.

Immunohistochemistry (IHC) exploits the principle of antibodies binding specifically to antigens (i.e., proteins) in biological tissues. IHC is widely used in basic research to determine the localization and distribution of biomarkers in biological tissue. For the visualization of the antibody-antigen interaction, an antibody is conjugated to an enzyme. A commonly used enzyme such as peroxidase can catalyze a color-producing reaction or the antibody can be tagged to a fluorophore which then could be detected under the appropriate fluorescent light.

The experiments presented in this chapter were designed to address the hypothesis that the severity of lung tissue toxicity will correlate to the concentration of BPDE-protein adducts in hair. To determine the severity of lung tissue toxicity we: 1) Measured alveolar wall thickness and counted neutrophils in the lung tissue of control rats and B(a)P dosed rats by subjective means; 2) Measured nuclear space, cellular space, and air space by objective means; 3) Employed IHC to determine if MPO increases in rat lung tissues from B(a)P treated rats.

Materials and Methods

Animals

Male Long-Evans rats (200-225 g) were individually housed in cages with wire mesh bottoms and maintained under controlled temperature and lighting conditions (12 hr light/dark cycle) and provided with food and water ad libitum. All procedures were in compliance with the National Institutes of Health *Guide for the Care and Use of Laboratory Animals* [120].

Chemicals and reagents

B(a)P used for dosing solutions was purchased from Sigma-Aldrich® (St. Louis, MO). Containers with formalin solution (10%) for tissue fixation were obtained from ARUP laboratories (Salt Lake City, UT). All other chemicals, reagents were obtained by the laboratories of ARUP Laboratories (Salt Lake City, UT) for H&E staining and IHC Services (Smithville, TX) for MPO staining. For ICH preparations the protein blocking solution was obtained from Signet Pathology Systems (Dedham, MA); The avidin /biotin blocking kit was purchased from Zymed Labs (San Francisco, CA); SuperBlock was purchased from Pierce Chemical Company (Rockford, IL); Antibodies were obtained from Signet™ Laboratories (Dedham, MA) and New Fuchsin substrate from Kirkegaard & Perry Labs (Gaithersburg, MD).

Experimental protocol and lung tissue collection

Two experimental groups were evaluated for evidence of the described histopathological changes as outlined below.

Group 1: Rats were administered 40 mg/kg of B(a)P (in corn oil) (n=10) i.p. once daily for 7 days. Control rats (n=5) were dosed i.p. once daily with corn oil for seven days.

Group 2: Rats were administered 160 mg/kg of B(a)P (in corn oil) (n=10) i.p. once daily for 7 days. Saline control rats (n=5) were administered sterile saline solution i.p. once daily for 7 days. Corn oil control rats (n=5) were dosed i.p. once daily with corn oil for 7 days.

Solutions of B(a)P in corn oil were prepared at 25 and 100 mg/mL for the 40 and 160 mg/kg doses, respectively. The volume of corn oil administered given i.p. to the corn oil control rats was based on the weight of the animal. This was done in order to keep the dosed volume of corn oil consistent between all experimental groups. The volume of saline was also based on the weight of the animal, therefore keeping the dosed volume equivalent to the other groups. For this study, the doses of B(a)P given are high and represent chronic lifetime doses of B(a)P in humans. In order to evaluate whether vehicle (corn oil) had any effect on inflammation or other events in the lung, an additional control group (saline dosed rats) was included with Group 2.

Fourteen days after the first dose, the animals were anesthetized with chloral hydrate (450 mg/kg). After hair and blood were collected (as described in Material and Methods section in Chapter 2), the animal's diaphragm on each side was carefully pierced to allow the lungs to collapse. The lungs were then carefully extracted by the trachea, avoiding actual contact with the lung at all times. The left lobe was placed in 10% formalin for at least 72 hours before gross

sectioning of tissue was performed. The location of the nickel-thick section of lung tissue used for sectioning and staining for H&E and IHC can be seen in Figure 3.2.

H&E staining of lung tissue

All of the H&E procedures were performed at ARUP laboratories (Salt Lake City, UT). The nickel-thick gross section of lung tissue was allowed to equilibrate in 10% formalin overnight. The next day, the tissue was paraffin embedded, then 3-5 micron paraffin sections were placed on positive charged slides and allowed to air dry at room temperature. Using an automated staining system (Tissue-Tek® Prisma™), the slides were first deparaffinized in a 65°C drying oven then taken through a series of xylene, alcohol, water, Harris hematoxylin, acetic acid, and eosin washes. After the final rinsing and drying steps were complete, slides were transferred to an automated Tissue-Tek® Film™ for coverslipping.

Immunohistochemistry staining of lung tissue for MPO

All of the MPO staining procedures were performed at IHC Laboratories (Smithville, TX). Five micron paraffin sections were placed on positive charged slides and allowed to air dry at room temperature. The slides were then deparaffinized with ProPar® and hydrated down though a series of alcohols to covered with a protein blocking solution for 30 mins, and subsequently rinsed in Tris buffer. An avidin/biotin blocking procedure was then performed, streptavidin-alkaline phosphatase linking reagent was applied and incubated for 30 mins

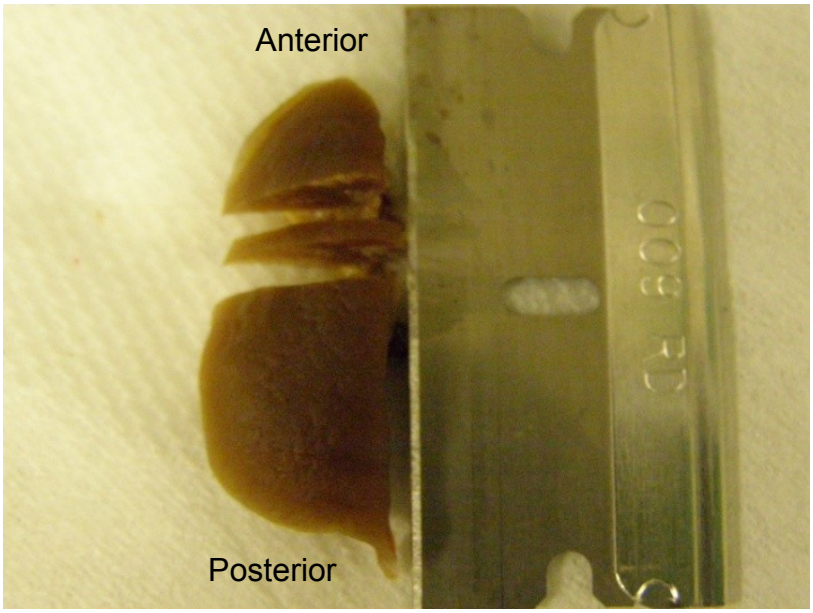

Figure 3.2 *Rat lung indicating the gross section of lung tissue used for paraffin embedding, sectioning, and H&E and immunohistochemistry staining.* The nickel-thick section contains the pulmonary artery and main bronchus.

in water. Slides were then placed into a 10 uM citrate buffer (pH 6.0) and heated in a microwave to boiling, then held at the boiling temperature for 6 mins. The slides were allowed to cool for 20 mins at room temperature. Each tissue section was Slides were again rinsed in Tris buffer and New Fuchsin substrate applied. Color development was monitored microscopically, then slides were washed in distilled water and counterstained in Mayers' hematoxylin. Slides then went through a brief rinse in an aqueous ammonia solution, then distilled water, then dehydrated though a series of alcohols. Slides were dipped in ProPar®, then mounted.

Subjective analysis of lung tissues

An initial observation of the H&E stained lung tissue obtained from a pilot study in rats administered B(a)P (80 mg/kg, n=10) and normal untreated rats (n=4) revealed that B(a)P appeared to cause alveolar wall thickening (possible hyperplasia or hypertrophy based), decreased air space, and an increase in neutrophils and activated macrophages. Therefore, in our 40 mg/kg and 160 mg/kg dosed rats groups, along with appropriate vehicle (corn oil) control rats and saline control rats, we subjectively measured the percentage of alveolar wall thickening and number of neutrophils evident in ten random 40X images taken around the pulmonary artery and main bronchus of each rat (analyst was blinded to treatment groups).

The percentage of alveolar wall thickening was determined by observing the increase in the number of cells that made up the alveolar wall in ten 40X fields (rounded to the nearest 5%). For the average neutrophil count

measurement, the exact number of neutrophils were recorded in 10 40X fields. The ten values obtained from each rat for percentage of alveolar wall thickening and neutrophil count were then averaged, yielding a mean value per rat. Statistical tests were then performed on these mean values between each of the groups tested. Subjective measurements were done under the guidance of Dr. Lawrence McGill (a veterinarian and board certified veterinarian pathologist) at ARUP Laboratories.

Objective analysis of lung tissue

ImageJ is a Java-based image processing program developed at the National Institutes of Health [168]. We employed this software as a second approach for assessing histopathological changes in lung tissues obtained from the control and B(a)P dosed rats. Using this software, and digital images of the H&E stained lung tissue, we performed several densitometric measurements.

First, the analyst was blinded to treatment group, then ten random fields (at 40X magnification) around the pulmonary artery and main bronchus were selected (examples shown in Figure 3.3). Because densitometric measurements of cellular content were assessed, fields only containing alveolar epithelial cells were taken (to avoid offset of other lung parenchyma of differing cellular density). These images were all taken under the same camera and scope settings (i.e., exposure, contrast, etc.). These images were then analyzed in Image J using pixel value statistics of user-defined selections of intensity thresholded objects. The threshold intensity was set for each measurement of interest, then held constant for all sequential image measurements. The thresholded

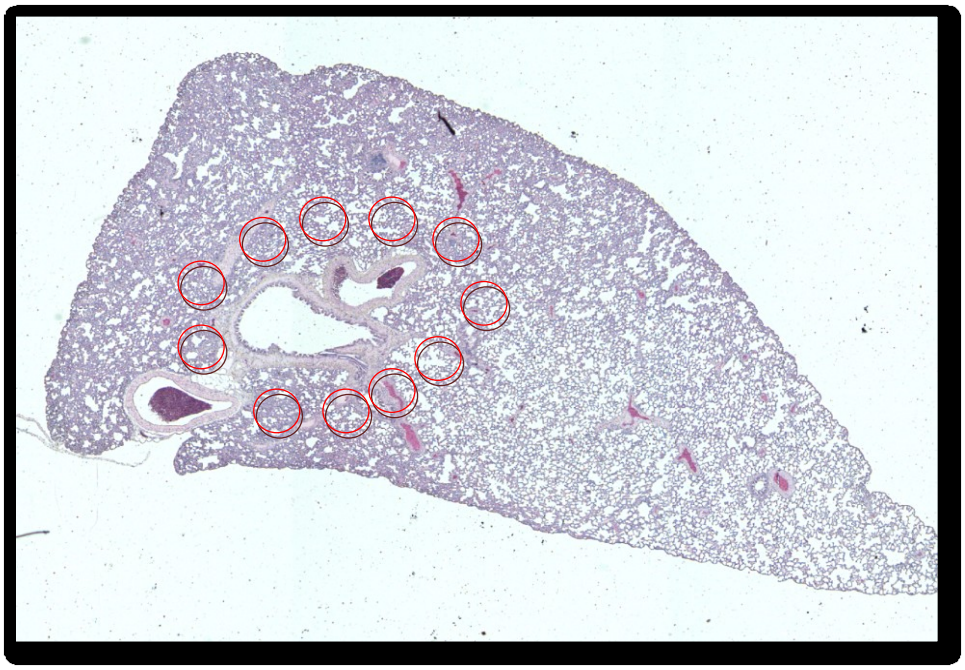

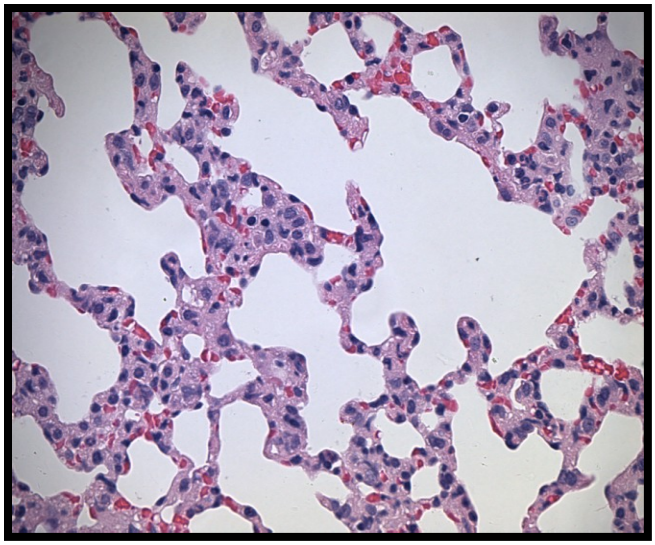

Figure 3.3 *Representative digital images of H&E stained lung tissues.* Whole lung (10X) (top) and alveolar cells (40X) (bottom). Red circles around the pulmonary artery and main bronchus are representative areas for obtaining 40X images for ImageJ measurements.

measurements included: 1) Cell Count (measure of hematoxylin stained nuclear space), Cellular Space (measure of eosin stained cytoplasmic material plus hematoxylin stained nuclear space), Air Space (measure of space not stained with hematoxylin or eosin), and ratios of these measures. (Images of these measurements are represented above their respective data in the Results section.) The "Cell Count" measurement may be representative of hyperplasia. "Cellular Space" may be representative of hypertrophy. Decreased "Air Space" may be indicative of hyperplasia, hypertrophy, and/or inflammation. A smaller than control value for the ratio of nuclear space to air space could be representative of hypertrophy. Whereas, a larger value than control value for the ratio of cellular space to air space could be indicative of hyperplasia, hypertrophy, and/or inflammation. Figure 3.3 represents a whole lung slice showing representative areas where 40X images were obtained, and an example of a 40X image of alveolar cells of which ImageJ densitometric measurements were taken.

Statistics

Subjective measures of the percent of alveolar wall thickening and average neutrophil counts for the 40 mg/kg dosed rats and corresponding corn oil control rats were compared by a two-tailed Student's t-test. Objective ImageJ results for Cell Count, Cellular Space, Air Space, and ratios were also compared by a two-tailed Student's t-test between these two groups. Subjective measures of the percent of alveolar wall thickening and average neutrophil counts for the 160 mg/kg dosed rats and corresponding saline control and corn oil control rats

were compared by a one-way ANOVA. Objective ImageJ results for Cell Count, Cellular Space, Air Space, and ratios between these groups were also compared by a one-way ANOVA. All statistics were performed using Graph Pad Prism® software (version 5.01) (La Jolla, CA). Differences were considered significant at $\alpha \leq 0.05$.

Results

There was no statistical difference in the subjective measurement of alveolar wall thickening or average neutrophil counts between 40 mg/kg dosed rats and the corresponding corn oil control rats (Figure 3.4 A-B). There was also no statistical difference in the subjective measurement of the alveolar wall thickening or average neutrophil count between 160 mg/kg dosed rats and the corresponding saline control and corn oil control rats (Figure 3.4 C-D).

The objective ImageJ measurements for Cell Count and Cellular Space can be seen in Figure 3.5. There was no statistical difference between 40 mg/kg dosed rats and the corresponding corn oil controls for Cell Count or Cellular Space. There was also no statistical difference between 160 mg/kg dosed rats and the corresponding saline control and corn oil control rats for Cell Count or Cellular Space (Figure 3.5).

The objective ImageJ measurements for Air Space can be seen in Figure 3.6. There was no statistical difference between 40 mg/kg dosed rats and the corresponding corn oil controls for Air Space. There was also no statistical difference between 160 mg/kg dosed rats and the corresponding saline control and corn oil control rats for Air Space (Figure 3.6).

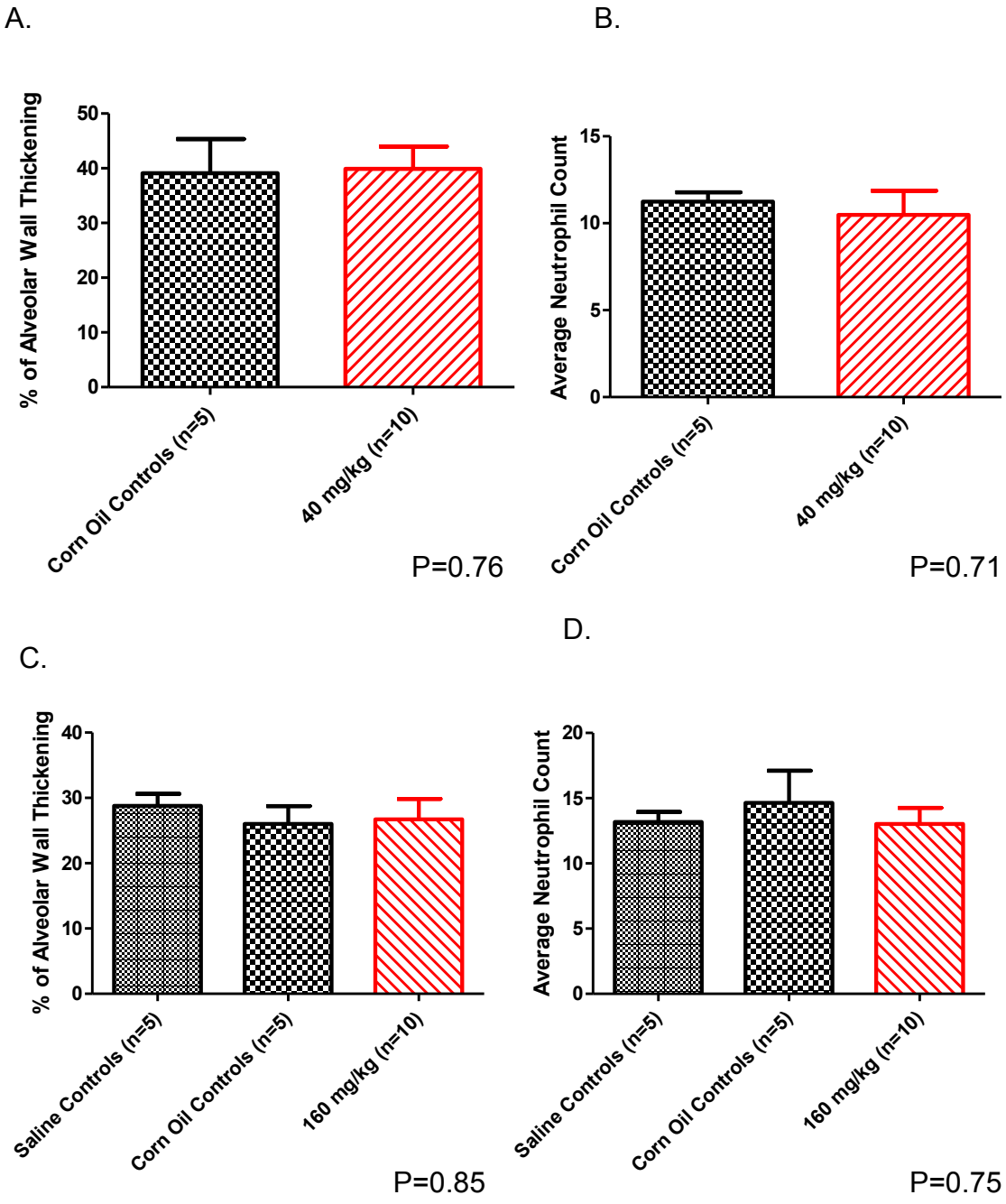

Figure 3.4 *Subjective measurements (mean ± SEM) for alveolar wall thickening and neutrophil counts for 40 and 160 mg/kg doses rats.* Panels A&B) There is no statistical difference between alveolar wall thickening or neutrophil count for 40 mg/kg dosed rats and corresponding corn oil control rats (P values for Student's t-tests shown). Panels C&D) There is no statistical difference between alveolar wall thickening or neutrophil count for 160 mg/kg dosed rats and corresponding saline control and corn oil control rats (P values for ANOVA shown).

Figure 3.5 *ImageJ results (mean ± SEM) for Cell Count and Cellular Space.* Thresholded area is shown in red above bar charts and corresponds to the percent area fraction shown on the y-axis. A&B) Results for 40 mg/kg dosed rats and corresponding corn oil control rats. There is no statistical difference between 40 mg/kg dosed rats and corresponding corn oil controls for Cell Count or Cellular Space. (P values for Student's t-tests shown). C&D) Results for 160 mg/kg dosed rats and corresponding saline and corn oil control rats. There is no statistical difference between 160 mg/kg dosed rats and corresponding saline control and corn oil control rats for Cell Count or Cellular Space. (P values for ANOVA tests shown)

A.

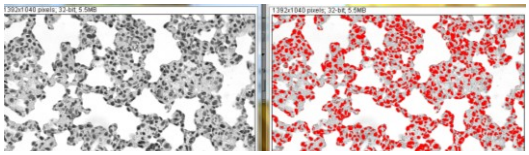

"Cell Count"

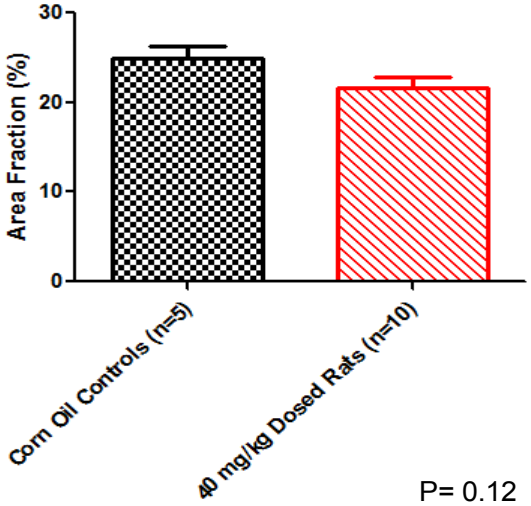

P= 0.12

B.

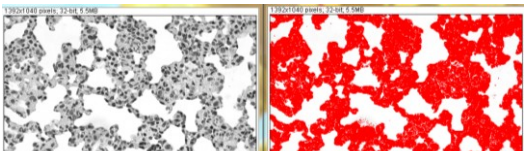

"Cellular Space"

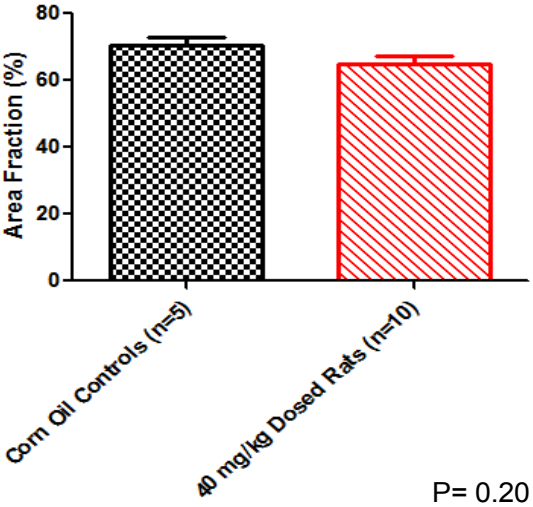

P= 0.20

C.

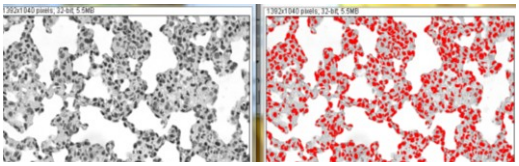

"Cell Count"

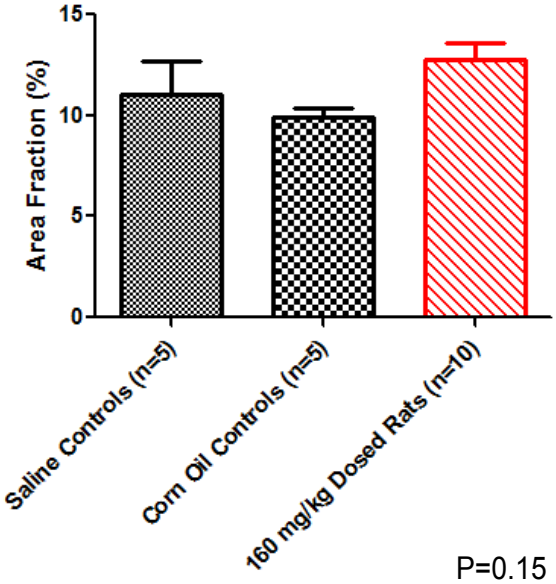

P=0.15

D.

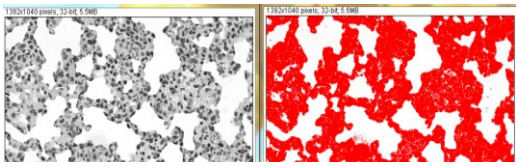

"Cellular Space"

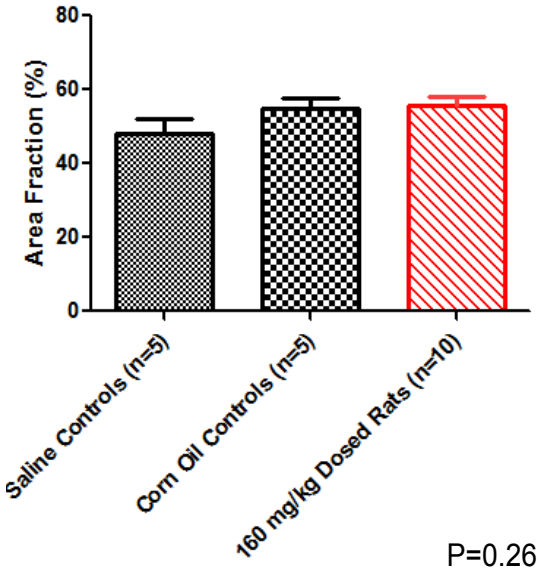

P=0.26

Figure 3.6 *ImageJ results (mean ± SEM) for Air Space.* Thresholded area is shown in red above bar charts and corresponds to percent area fraction shown on the y-axis. A) Results for 40 mg/kg dosed rats and corresponding corn oil control rats. There is no statistical difference between 40 mg/kg dosed rats and corresponding corn oil controls for Air Space. (P values for Student's t-tests shown). B) Results for 160 mg/kg dosed rats and corresponding saline control and corn oil control rats. There is no statistical difference between 160 mg/kg dosed rats and corresponding saline and corn oil controls for Air Space. (P values for ANOVA tests shown)

A.

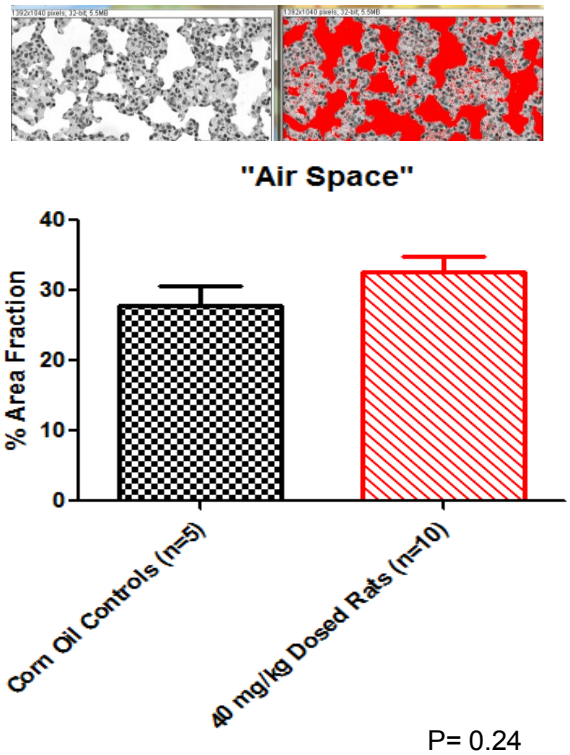
"Air Space"
% Area Fraction
40
30
20
10
0
Corn Oil Controls (n=5)
40 mg/kg Dosed Rats (n=10)

P= 0.24

B.

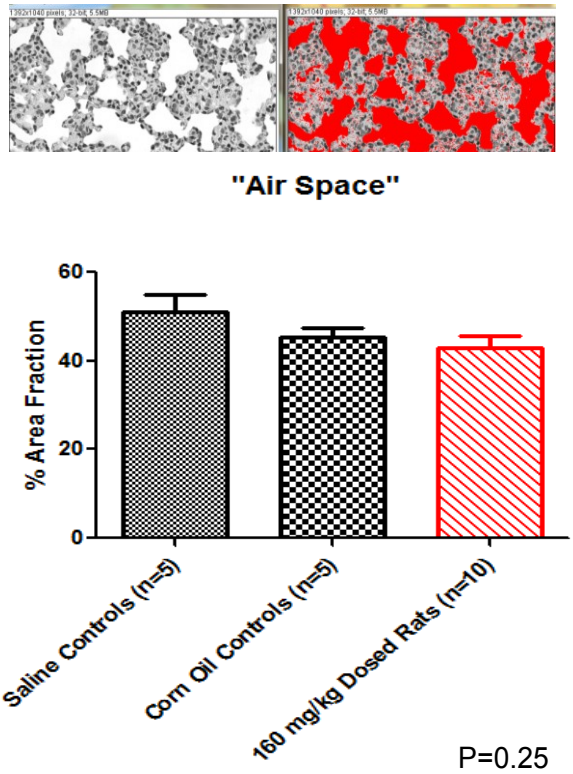
"Air Space"
% Area Fraction
60
40
20
0
Saline Controls (n=5)
Corn Oil Controls (n=5)
160 mg/kg Dosed Rats (n=10)

P=0.25

The measurements for the ratios of nuclear space to cellular space, and cellular space to air space, from ImageJ results can be seen in Figure 3.7. There was no statistical difference between 40 mg/kg dosed rats and corresponding corn oil controls for either ratio. There was also no statistical difference between 160 mg/kg dosed rats and corresponding saline and corn oil controls for either ratio.

The results from MPO staining from 160 mg/kg dosed rats (n=3) and corresponding corn oil control rats (n=3) are shown in Figure 3.8. There was a significant difference in the number of MPO stained cells between these two groups. The mean $\pm$ SEM was 2.0 $\pm$ 0.3 for the corn oil control rats 3.1 $\pm$ 0.3 for the 160 mg/kg dosed rats.

Discussion

We determined that there is a significant difference in the IHC staining for MPO content between B(a)P dosed rats and control rats (Figure 3.8). However, we were unable to determine a statistically significant difference the lung tissues between B(a)P dosed rats and control rats using the described subjective and objective measures within this chapter. This lack of significant difference may be due to several reasons: 1) There may be a lack of sensitivity in methods used for both subjective and objective measurements; 2) The lung tissues from animals were not insufflated at a constant pressure prior to collection; 3) The dosing paradigm included only one time point (Day14), seven days after the last B(a)P dose; 4) The route of administration by i.p. may not be appropriate for short-term studies of B(a)P-induced toxicities in the lung; 5) Artifacts of H&E staining

Figure 3.7 *Ratios of nuclear space to cellular space and cellular space to air space for ImageJ results (mean ± SEM).* A&B) Results for 40 mg/kg dosed rats and corresponding corn oil control rats. There is no statistical difference between 40 mg/kg dosed rats and corresponding corn oil controls for either ratio. (P values for Student's t-tests shown). C&D) Results for 160 mg/kg dosed rats and corresponding saline control and corn oil control rats. There is no statistical difference between 160 mg/kg dosed rats and corresponding saline and corn oil controls for either ratio. (P values for ANOVA tests shown)

A.

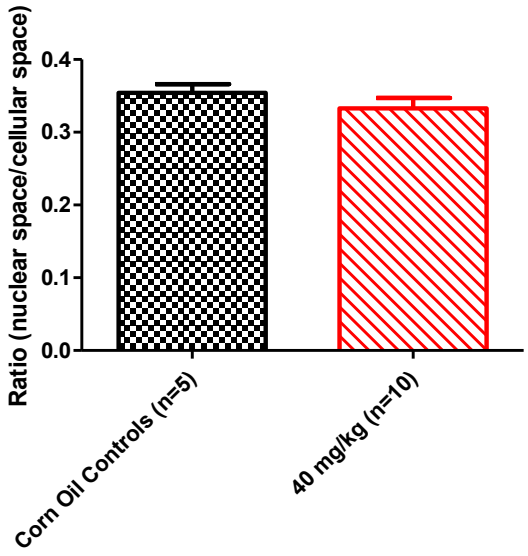

P=0.34

B.

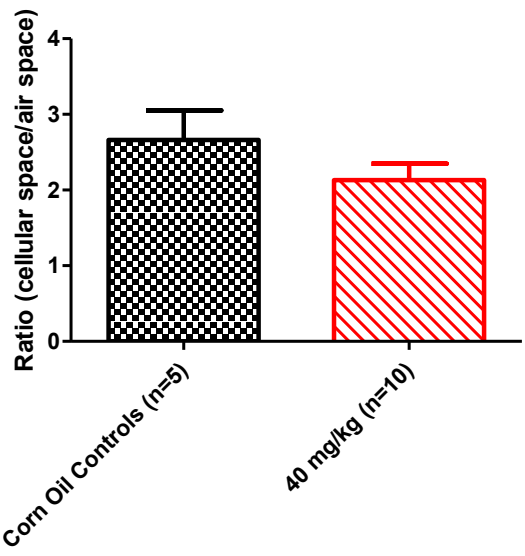

P=0.22

C.

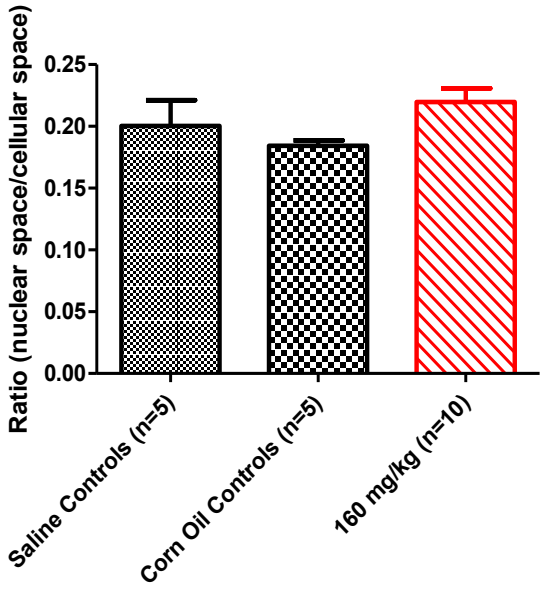

P=0.064

D.

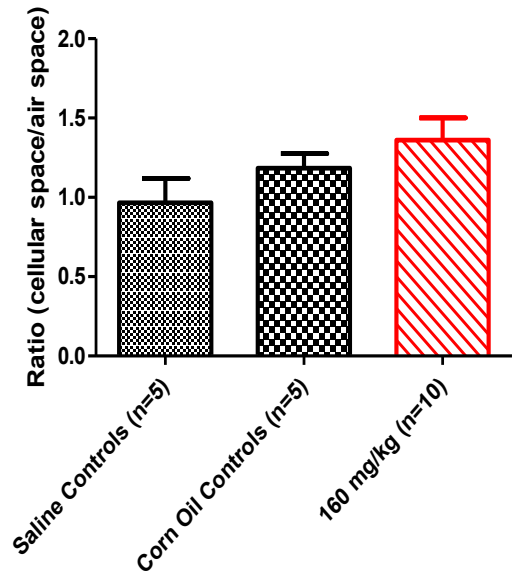

P=0.27

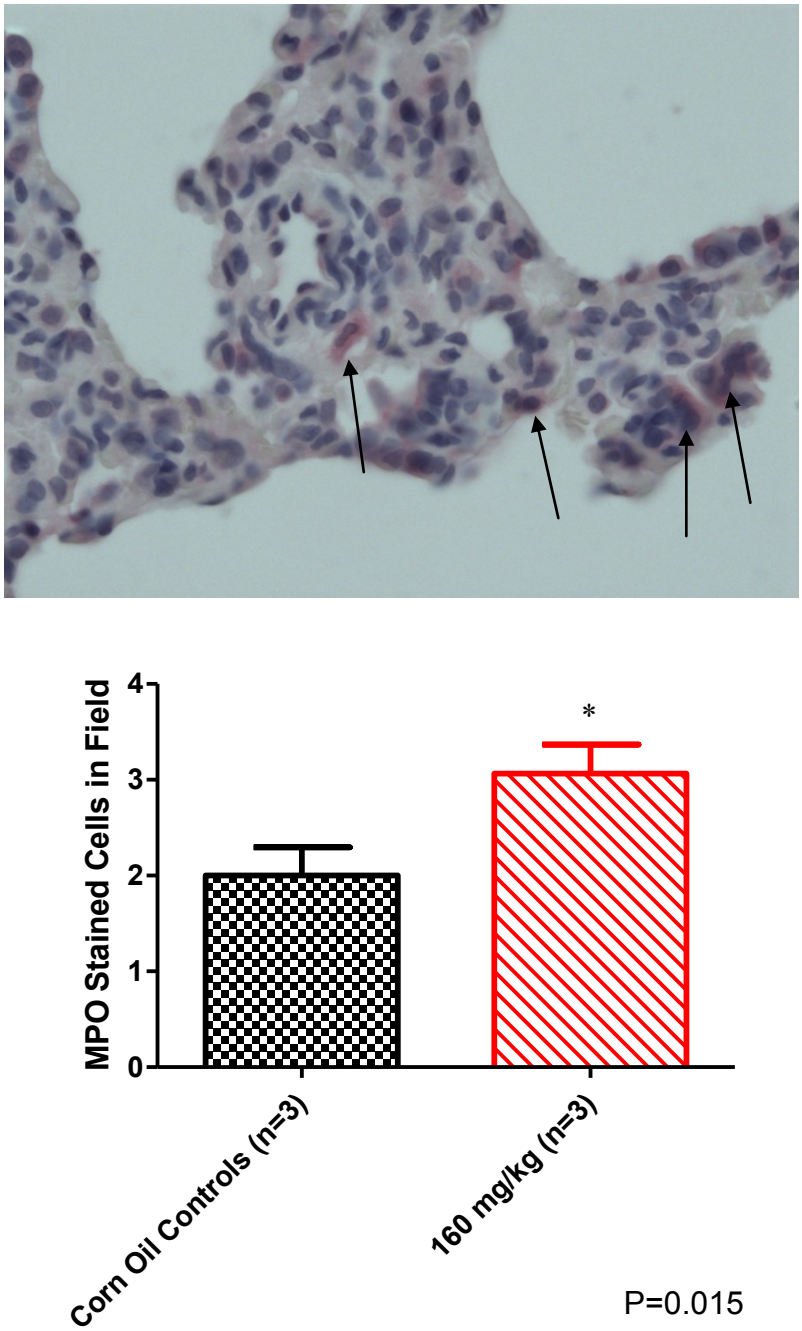

Figure 3.8 *Digital 100X image showing MPO stained cells (top)* and r*esults (mean ± SEM) for MPO staining (bottom).* There is a significant difference between the number of MPO stained cells between 160 mg/kg dosed rats and corresponding corn oil control rats (P value from Student's t-test shown).

and residual nonuniform blood distribution in lung tissue may be contributing to discrepancies in the ImageJ measurements taken; 6) There are a multitude of cell types in the lung and we only performed measurements on one cell type (alveolar epithelial cells). These topics will be expanded upon below.

The use of deflated lung tissue

Deflated lung tissue is commonly used to examine gross histopathological changes (i.e., hyperplasia, hypertrophy, metaplasia, neoplasia, necrosis, and tumors). Insufflated lung tissues are commonly used for morphometric analyses of the numbers of bronchi, bronchioli and alveolar ducts, along with air space and space and pulmonary vascular bed measurements. Additionally, using morphometric analyses, qualitative and quantitative measurements can be performed on lung tissues. We found that using deflated lung tissue resulted in inconsistent atelectasis (see top panel of Figure 3.9), which may have resulted in discrepancies in the densitometric measurements taken by ImageJ (i.e. higher cellular space percent area threshold values due to collapsed tissue and not because of an increase in cell numbers or size).

Dosing paradigm

Recognizing that lung clearance and lung cell turnover is rapid, earlier time points for inflammatory responses may have resulted in a more pronounced difference between B(a)P dosed rats and control rats. However the current methods described in this chapter may still have not been sensitive enough to detect a significant difference. Literature supports that with later time points

(several months to a year), metaplasia, neoplasia, and possible tumor formation is supported in rats dosed this high with B(a)P [71, 72, 169-171]. From H&E stained lung tissues from our pilot experiment (rats dosed at 80 mg/kg) and the 40 mg/kg and 160 mg/kg dosed rats detailed in this chapter, we did observe increased in alveolar wall thickness, edema, and macrophage hyperplasia (representation shown in Figure 3.9 bottom panel). We also noted there was decreased weight gain (from Day 0 to Day 14) in B(a)P dosed rats as compared to the control rats (Figure 3.10), which may also be contributing to the toxicity of B(a)P.

Artifacts of H&E staining

Slight differences in the thickness of the lung tissue sectioned by a microtome cutting device can contribute to more, or less, H&E dye uptake. This artifact of H&E staining may contribute to higher percent area thresholded measurement if the slice was thicker (thus more dye uptake), and conversely a trying to compare experimental groups. The same microtome should be used for all samples, and the same technician should do all the paraffin blocked tissue sectioning. Additionally, samples should all be processed together using the same batch of reagents and dyes.

Cell type chosen

The lung contains over 40 different cell types and pneumotoxins are thought to only exert their toxic effects on six of these cell types. Since it is known that there is more diversity in the cellular bioactivation and covalent

Figure 3.*9 Images from H&E stained lung tissue showing: A) Atelectasis in tissue from Saline Control Rat. B) Edema and macrophage hyperplasia in tissue from 160 mg/kg dosed rat*. A) Yellow dashed line indicates one of the areas showing atelectasis. B) Red oval indicates an area of edema. Arrows indicate some activated macrophages.

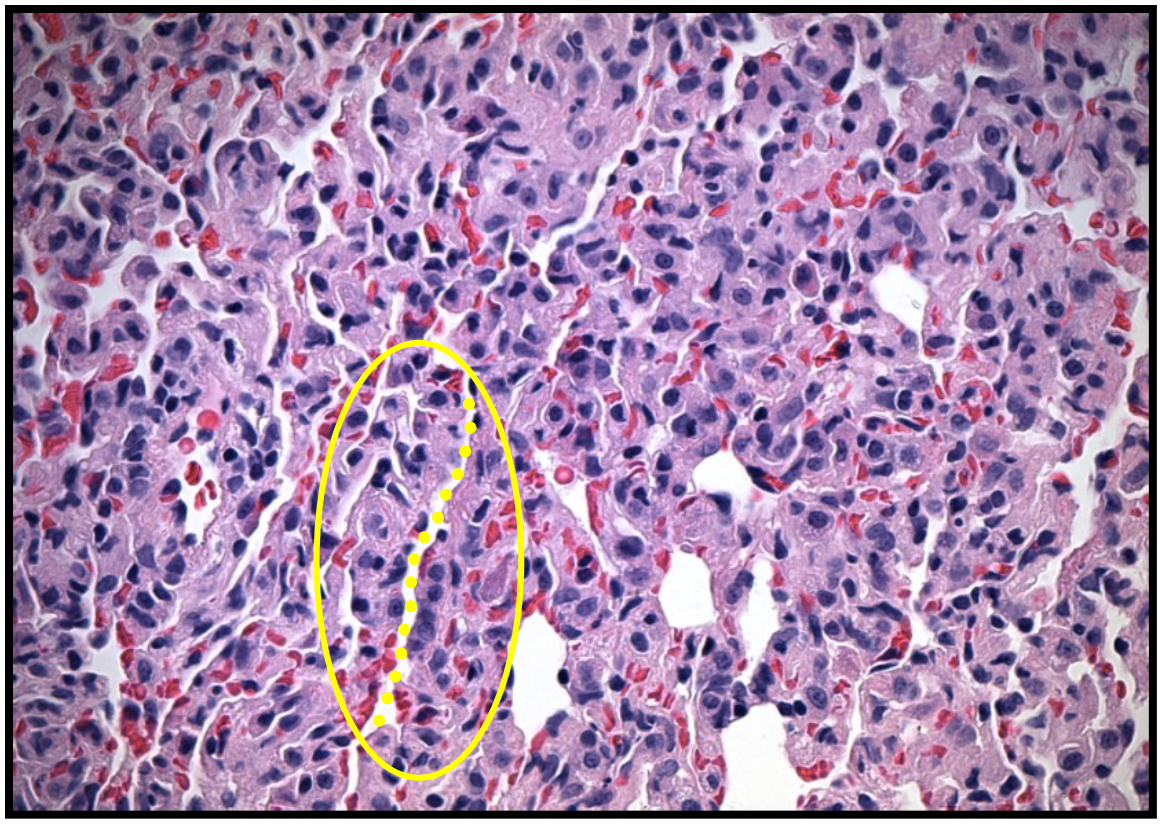

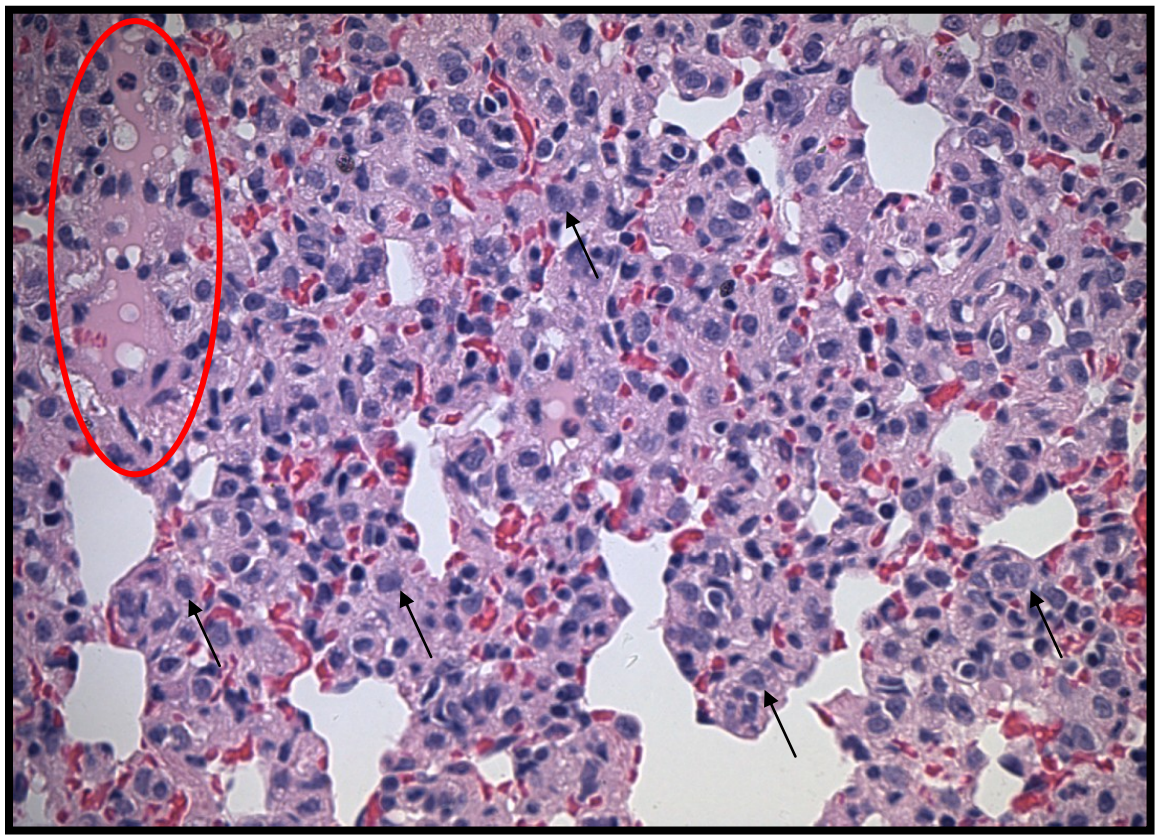

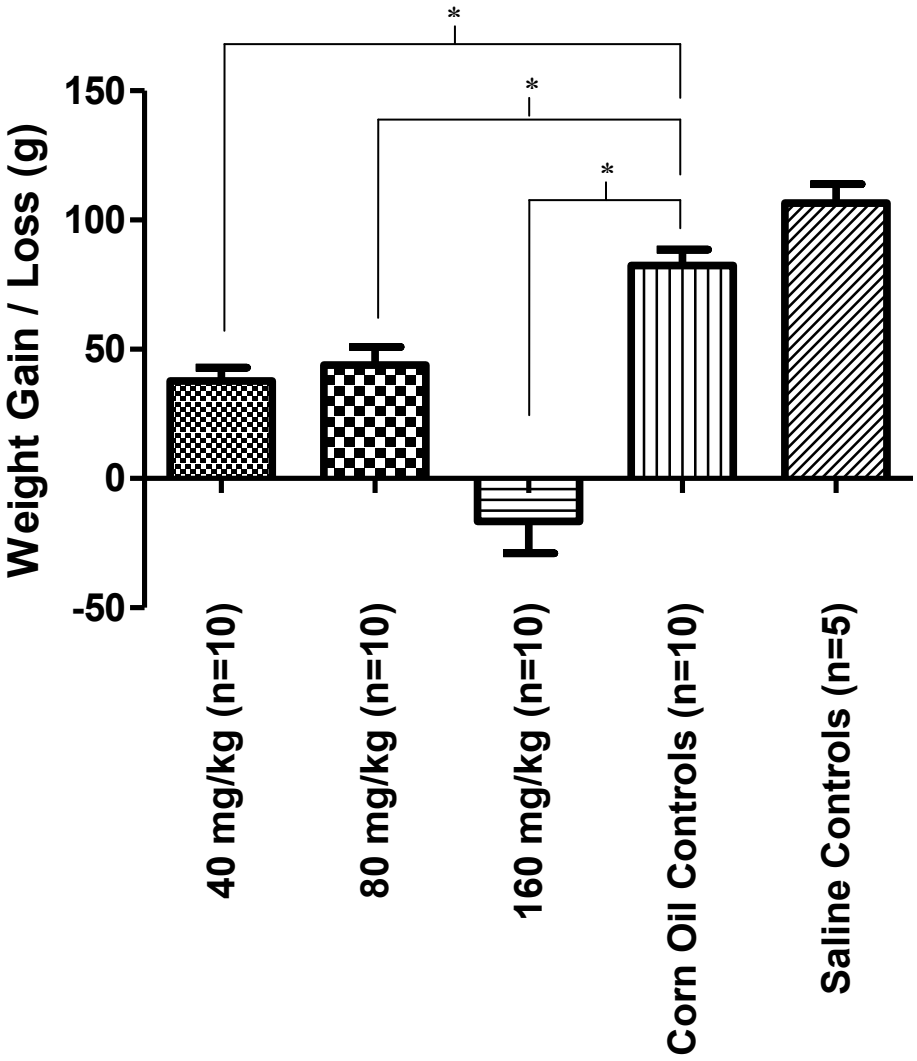

Figure 3.10 *Results for weight gain/loss from Day 1 to Day 14.* The average weight gain/loss for all B(a)P dosed rats were significantly different than the vehicle control (corn oil) rats (Student's t-test, $p<0.05$). Saline control rats are shown for representative purposes only.

binding to proteins and DNA in the lung, as compared to hepatic cellular populations [147], this demonstrates the importance of the examination of ower percent area thresholded measurement if the slice was thinner (thus less dye uptake). Also, different batches of H&E dyes could conceivably affect percent area thresholded measurements. It is therefore important that protocols remain consistent between the lung tissues processed for H&E staining when specific cell types in the lung. The heterogeneous distribution of drug-metabolizing enzymes among lung cells [172] may greatly enhance the risk for cytotoxicity in certain cell types.

Clara cells have been demonstrated to be more susceptible to electrophilic intermediates (like the epoxide) than other lung cells [147], but the alveolar type II cells are considered to be at high risk for B(a)P-induced tumor formation [142]. A number of studies have also demonstrated that alveolar type II cells are important in the modulation inflammatory and immune events in the lung [173, 174]. These cells also have greater volume densities of mitochondria and endoplasmic reticulum than many of the other cell types, supporting that higher metabolic activities are present in these cells [175]. Unfortunately, the metabolic capacity of alveolar type I cell is unknown, due to the inability to isolate type I cells for *in vitro* studies. While there are greater numbers of alveolar type II cells, the alveolar type I cells covers >95% of the alveolar surface, and may mask effects in the less prominent alveolar type II cell population. The alveolar epithelial cells, in general, are where we observed the most distinct gross histopathology differences between the B(a)P dosed rats and the control rats

(see images in Figure 3.11 and Figure 3.12). The Clara cells however, contain the highest amounts of several CYP450 enzymes [147], and further examination of these cell types is warranted.

Experiments not detailed in this chapter

The location around the pulmonary artery and main bronchus were chosen because we hypothesized that B(a)P given i.p. would be systemically introduced via the circulation, and thus the distribution of the resultant injury would be dependent on the pattern of blood flow to the lung. While systemically introduced toxicant lung injury is thought to be quite uniform [175], the posterior sections of the lower lobes in rat lungs show increase toxicities with the PAH naphthalene [176]. We thus considered that different regions of the lung may have greater toxicities associated with B(a)P exposure based on blood pooling effects. Based on this assumption, subjective and objective measurements described in this chapter, were performed on the posterior lobe and the anterior ventral portion of the lobe. However, analysis of these distinct regions did not reveal a significant difference between B(a)P dosed animals and controls (data not shown).

In addition to evaluation of regional differences, Red O staining was employed to decipher whether the “spongy” appearance of macrophages in B(a)P dosed animals (Figure 3.9 bottom panel) was due to the presence of residual corn oil. Red O staining indicates fat or lipids in fresh frozen tissue sections. This type of staining allows for the detection of fat / lipids occurring in

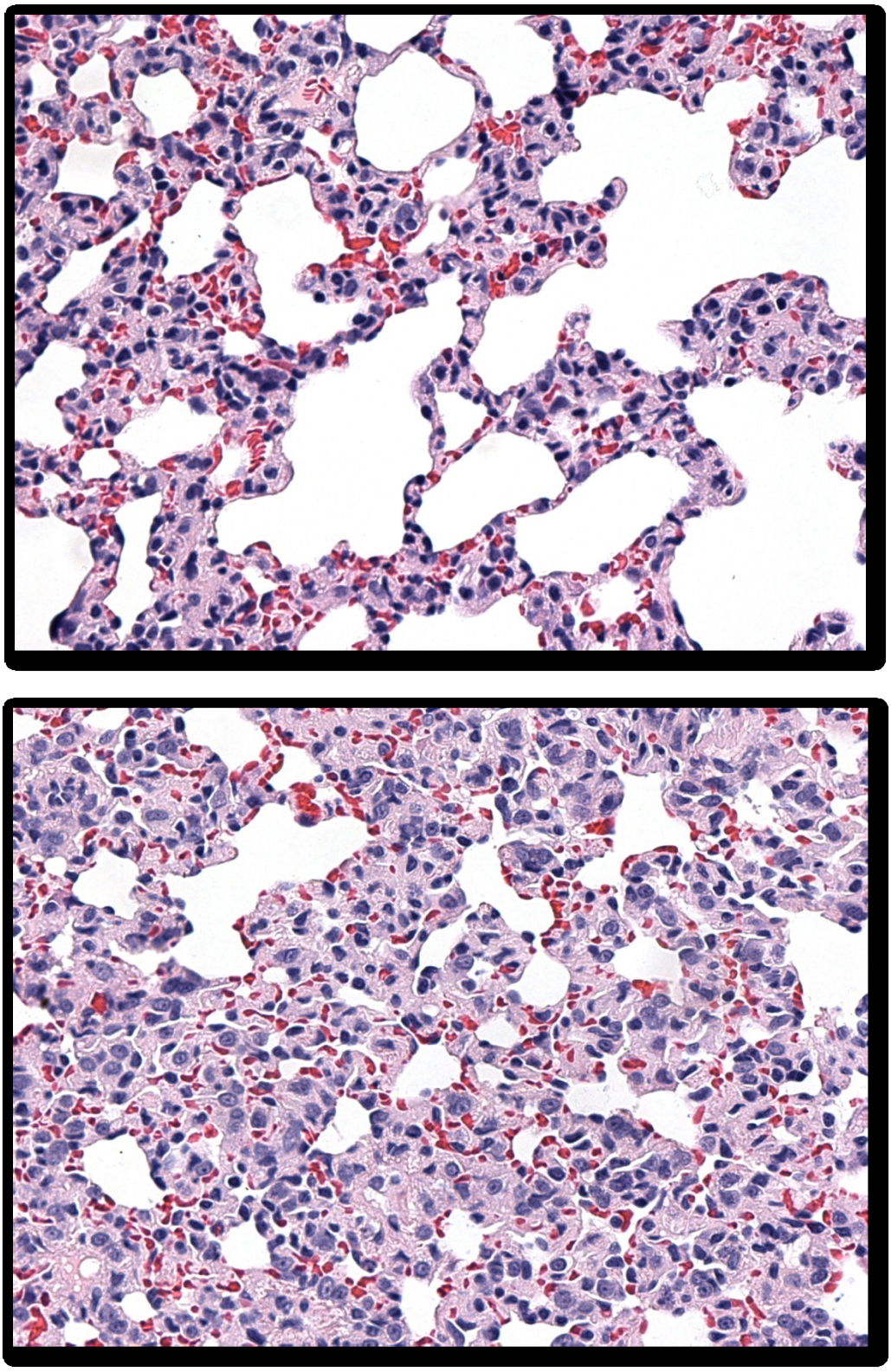

Figure 3.11 *Representative H&E images of corn oil control rat lung (top panel) and corresponding 40 mg/kg dosed rat lung (bottom panel).*

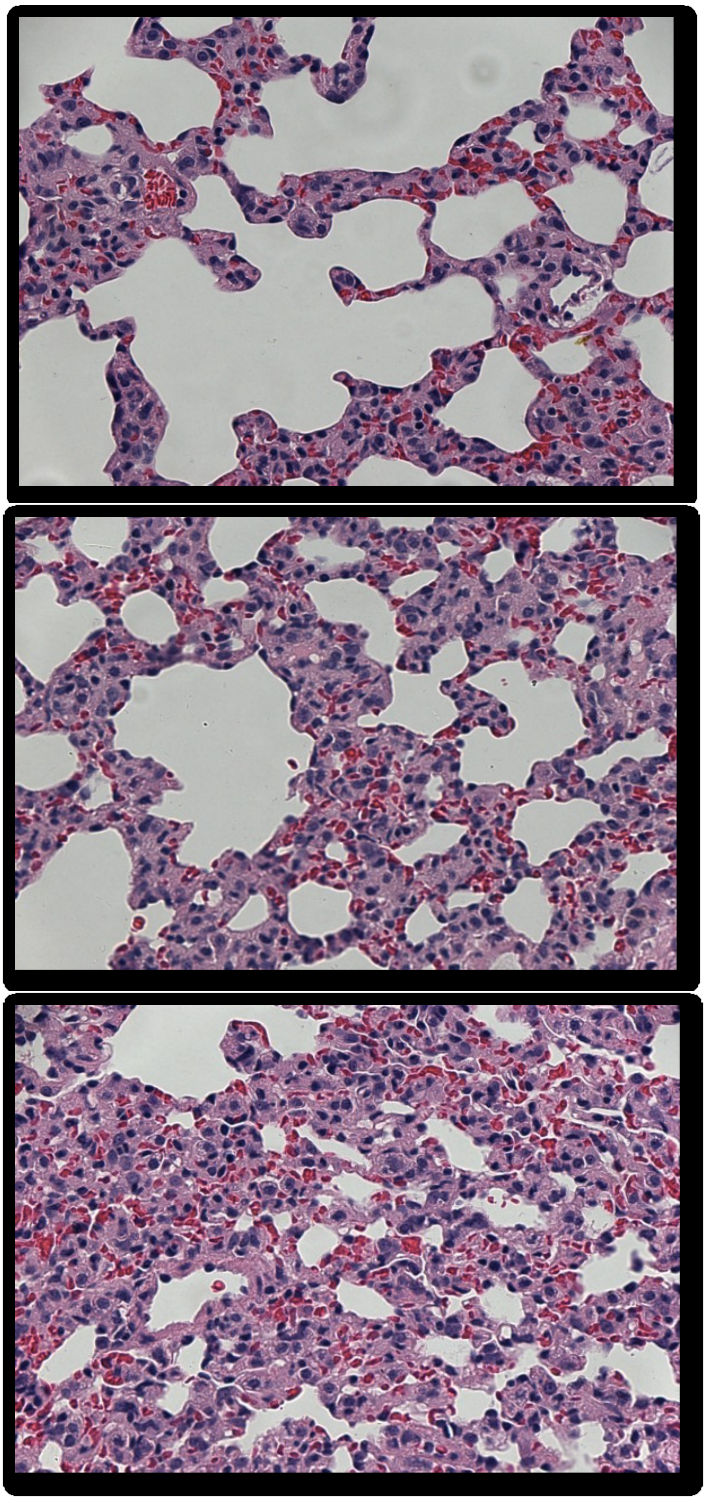

Figure 3.12 *Representative H&E images of saline control rat lung(top panel), corn oil control rat lung (middle panel) and corresponding 160 mg/kg dosed rat lung (bottom panel).*

abnormal places (e.g., tumors arising from fat cells (liposarcomas)). Tissues (n=3, corn oil controls; n=3, 40 mg/kg) from this experiment indicated the "spongy" appearance in macrophages was not due to the presence of corn oil, and B(a)P dosed animals and corn oil controls had similar staining patterns (which was very little to no stain present) (data not shown).

Extrapolation from animal to human studies

There may be unique differences in the genetic variation and regulation of specific proteins within the lung that should be considered when comparing lung toxicities in rats and humans. Spontaneous lung tumors in murine strains have been demonstrated to have similar histopathology and molecular characteristics to human adenocarcinomas [177, 178] . However, only rudimentary respiratory bronchioles are present in rodent lungs, and the populations of cells in rats vs. humans are different, as well as cellular metabolism and cellular defense mechanisms [175]. There are also known differences in the sensitivity of alveolar macrophages to xenobiotics in murine strains [179]. While there has been a great deal of information obtained on xenobiotic induced lung injury, more important questions still remain to be answered. Particularly, it is important to determine if the human lung is more sensitive to B(a)P-induced toxicities than the rat lung.

Future directions

Whole-genome microarrays in normal human epithelial cells exposed to BPDE show induction of numerous inflammatory factors [180]. These include genes that encode for pro-inflammatory cytokines and enzymes related to

prostaglandin synthesis and signaling. In addition, Podechard *et al*. have demonstrated that interleukin-8 (a pro-inflammatory cytokine) induction by B(a)P is aryl hydrocarbon receptor-dependent and leads to lung inflammation and to increased oxidative stress [145]. With this, and numerous other data stemming from research on B(a)P-induced inflammation, biochemical markers for inflammatory pathways in the lung tissue is warranted. Flow cytometry for specific inflammatory markers and specific inflammatory cell types could provide much higher sensitivity than our described methods, and may be able to better determine whether measureable differences are present in lung tissues from B(a)P dosed rats and control rats.

Experiments could be repeated with insulflated lung tissue and then morphometric measurements (or quantitative morphology) could be performed. Morphological abnormalities are the most reliable evidence we have to date for alveolar epithelial cells, since there are a lack of epithelial specific biochemical markers [175].

Electron photomicroscopy could provide better resolution of the cell types in lung tissue in order to examine any epithelial injuries or abnormalities in cell structure. Potential increases in the number of cells undergoing DNA synthesis can also be evaluated by this type of microscopy.

Cellular necrosis can contribute to an increase in alveolar protein concentrations. Injured cells release soluble enzymes from the cell's cytosol into extracellular fluids. These soluble enzymes can then be measured and used as indicators of cytotoxicity.

Very few studies have examined BPDE-protein adduct formation and specific tissue toxicities [181, 182]. The experiments detailed in this chapter aimed to understand whether or not B(a)P and/or BPDE-protein adduct concentrations in hair can serve as biomarkers, not only of exposure to B(a)P, but also as a predictor of increased lung toxicities. Further research will be needed to elucidate if the presence of BPDE-protein adducts in biological matrices such as hair and specific lung toxicities are associated.

In conclusion, despite more than 80 years since B(a)P has been isolated, much still remains to be learned about the underlying mechanisms that contribute to B(a)P-induced lung toxicity. A better understanding of the biochemical events that surround these toxicities would help us better recognize the relationship between functional alterations and structural changes in the lung. The cellular fate of metabolic and inflammatory induced injury after B(a)P exposure are important factors to improving our current knowledge of lung toxicology in B(a)P exposed animals.

CHAPTER 4

BIOMARKERS OF BENZO(A)PYRENE EXPOSURE IN THE HAIR AND BLOOD OF SMOKERS AND NONSMOKERS

Introduction

Smoking causes about 440,000 deaths and generates an estimated $157 billion in health-related economic losses in the United States annually [183]. Lung cancer is the leading cause of cancer death in the United States and is the most common type of tumor worldwide [184]. Since tobacco smoking is the single most important risk factor for development of lung cancer, it is strongly implicated as the causative agent [184]. It is also well established that active tobacco smoking can cause cardiovascular diseases, respiratory illnesses and other serious and often fatal health conditions. Moreover, evidence is rapidly accumulating that both platelet and endothelial function, arterial stiffness, atherosclerosis, oxidative stress, inflammation, heart rate variability, energy metabolism, and increased infarct size are seen not only in the active smoker, but also in nonsmokers exposed to environmental tobacco smoke (ETS) [185]. Although several studies have demonstrated the usefulness of biomarkers, such as cotinine, for ETS and particulate tobacco smoke (PTS) exposure, these biomarkers have limited utility because they do not directly address toxicity.

Therefore, more studies are needed to develop new and enhanced biomarkers that will address tobacco smoke exposure and the toxicity risks associated with smoking and exposure to ETS. Advantages of improved biomarkers include: 1) They can be used in epidemiological and health surveillance programs as well as new product and harm-reduction studies. 2) They can improve quantitative risk assessments and exposure reduction studies for tobacco smoke exposures. 3) They can provide a tool for assessing individual exposure for smoking intervention programs and chemoprevention studies. 4) They can provide data for studies regarding smoking cessation in special populations such as adolescents, pregnant women, or medical patients with smoking-related diseases. 5) They can be used to evaluate and improve upon the accuracy of self-reported status smoking in observational studies, as well as expand our knowledge on the utility of hair biomarkers for determining ETS and PTS exposures.

The Environmental Protection Agency (EPA) estimates that the exposure to B(a)P is 1-3 ug/day for nonsmokers [76]. It has been determined that the predominant pathways of exposure to B(a)P for nonsmokers is through inhalation of polluted air and ingestion of food containing B(a)P [186]. The major route of exposure for smokers, however is through inhalation of PTS and ETS [186]. The amount of B(a)P exposure in smokers can vary widely, but has been approximated at 1-30 ug/pack/day [63, 82-85]. Polycyclic aromatic hydrocarbons (PAHs) have also been demonstrated to be 3-4 times higher in ETS [187], so indoor smoking can lead to even higher levels of B(a)P exposure [186]. Although

it is considered a minor route of exposure, B(a)P can also be absorbed through the skin [188].

The metabolic activation and detoxification of B(a)P varies widely among humans and a large interindividual variation has been noted [73, 127, 189-193]. Higher metabolic activity to form the reactive metabolite BPDE, or lower detoxification of BPDE, would presumably be associated with a higher risk of cancer. Measurement of biomarkers that can reflect this higher cancer risk would be of great importance. Using a biomarker in a surrogate tissue such as hair, whose collection is noninvasive and which serves as a marker for cumulative exposures, would have major advantages over tradition matrices. Additionally, hair biomarkers for nicotine and cotinine have been demonstrated to identify exposure for up to 10 weeks posttobacco use, thus providing a larger window of detection and a more accurate account of tobacco smoke exposure [194].

Protein adducts can serve as a measure of internal dose of a carcinogen. While DNA is the target in carcinogenesis, BPDE-DNA adducts levels are generally too low to detect in blood [60]. For this reason, protein adducts are employed as surrogates for DNA adducts because of their greater availability from blood. Additionally, BPDE-protein adduct levels have been demonstrated to reflect genetic damage, and have a strong degree of correlation with BPDE-DNA adducts [60, 98, 127]. Previous methods have used BPDE adducts to Hb and serum albumin as surrogates for BPDE-DNA adducts [60, 98, 127]. These protein adducts are much easier to collect in large quantities, compared to DNA adducts, and they are not subject to enzymatic repair [127]. Since it is difficult to

obtain lung tissue from human subjects, the ability to establish a relationship between B(a)P and/or BPDE-protein adducts in hair to that found in the lung, would be an invaluable tool for assessing toxic ETS and PTS exposures.

The experiments presented in this chapter were designed to address the following objectives: 1) Develop sensitive and specific GC/MS analytical methods to detect B(a)P and BPDE-protein adducts in human hair; 2) Determine the differences of B(a)P incorporation in smokers (those exposed to PTS) and nonsmokers (those with no exposure to PTS or ETS) hair; 3) Determine the differences in BPDE-protein adducts in the hair and Hb (from blood) of smokers and nonsmokers; 3) Determine if the concentration of B(a)P and/or BPDE-protein adducts in hair correlate to the concentration of the well characterized BPDE-Hb adduct (the positive control); 4) Verify self-reported status of smokers and nonsmokers by determining nicotine and cotinine concentrations in plasma. We hypothesized that we will be able to detect a significant difference in the concentration of B(a)P and BPDE-protein adducts measured in hair from heavy smokers vs. nonsmokers.

Materials and Methods

Chemicals and reagents

Benzo(a)pyrene (1 mg/mL) was purchased from SPEX Certiprep®, Inc. (Metuchen, NJ), Restek (Austin, TX), and AccuStandards® (2 mg/mL) (New Haven, CT) for the preparation of calibration curves and quality control samples. The internal standard B(a)P-d_{12} (1 mg/mL), was purchased from SPEX

Certiprep®, Inc. (Metuchen, NJ). BPT (5 mg) was purchased from the National Cancer Institutes Chemical Repository (Midwest Research Institute, Kansas City, MO). The internal standard [$^{13}C_6$]-BPT (1 mg), was purchased from Cambridge Isotopes Laboratories, Inc. (Andover, MA) by Dr. Stephen Hecht of Masonic Cancer Center (University of Minnesota), and generous gift of a 1200 ng/mL [$^{13}C_6$]-BPT solution (1mL in DMSO) was provided for this dissertational research. (−)-Nicotine hydrogen tartrate salt was obtained from Sigma-Aldrich® (St Louis, MO). (−)-Cotinine, (±)-cotinine-d_3 and (±)-nicotine-d_3 were obtained from Cerilliant (Austin, TX). Hexane, dichloromethane (DCM), methanol, acetonitrile, ethyl acetate were all GC/MS or high performance liquid chromatography grade and purchased from Burdick & Jackson® (Morristown, NJ & Muskegon, MI). Acetone (GC/MS grade) was purchased from EMD (Gibbstown, NJ), and anhydrous tetrahydrofuran (THF) was purchased from Sigma-Aldrich® (Milwaukee, WI). Ammonium acetate and glacial acetic acid were obtained from Spectrum (Gardena, CA). Proteinase K (from *Tritirachium album*, activity ≥30 units/mg) was purchased from Sigma-Aldrich®. The derivatization agent (*N*-Methyl-*N*-(trimethylsilyl) trifluoro-acetamide activated II, MSFTA II) was purchased from Fluka (Castle Hill, New South Wales, Australia), Sep-Pak® C18, 3cc solid phase extraction (SPE) cartridges were purchased from Waters Corporation (Milford, Massachusetts). Oasis® HLB and MCX (60 mg, 3mL) cartridges were purchased from Waters (Milford, MA). Trichloroacetic acid, concentrated formic acid, concentrated ammonium hydroxide, and all other reagent grade chemicals were purchased from Fisher Scientific (Pitsburg, PA),

Sigma-Aldrich® and Fluka. Water used was house-prepared Milli-Q water. Helium and ammonia gases used for GC/MS analysis were purchased from Airgas, Inc. ® (Salt Lake City, UT). Lyophilized human hemoglobin was obtained from Sigma-Aldrich®. RBC lysis buffer was purchased from Roche (Branford, CT) and phosphate buffered saline solution from Teknova (Hollister, CA). Sodium heparin Vacutainers® were purchased from BD (Franklin Lakes, NJ). Nicotine- and cotinine-free human plasma was obtained from BioChemed (Winchester, Virginia, USA). Hair collection kits were obtained from AgriYork (York, England).

Stocks and solutions

Intermediate stock solutions of B(a)P and B(a)P-d_{12} were prepared in 1:1 acetone/DCM at a concentration of 5000 and 500 ng/mL. Intermediate stock solutions of BPT were prepared in fresh anhydrous THF at a concentration of 5000 and 100 ng/mL. Intermediate stock solutions of [$^{13}C_6$]-BPT were prepared in fresh anhydrous THF at a concentration of 100 ng/mL. Since B(a)P and BPT are light and air sensitive, all solutions were made in amber vials with septum screw caps to avoid over exposure to light and air and stored at -20°C in air-tight jars. Matrix-fortified calibration curves and quality control samples were prepared daily. The quality control samples for B(a)P that were prepared with each batch of samples, and for determination of assay imprecision and accuracy, were fortified with a reference material from a different manufacturer than that used to prepare the calibration curve for B(a)P. Since no other commercial source was available for BPT, a separate stock and intermediate solution for the quality Control samples were prepared by the Center for Human Toxicology personnel.

For nicotine and cotinine assays, the deuterated internal standards were prepared in a single combined working solution in methanol at 1 µg/mL. This solution was stored in the freezer at -20°C until required for an analytical batch. For nicotine and cotinine, three combined calibrator working solutions were prepared in methanol at concentrations of 10 µg/mL,1 µg/mL and 0.1 µg/mL for nicotine and cotinine. Nicotine hydrogen tartrate salt (weight corrected for nicotine) was selected as it was determined to be more stable over time than nicotine free base. Separate methanolic working solutions were prepared for quality control samples at the same concentrations as the calibrator working solutions. All working solutions were stored in the freezer at −20 °C until required for an analytical batch.

Human clinical trial participants

To optimize the potential for detecting of B(a)P and/or BPDE-protein adducts (assuming incorporation may be dependent upon melanin content), only dark pigmented hair samples were obtained from subjects enrolled in human clinical trials approved by the Institutional Review Board at the University of Utah and the University at Buffalo, SUNY (Buffalo, NY). The study participants were subdivided into two groups. ***Group 1*** consisted of male and female nonsmoking participants, and ***Group 2*** consisted of male and female heavy-smoking participants (defined as smoking at least one pack of cigarettes per day).

Group 1 participants (nonsmokers) were screened by telephone using a questionnaire to exclude participants with potentially higher levels of nonsmoking-related B(a)P exposure (See *Appendix* for Screening

Questionnaire). Any subject with higher than normal consumption of smoked or charbroiled foods were excluded, along with any subject with known occupational exposure to B(a)P. Hair samples from nonsmoking participants meeting inclusion criteria (n=20) were collected by personnel from the Center for Human Toxicology at the Center for Clinical and Translational Science at the University of Utah Hospital. A "pencil-width" amount of hair (about 90-120 strands) was cut as close to the scalp as possible from each participant in the posterior vertex region of the scalp (see Figure 4.1). Hair samples were then placed in a hair collection kit to mark the root end, and stored in the dark at 4°C in a Ziploc® bag until further sample preparation.

Fresh whole blood was also obtained from the ***Group 1*** participants by venipuncture at the Center for Clinical and Translational Science (University of Utah Hospitals, Salt Lake City, UT). All blood samples were collected in sodium heparin BD Vacutainers®. Whole blood samples were then centrifuged at 3000 rpm for 10 mins to separate plasma from red blood cells (RBCs). The plasma portion (collected for determination of nicotine and cotinine levels on all participants to verify nonsmoking status) was transferred to silanized glass culture tubes and stored at -20°C until preparation for nicotine and cotinine analysis. The RBC portion remaining in the Vacutainer® was stored at 4°C until Hb preparaton.

Group 2 participants (heavy smokers), were screened by telephone by Dr. Stephen Tiffany's laboratory at the University at Buffalo, SUNY (Buffalo, NY). Heavy smokers (n=30) self-reported to have smoked at least one pack (20

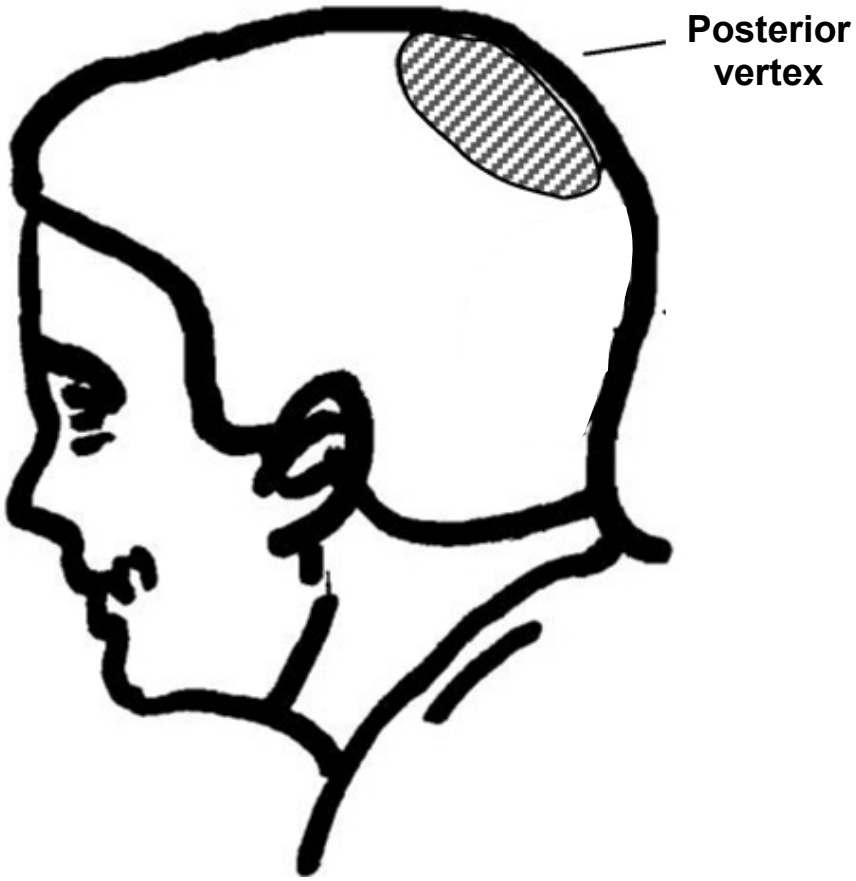

Figure 4.1 *Drawing illustrating the posterior vertex region where hair was collected. (*Adapted from [195].) Hair samples are collected from this region since approximately 85% of hairs in this region are in the active growth phase (anagen phase).

(using questions 7-9 on Screening Questionnaire, see *Appendix*), and collected cigarettes) per day. A "pencil-width" amount of hair (about 90-120 strands) was cut as close to the scalp as possible from each participant in the posterior vertex region of the scalp, then placed in a hair collection kit to mark the root end and shipped to the Center for Human Toxicology. Upon arrival, hair collection kits were placed placed in Ziploc® bags and stored in the dark at 4°C until sample preparation.

Fresh whole blood was also obtained from the ***Group 2*** participants by venipuncture by a registered nurse employed by the University at Buffalo, SUNY (Buffalo, New York). All blood samples were collected in sodium heparin BD Vacutainers®. Whole blood samples were then centrifuged at 3000 rpm for 10 mins to separate plasma from red blood cells (RBCs). The plasma portion (collected for determination of nicotine and cotinine concentrations on all participants to verify self-reported current smoking status) was transferred to silanized glass culture tubes and stored at -20°C until shipped to the Center for Human Toxicology. The RBC portion remaining in the Vacutainer® was stored at 4°C until shipped. Plasma and RBCs were kept cold during transport with ice packs. Plasma samples were then stored at -20°C until preparation for nicotine and cotinine analysis. The RBCs were stored at 4°C until Hb preparation.

B(a)P Assay

B(a)P: Hair preparation and extraction

The first three centimeters of hair from the root end was removed from

each sample, then homogenized by cutting into 2-3 mm segments. Hair (100 mg, ±10%) was then accurately weighed (Mettler Toledo, AG104). The hair samples analyzed therefore represent approximately the last 3 months of exposure based on an assumption of an average 1 cm/month growth rate [11]. B(a)P-d_{12} internal standard (IS) (100 pg/mg) was then added to each sample. Calibrators (10-100 pg/mg) and QC's (45, 60, 80 pg/mg) were concurrently prepared by fortification of B(a)P and IS to analyte-free (blank) human hair. After digestion of the hair in 1.0 mL of 1 N sodium hydroxide for 1 hr in a shaker, a 0.100 mL aliquot of concentrated hydrochloric acid was added to neutralize the sample. Samples were then centrifuged at 3500 rpm for 4 mins and subsequently subjected to solid phase extraction (SPE). The SPE was performed as follows: 2.5 mL of methanol followed by 2.5 mL of Milli-Q water was used to condition the column. The liquid portion from the centrifuged hair sample was then decanted into the SPE cartridge (to improve complete transfer, 1 mL of Mill-Q water was added to each hair sample, centrifuged again at the specified conditions, and the liquid portion decanted into the SPE cartridge). The columns were then washed with 2.5 mL of water followed by 2.5 mL of 10% aqueous methanol (v/v). Samples were eluted by the addition of two volumes of 2.5 mL 1:1 acetone/ dichlormethane. Eluents from samples were dried under a constant stream of nitrogen in a Zymark Turbovap® LV evaporator at 55°C. Residues were then reconstituted in 0.100 mL of 1:1 acetone/ dichloromethane and analyzed by GC/MS-EI- SIM (see *GC/MS-EI-SIM analysis for B(a)P* section for additional details).

BPT Assays

BPT: Hair preparation and extraction

Multiple digestion and extraction methods were initially evaluated in order to detect BPT and IS fortified to analyte-free human hair. First, the enzymatic extraction method for the release of BPT from BPDE-protein adducts in rat hair, which we previously validated (Chapter 2, *Materials and Methods* section), was evaluated for use with human hair. Preparation and extraction were as follows: Analyte-free (blank) human hair (100 mg ($\pm$10%)) was weighed (Mettler Toledo, AG104) and BPT and [$^{13}C_6$]-BPT IS (100 pg/mL) were added. To each hair sample, 2 mL of 200 ug/mL Proteinase K in incubation buffer (50 mM Tris buffer, 5 mM calcium chloride, pH 8.5) was added to liberate any bound analyte from hair shaft constituents. Samples were then placed in a sonicator for 1 hr (~37°C) and then transferred to a 37°C water bath and allowed to incubate overnight (total time ~20 hrs). After cooling, approximately 0.25 g of sodium chloride (NaCl) was added to each sample. A liquid-liquid extraction was then performed. Ethyl acetate (6 mL) was added to each hair digestion solution, which was then thoroughly vortex mixed followed by centrifugation at 3500 rpm for 4 mins. The liquid-liquid extraction was performed twice, and then the combined organic fractions were placed in a Zymark Turbovap® LV evaporator at 55°C under a constant stream of N_2 until dry. The residues were then derivatized by adding 50 uL of MSTFA and allowing for 15 mins reaction time in a heating block at 80°C. Samples, in MSTFA, were then transferred to autosampler vials for analysis by

GC/MS-NCI-SIM (see *GC/MS-NCI-SIM analysis for BPT* section for additional details).

In addition to the enzymatic digestion and extraction procedure outlined above, numerous other analytical digestions and extraction techniques were evaluated. These included: acidic (using varying concentrations of hydrochloric and sulfuric acid solutions), alkaline (using varying concentrations of sodium hydroxide and sodium sulfide solutions), and solvent digestions (using methanol) of BPT (and IS) fortified human hair samples. These hair sample digests were then coupled to either liquid-liquid (using hexane or ethyl acetate) and/or SPE (using various types of SPE cartridges) extraction techniques.

BPT: Hemoglobin preparation from whole blood and extraction

The RBCs from whole blood were isolated using a modified procedure from Ragin et al. [93]. Upon arrival of ***Group 1*** and/or ***Group 2*** samples to the laboratory, the RBC portion from whole blood was washed twice with equivalent volumes of 0.9% sodium chloride solution in Milli-Q water to remove any free, unbound BPT (from metabolism by epoxide hydrolase or reaction with water). One volume of phosphate buffered saline (PBS) was then added, and two volumes of RBC lysis buffer to re-suspend the RBCs (e.g., 3 mL RBCs then 3 mL of PBS and 6 mL of RBC lysis buffer). This was done to keep volumes of reagents used consistent between samples of differing volumes. The samples were then gently shaken for 10 mins for lysis of RBCs, followed by centrifugation at 2000 rpm to pellet ghost membranes. The supernatant was removed from each sample, and six volumes of ice-cold acetone (with 0.015% hydrochloric

acid) was slowly added dropwise to precipitate Hb. After 5 mins, the samples were centrifuged to pellet the precipitated Hb, and the excess fluid was decanted. The Hb pellet was then taken to dryness in a Zymark Turbovap® LV evaporator under a constant stream of nitrogen at 37°C and stored at -80°C until preparation for analysis. A 200 mg (± 10%) aliquot of Hb (prepared as described above) was weighed (Mettler Toledo, AG104) and IS (10 pg/mg) added. Calibrators (1.75-10 pg/mg) were concurrently prepared by fortification of BPT and IS to analyte-free (blank) human Hb. Two milliliters of NANOpure™ water and 30 uL of 6 N hydrochloric acid were added to each Hb sample, tightly capped, and placed in a water bath for 3 hrs at 90°C. Samples were allowed to cool, then approximately 0.25 g of sodium chloride was added to each sample. A liquid-liquid extraction was then performed. Ethyl acetate (6 mL) was added to each Hb hydrosylate, then thoroughly vortex-mixed, and centrifuged at 3500 rpm for 4 mins. The liquid-liquid extraction was performed twice, and the combined organic fractions were placed in a Zymark Turbovap® LV evaporator @ 52°C under a constant stream of N_2 until dry. MSTFA (50 uL) was added to the residues and a 15 min reaction time was allowed in a hot block at 80°C. Samples were then transferred to autosampler vials for analysis by GC/MS-NCI-SIM (see *GC/MS-NCI-SIM analysis for BPT* section for additional details).

Nicotine and cotinine: Plasma preparation and extraction

Plasma samples for participants were analyzed according to the laboratory's validated published method [196]. One mL of each participant's plasma sample was fortified with internal standards (50 ng/mL). Calibrators (1-

50 ng/mL for nicotine and 1-100 ng/mL for cotinine) and QC's (5, 25, 45 ng/mL for nicotine; 1, 10, 100 ng/mL for cotinine) were concurrently prepared by fortification of nicotine and cotinine plus respective internal standards to 1 mL of analyte-free plasma. To aid in matrix clean-up, 1 mL of 10 % aqueous trichloroacetic acid was added to each of the plasma samples, vortexed, and then centrifuged for 10 mins at 1100x g. The acidified plasma supernatant was then subjected to SPE using a combination of Oasis® HLB and Oasis® MCX mixed mode cartridges. The SPE cartridges were conditioned with 2 mL methanol followed by 2 mL 10% aqueous trichloroacetic acid. The samples were loaded onto the cartridges and subsequently eluted with 2 mL methanol containing 5% concentrated aqueous ammonium hydroxide (v/v). One hundred µL of 1% concentrated aqueous hydrochloric acid in methanol (v/v) were then added prior to evaporation of the eluant. Extracts were evaporated to dryness under a stream of air at 40 °C using a Zymark Turbovap® LV evaporator. Extracted plasma residues were reconstituted in 150 µL of initial mobile phase (10 mM ammonium acetate with 0.001 % formic acid (A) (pH 5): methanol (B) (85:15 v/v)). (See *LC-MS/MS analysis of nicotine and cotinine* section for additional details).

GC/MS-EI-SIM analysis for B(a)P

A Hewlett Packard (HP) GC 6890 was fitted with an Agilent DB-5UI-MS capillary column (part no. 122-5535UI, 30.0 m x 250 um x 0.25 um nominal). The injector was operated in the pulsed splitless mode (injection pulse 40 psi until 0.2 min, purge flow to split vent 30 mL/min at 0.75 min). The pressure of helium gas

was programmed to 17.0 psi (total flow 33.8 mL/min). The inlet heater temperature was set at 300°C and the transfer line was set at 300°C. The injection volume was 1 uL. The solvent delay was set at 7 mins. The initial oven temperature was set at 120°C for 1 min, then ramped to 250°C at 25°C/min A 2nd ramp to 320°C at 10°C /min followed, then oven was held at 320°C for 0.5 mins. The total run time equaled 16.7 mins. An HP MS 5973 was used to perform selective ion monitoring (SIM) to detect B(a)P at *m/z* 252 and its fragment at *m/z* 126. B(a)P-d_{12} was detected at *m/z* 264. To quantitate the results, ChemStation software (version: D.02.00.275) was used to generate calibration curves from peak area ratios of target analyte to the corresponding deuterated internal standard across the concentration range of specified calibrators.

GC/MS-NCI-SIM analysis for BPT

The same GC/MS system and column was used as stated in the GC/MS-EI-SIM analysis. The injector was operated in the pulsed splitless mode (injection pulse 17.6 psi until 1.33 min, purge flow to split vent 30 mL/min at 1.75 min). The pressure of helium gas was programmed to 24.3 psi (flow 2.2 mL/min, total flow 34.5 mL/min). Ammonia reagent gas pressure was set at 17.0 mL/min The inlet heater temperature was set at 280°C. The transfer line was set at 300°C. The injection volume was 2 uL and the solvent delay was set at 9.0 mins. The initial oven temperature was set at 120°C for 1 min, then ramped to 250°C at 20°C/min A 2nd ramp to 300°C at 8°C /min followed. The total run time equaled 13.75 mins. SIM was used to detect the derivatized BPT molecule at *m/z* 446 (no other fragment was present for inclusion in SIM). The derivatized ($^{13}C_6$)-BPT molecule

was detected at *m/z* 452. To quantitate the results, ChemStation software (version: D.02.00.275) was used to generate calibration curves from peak area ratios of target analyte to the corresponding deuterated internal standard across the concentration range of specified calibrators.

LC-MS/MS analysis of nicotine and cotinine

An Acquity UPLC® system (Waters®, Milford, MA) and a Discovery® HS F5 HPLC column (100 mm × 4.6 mm, 3 µm, Supelco®, Bellefonte, PA) was used for analysis of nicotine and cotinine to verify nonsmoking and heavy smoking self-reported status of participants. A gradient consisting of 10 mM ammonium acetate with 0.001 % formic acid (pH 4.97) (A), and methanol (B) was used at a flow rate of 0.6 mL/min The initial mobile phase condition was 15% B which was increased linearly to 76 % after 11 mins, then decreased back to the initial mobile phase condition of 15 % B after 11.6 mins and held for 3.4 mins to re-equilibrate the LC column. The mass spectrometer was operated in positive ion electrospray mode using multiple reaction monitoring (MRM) data acquisition. Two MRM transitions were monitored for both nicotine (163.2 → 130.0 and 163.2 →116.9) and cotinine (177.2 → 79.9 and 177.2→ 97.9). The following ESI conditions were applied: capillary voltage 3.25 kV; source temperature 100°C; desolvation temperature 350°C; desolvation gas (nitrogen) 600 L/h; cone gas (nitrogen) 50 L/h; collision cell pressure (argon) $7.38e^{-3}$ mbar; and collision gas flow rate 0.35 mL/min Mass spectrometric analysis was performed using a Quattro Premier XE™ triple quadrupole mass spectrometer (Waters® Corporation, Milford, MA) with MassLynx™ v 4.1 software. Calibration curves

generated from peak area ratios of target analyte quantification ions to their corresponding deuterated internal standard quantification ions, across the concentration ranges of the calibrators. The calibration graphs were generated using the TargetLynx™ feature of the MassLynx™ v 1.4 software and also using Microsoft® Office Excel 2007.

Results

Analytical method for B(a)P in human hair

We originally planned to validate a quantitative method for detection of B(a)P in human hair with a sensitivity at or below 1 pg/mg. However we were unable to achieve adequate reproducibility (CV<20%) at concentrations below 20 pg/mg; therefore, the following qualitative method was developed.

Figure 4.2 shows representative ion chromatograms for an extracted B(a)P-fortified (75 pg/mg) human hair and an extracted blank human hair sample. The assay was determined to be linear from 20 to 100 pg/mg. The limit concentration of analyte at which the qualifying secondary ion was present and the chromatograms for ions of interest showed Gaussian peak shape with S/N ratio $\geq$ 3.

Samples for determination of assay accuracy and imprecision were prepared with a stock solution purchased from a different manufacturer from that used to make the calibration curve standards. The intraassay accuracy and imprecision of the method were determined by analyzing replicate samples of multiplied by 100 to obtain a percentage. The percent CV calculated from the

Figure 4.2 *Representative ion chromatograms from (A) extracted analyte-free (blank) human hair sample and (B) an extracted B(a)P-fortified (75 pg/mg) human hair sample.* Analyte retention time (RT) is on the x-axis and signal intensity on the y-axis. B(a)P = 252 *m/z* and B(a)P-d_{12} = 264 *m/z*

A.

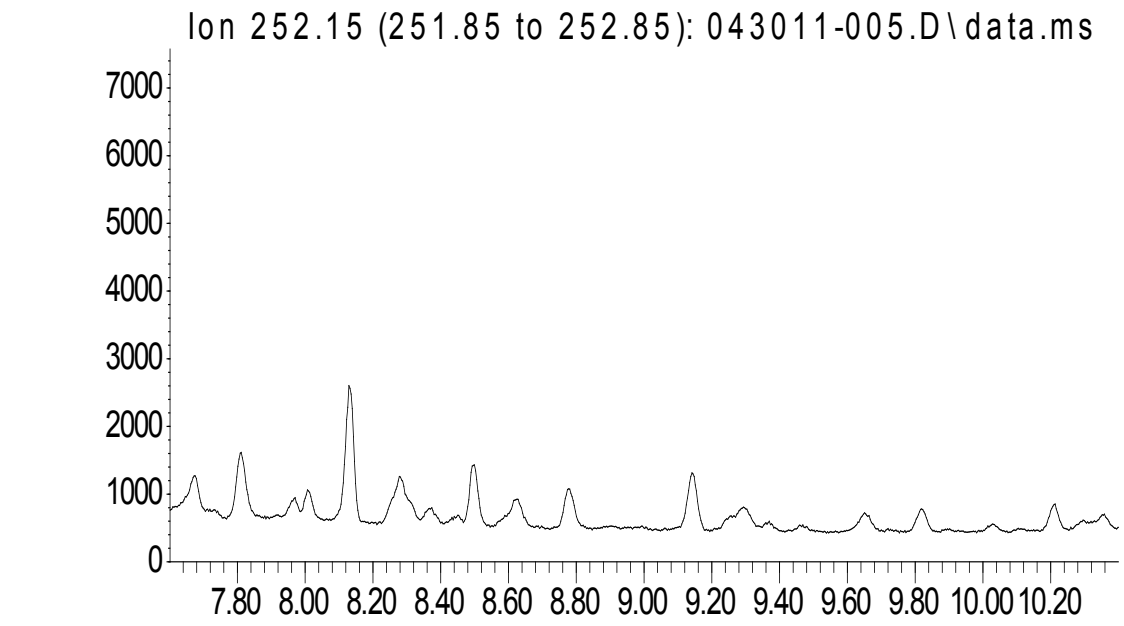
Abundance
Ion 252.15 (251.85 to 252.85): 043011-005.D\data.ms
7000
6000
5000
4000
3000
2000
1000
0
7.80 8.00 8.20 8.40 8.60 8.80 9.00 9.20 9.40 9.60 9.80 10.00 10.20
Time-->

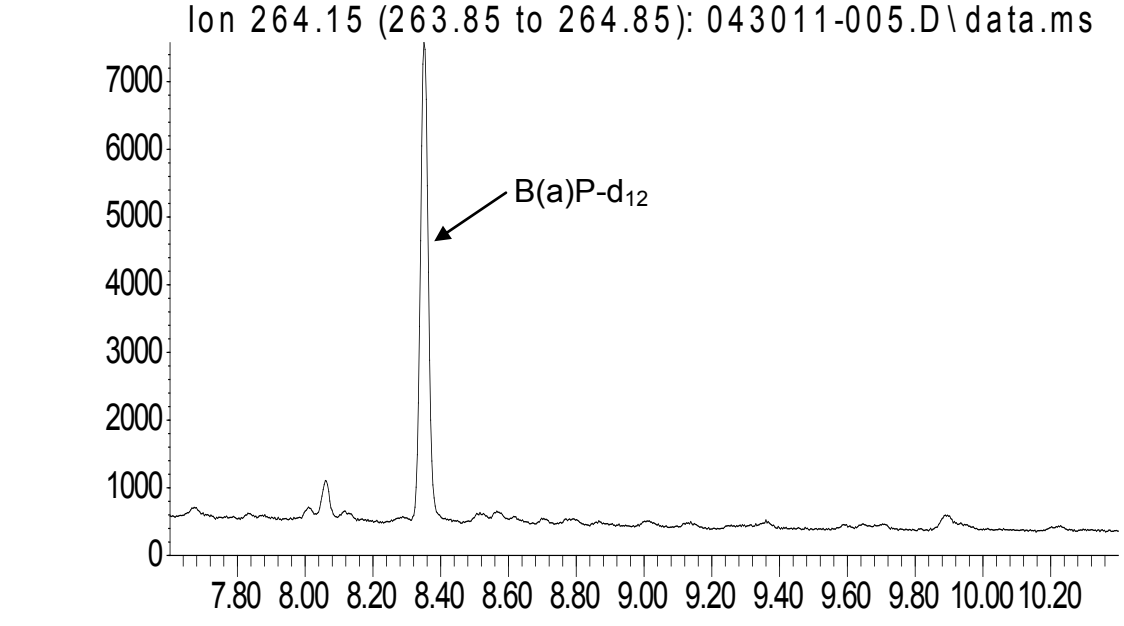
Abundance
Ion 264.15 (263.85 to 264.85): 043011-005.D\data.ms
7000
6000
5000
4000
3000
2000
1000
0
B(a)P-d12
7.80 8.00 8.20 8.40 8.60 8.80 9.00 9.20 9.40 9.60 9.80 10.00 10.20
Time-->

B.

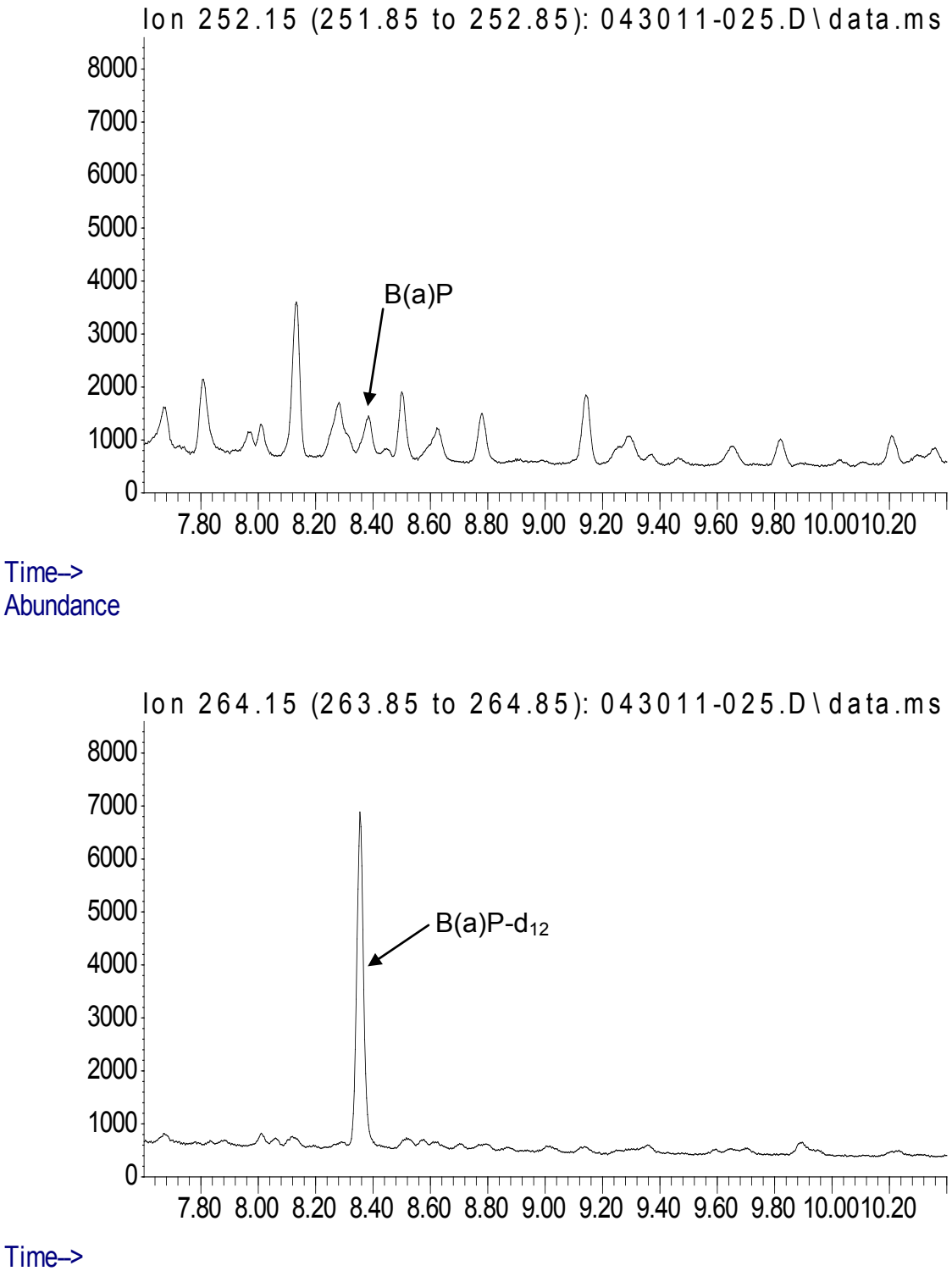
Abundance
Ion 252.15 (251.85 to 252.85): 043011-025.D\data.ms
8000
7000
6000
5000
4000
3000
2000
1000
0
B(a)P
7.80 8.00 8.20 8.40 8.60 8.80 9.00 9.20 9.40 9.60 9.80 10.00 10.20
Time-->
Abundance
Ion 264.15 (263.85 to 264.85): 043011-025.D\data.ms
8000
7000
6000
5000
4000
3000
2000
1000
0
B(a)P-d12
7.80 8.00 8.20 8.40 8.60 8.80 9.00 9.20 9.40 9.60 9.80 10.00 10.20
Time-->

mean observed concentrations of samples tested is an estimated of imprecision. The percent CV was calculated by dividing the standard deviation of the samples tested by the mean observed concentration of the samples. This value was then of detection (LOD) was 20 pg/mg. The LOD was defined as the lowest multiplied by 100 to obtain a percentage. Acceptable accuracy (% difference compared to target concentration within ± 20 %) and imprecision (%CV<20) for low, medium and high concentrations of B(a)P-fortified human hair were demonstrated within an analytical batch (Table 4.1).

Analytical Method for BPT in Human Hair

Figure 4.3 shows representative chromatograms from an extracted 10 pg/mg BPT-fortified 100 mg human hair sample (same preparation and extraction as described in Chapter 2 for rat hair). The chromatographic peaks indicated for BPT and IS in this figure illustrate the significantly reduced sensitivity and recovery of BPT in fortified human hair, as compared to that observed for rat hair (refer to Figure 2.6 in Chapter 2 for 5 pg/mg BPT-fortified rat hair chromatograms). The IS response is approximately 95% lower than what was observed for rat hair matrix. Therefore, the digestion and extraction procedure that was used for the rat hair was determined to be inadequate for determination of BPT in human hair.

Several other digestions and extractions of BPT and IS fortified human hair samples were attempted. The details for these digestions and extractions are shown in Table 4.2. For most digested and extracted samples, we were unable to detect the BPT that was fortified, with the exception of one procedure,

Table 4.1

Accuracy and imprecision of B(a)P-fortified human hair

	Target Concentration pg/mg	n[a]	Mean Concentration pg/mg	% of Target	%CV[b]
Intraassay					
	45.0	3*	40.9	90.8	2.9
	60.0	3*	63.2	105.3	12.6
	80.0	4	82.7	103.4	16.6
	Target Concentration pg/mg	**n[a]**	**Mean Concentration pg/mg**	**% of Target**	**%CV[b]**
LOD					
	20.0	4	23.1	115.7	6.0
ULOD					
	100.0	4	98.9	98.9	15.1

[a] Number of quality control replicate samples used
[b] CV= coefficient of variation
* Replicate sample in set did not get injected

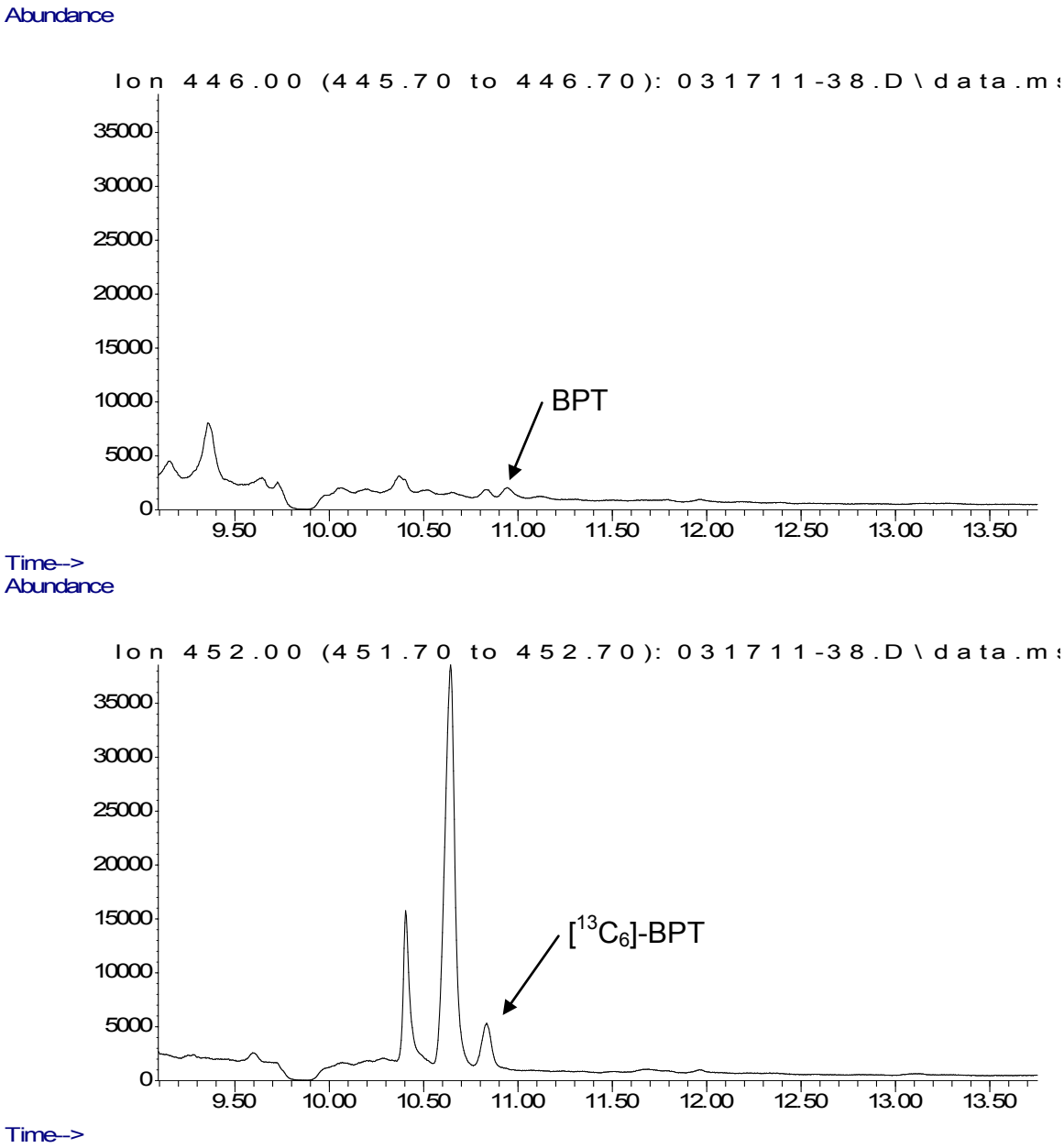

Figure 4.3 *Ion chromatograms from an extracted BPT-fortified (10 pg/mg) human hair sample.* These chromatograms illustrate the reduced sensitivity for the detection of BPT in human hair (refer to Figure 2.6 in Chapter 2 for 5 pg/mg BPT-fortified rat hair ion chromatograms). Analyte retention time (RT) is on the x-axis and signal intensity on the y-axis. B(a)P = 252 *m/z* and B(a)P-d_{12} 264 *m/z*

Table 4.2

BPT-fortified human hair digestions and extractions

Concentration of BPT added (pg/mg)	Amount of hair used (mg)	Digestion	Extraction	Detection	Reference**	Notes
5	100	1 mL of 2.5 M NaOH and sonication for 2 hrs	Liquid-liquid with hexane*	ND	[59]	#
5	100	1 mL of 1 N NaOH and sonication for 1 hr	Liquid-liquid with ethyl acetate*	ND	n/a	#
5	100	1 mL of 2.5 M NaOH and sonication for 2 hrs	SPE with Oasis® MAX cartridge*	ND	[197]	#
5	100	1 mL 1 M Na_2S, 37°C overnight	Liquid-liquid with ethyl acetate*	ND	[198]	#
5	50	2 mL 1 M Na_2S, 37°C overnight	Liquid-liquid with ethyl acetate*	ND	[198]	#
10	100	1 mL proteinase K solution, 1 hr sonication, and over-night incubation at 37C	Liquid-liquid with ethyl acetate	ND	[199]	#
10	200	1 mL proteinase K solution, 1 hr sonication, and overnight incubation at 37C	Liquid-liquid with ethyl acetate	ND	[199]	#
80	100	1 mL proteinase K solution, 1 hr sonication, and overnight incubation at 37°C	SPE with C18 cartridge	<10%	[199]	#
80	100	1 mL 1 M Na_2S, 2 hrs sonication	Liquid-liquid with ethyl acetate*	ND	[198]	#
80	100	2 mL of 1 N HCl overnight digestion at room temperature	SPE with C18 cartridge	ND	[109]	#
100	100	30 uLof 6 N H_2SO_4, 3 hrs incubation at 90°C	Liquid-liquid with ethyl acetate followed by SPE with C18 cartridge	ND	[93]	***
100	100	60 uL of 6 N H_2SO_4, 3 hrs incubation at 90°C	Liquid-liquid with ethyl acetate followed by SPE with C18 cartridge	ND	[93]	***
100	100	120 uL of 6 N H_2SO_4, 3 hrs incubation at 90°C	Liquid-liquid with ethyl acetate followed by SPE with C18 cartridge	ND	[93]	***
100	100	Sonication in 3 mL of methanol	n/a	ND	[109]	#

ND – not detected; * Sample was neutralized with hydrochloric acid before extraction; **Methods were modified slightly; ***Peak for BPT may be shifted; #Poor chromatography

in which we were able to recover approximately 10% of the BPT that was added. Varying the ionic strength of the digestion solutions used, and/or the temperature and length of the digestion, did not improve the detection of BPT in human hair. Furthermore, poor chromatography, as defined by lack of Gaussian peak shape, was observed for most of the samples. In summary, we were unable to develop a GC/MS method for BPT in human hair with a sensitivity below 100 pg/mg BPT in fortified human hair.

Analytical method for BPT: Hemoglobin

Figure 4.4 shows representative chromatograms for an extracted 1.75 pg/mg calibration standard and an extracted blank human Hb sample. The assay was determined to be linear from 1.75 to 10 pg/mg. The LLOQ and ULOQ were 1.75 and 10 pg/mg, respectively. The coefficient of variations (CV) for intra- and interassay imprecision were less than 10% (Table 4.3).

The stock and intermediate solutions for accuracy and imprecision for intra- and interassay samples were made by the quality control officer or other Center for Human Toxicology personnel (since only one commercial supplier exists for BPT). The stock and intermediate solutions used to make the calibration standards were prepared by Sarah Campbell.

Accuracy was calculated by first dividing the observed concentration by the target concentration then multiplying by 100 to obtain a percentage. The percent CV calculated from the mean observed concentrations of samples tested estimates imprecision. The percent CV was calculated by dividing the standard

Figure 4.4 *Representative ion chromatograms from (A) extracted analyte-free (blank) human Hb sample and (B) an extracted BPT-fortified (1.75 pg/mg, LLOQ) human Hb sample.* Samples shown were also fortified with the internal standard ($^{13}C_6$)-BPT. Analyte retention time (RT) is on the x-axis and signal intensity on the y-axis. Derivatized BPT = 446 *m/z* and derivatized [$^{13}C_6$]-BPT = 452 *m/z*

A.

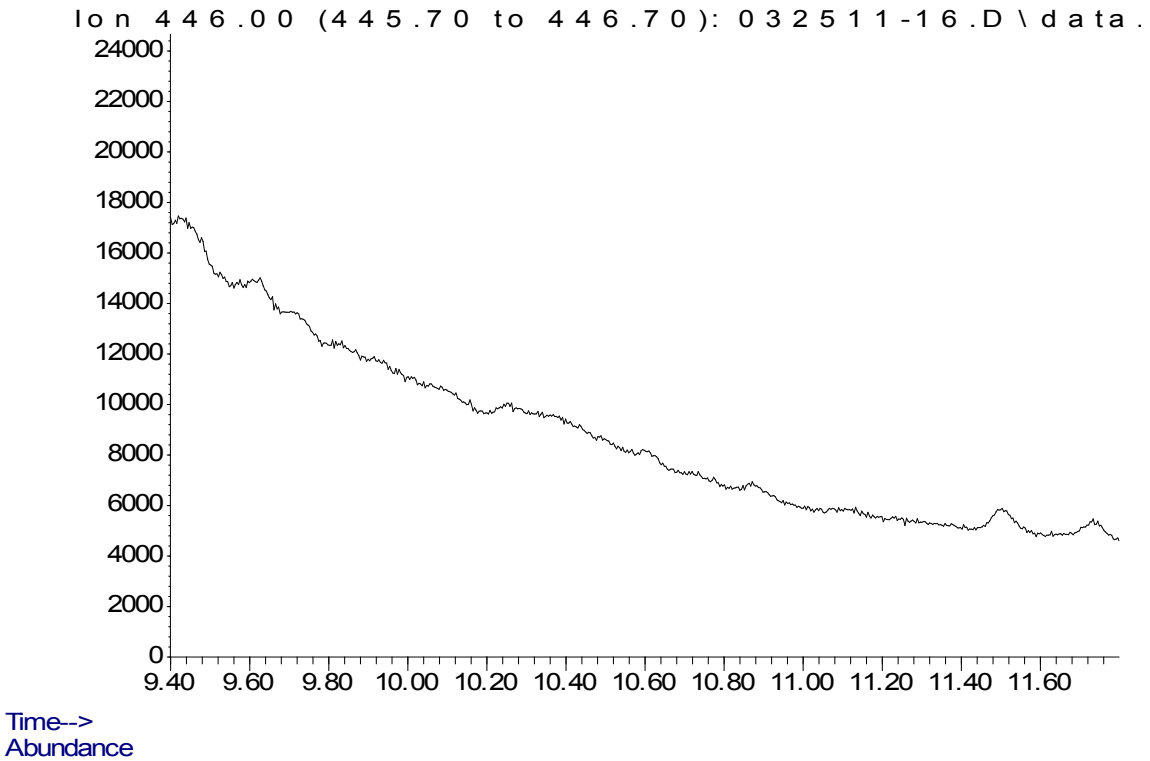
Abundance
Ion 446.00 (445.70 to 446.70): 032511-16.D \ data.
24000
22000
20000
18000
16000
14000
12000
10000
8000
6000
4000
2000
0
9.40 9.60 9.80 10.00 10.20 10.40 10.60 10.80 11.00 11.20 11.40 11.60
Time-->

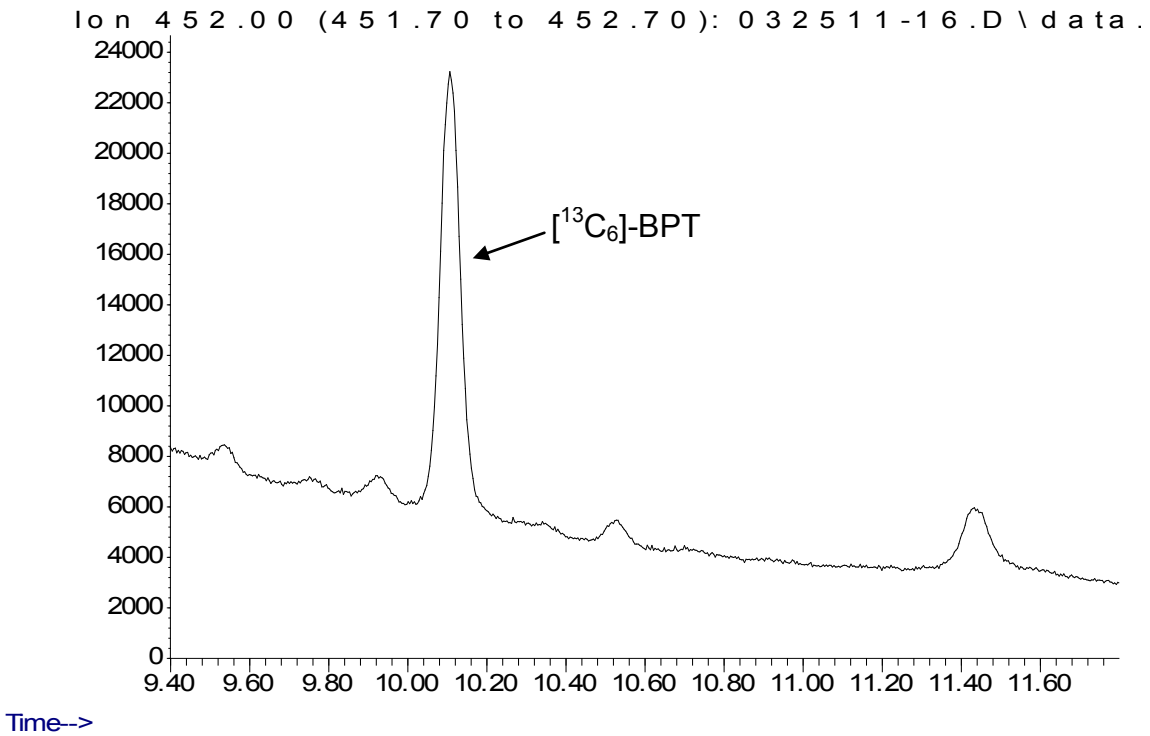
Abundance
Ion 452.00 (451.70 to 452.70): 032511-16.D \ data.
24000
22000
20000
18000
16000
14000
12000
10000
8000
6000
4000
2000
0
[13C6]-BPT
9.40 9.60 9.80 10.00 10.20 10.40 10.60 10.80 11.00 11.20 11.40 11.60
Time-->

B.

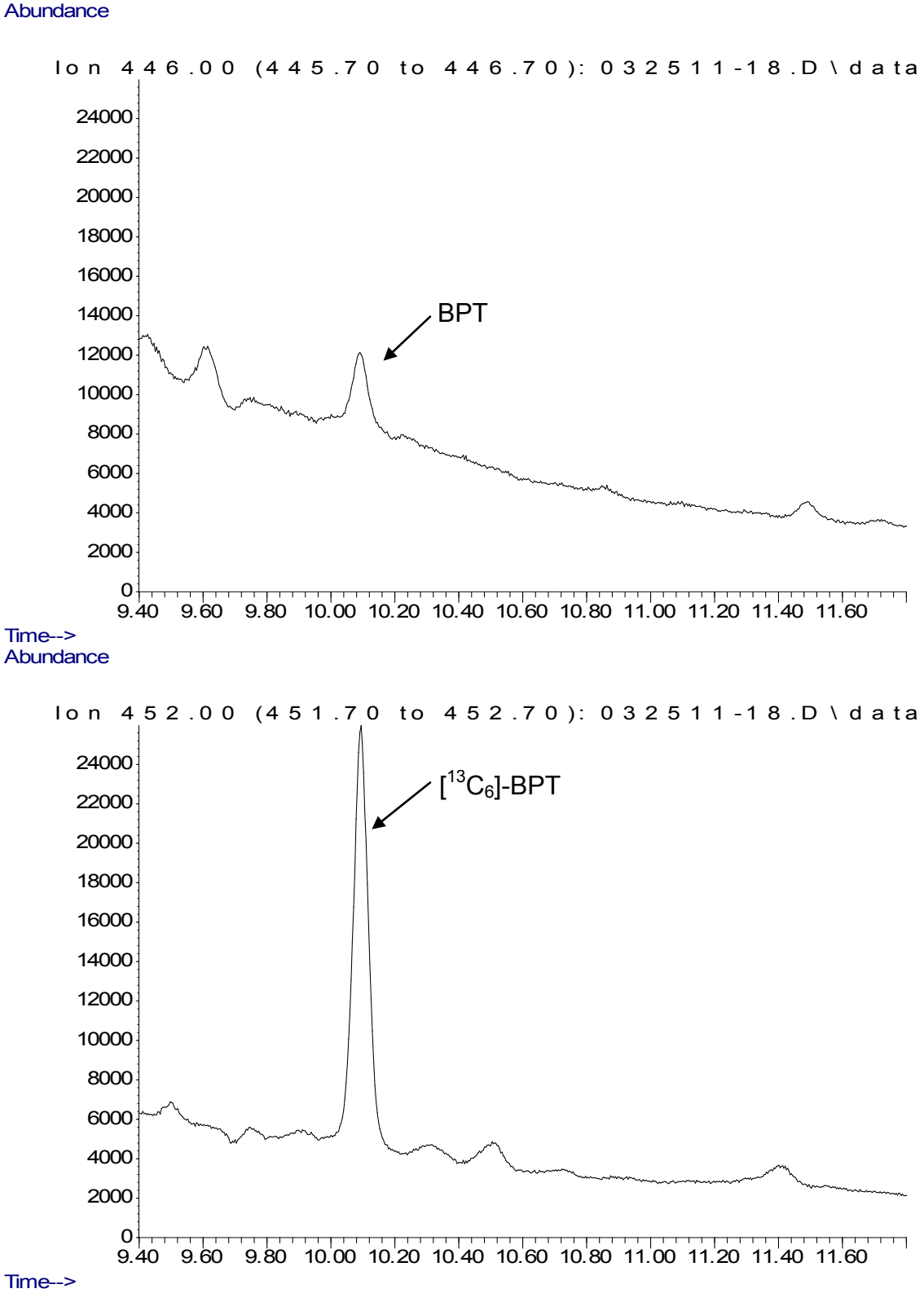
Abundance
Ion 446.00 (445.70 to 446.70): 032511-18.D \ data
24000
22000
20000
18000
16000
14000
12000
10000
8000
6000
4000
2000
0
BPT
9.40 9.60 9.80 10.00 10.20 10.40 10.60 10.80 11.00 11.20 11.40 11.60
Time-->
Abundance
Ion 452.00 (451.70 to 452.70): 032511-18.D \ data
24000
22000
20000
18000
16000
14000
12000
10000
8000
6000
4000
2000
0
[13C6]-BPT
9.40 9.60 9.80 10.00 10.20 10.40 10.60 10.80 11.00 11.20 11.40 11.60
Time-->

Table 4.3

Accuracy and Imprecision of BPT-fortified Human Hb

	Target Concentration pg/mg	n[a]	Mean Concentration pg/mg	% of Target	%CV[b]
Intraassay					
	3.75	5	3.56	94.8	6.3
	6.25	5	5.93	94.8	8.2
	8.75	5	9.05	103.5	5.5
Interassay					
	3.75	15	3.70	98.6	6.5
	6.25	15	6.19	99.1	5.9
	8.75	15	9.22	105.4	7.8

	Target Concentration pg/mg	n[a]	Mean Concentration pg/mg	% of Target	%CV[b]
LLOQ					
	1.75	4*	1.60	91.3	17.2
ULOQ					
	10.00	5	10.05	100.5	8.4

[a] Number of quality control replicate samples used
[b] CV= coefficient of variation
*Sample in group did not get injected

deviation of the samples tested by the mean observed concentration of the samples. This value was then multiplied by 100 to obtain a percentage.

The intraassay accuracy and imprecision were determined by analyzing five replicate samples of analyte-free human Hb fortified with known amounts of BPT at 3.75, 6.25, and 8.75 pg/mg, and analyzed within a single batch. The intra- assay accuracy ranged from 94.8-103.5% of the theoretical target concentrations. The intraassay imprecision ranged from 5.5- 8.2%.

Interassay accuracy and imprecision were determined by comparing calculated concentrations from replicates (n=5 for each concentration, total n=15) of analyte-free human Hb samples fortified with BPT at 3.75, 6.25, 8.75 pg/mg and analyzed in three separate analytical batches on 3 separate days. The interassay accuracy ranged from 98.6 -105.4% of the theoretical target concentrations. The interassay imprecision ranged from 5.9-7.8%.

The LLOQ was evaluated by the analysis of five replicates of BPT-fortified to analyte-free human Hb at 1.75 pg/mg. The average accuracy for these samples was 91.3%, and the imprecision was 17.2%.

The ULOQ was evaluated by the analysis of five replicates of BPT-fortified to analyte-free human Hb at 10 pg/mg. The average accuracy for these samples was 100.5%, and the imprecision was 8.4%.

Results for clinical trial participants

The analytical results for heavy smoking and nonsmoking participants are presented in Table 4.4 along with the demographics for each participant.

First, the self-reported smoking status for 25 of 30 participants was

Table 4.4

Results for human clinical trial samples

SUBJECT	GENDER	AGE	HAIR COLOR	BRAND	CPD	Hair B(a)P[a]	Hair BPDE-protein adducts[b]	Hb BPDE-Hb Adducts[c] (pg/mg)	Plasma Nicotine[e] (ng/mL)	Plasma Cotinine[f] (ng/mL)
101	M	38	Brown	Seneca	28	Negative	QNS	ND	29.3	351.2
102	F	25	Black	Newport Menthol	25	Negative	QNS	9.1	20.7	488.0
103	F	42	Brown	Niagara Light 100's	30	Negative	QNS	ND	NA	NA
104	F	32	Black	Marlboro menthol	26	Negative	QNS	ND	7.1	148.3
105	F	30	Light Brown	Exact Lights	25	**Positive**	QNS	ND	13.9	137.1
106	M	33	Brown	Newport	20	Negative	QNS	ND	ND	303.3
107	F	19	Auburn	Marlboro	22	Negative	QNS	ND	23.7	327.4
109	F	29	Brown	Seneca	23	Negative	QNS	ND	24.2	413.2
111	F	38	Dark Brown	Marlboro Lights	25	Negative	QNS	ND	12.8	243.0
112	M	40	Black	Marlboro	20	Negative	QNS	ND	11.4	202.7
114	F	37	Brown	Newport	30	**Positive**	QNS	ND	18.2	371.4
115	M	45	Black	Exact lights	25	Negative	QNS	ND	14.8	247.6
116	F	28	Brown	Newport	30	**Positive**	QNS	ND	23.6	353.8
117	M	42	Dark Brown	Newport	25	Negative	QNS	ND	13.4	148.5
118	M	30	Brown	Marlboro	20	Negative	QNS	ND	11.9	246.4
120	M	21	Light Brown	Marlboro Reds	25	Negative	QNS	ND	11.6	164.9
122	M	27	Dark Brown	Marlboro	30	**Positive**	QNS	ND	NA	NA
123	M	39	Dark Brown	Newport 100’s	20	Negative	QNS	9.7	12.8	94.9
124	M	23	Brown	Signal	20	Negative	QNS	ND	14.5	294.8

CPD – cigarettes per day; ND – not detected; QNS – quantity not sufficient; NA – not available
[a] – LOD 20 pg/mg; [b] – LOD not established; [c] – LLOQ 1.75 pg/mg; [d] – LLOQ 1 ng/mL; [e] – LLOQ 1 ng/mL

Table 4.4 *(continued)*

SUBJECT	GENDER	AGE	HAIR COLOR	BRAND	CPD	Hair B(a)P[a]	Hair BPDE-protein adducts[b]	Hb BPDE-Hb Adducts[c] (pg/mg)	Plasma Nicotine[e] (ng/mL)	Plasma Cotinine[f] (ng/mL)
125	M	28	Black	any brand	40	Negative	QNS	ND	14.5	247.3
126	M	43	Black	any brand	40	Negative	QNS	ND	NA	NA
127	M	28	Dark Brown	Seneca	30	Negative	QNS	ND	42.7	340.5
128	F	34	Dark Brown	Newport	20	Negative	QNS	ND	22.4	221.7
129	M	18	Dark Brown	Marlboro	20	Negative	QNS	ND	16.8	148.2
130	F	21	Dark Brown	Marlboro Lights	22	Negative	QNS	ND	12.8	175.0
131	F	30	Black	Seneca menthol lights	25	Negative	QNS	ND	19.8	176.7
132	F	36	Brown	Newport 100s	20	Negative	QNS	ND	NA	NA
134	F	28	Black	Newport	30	Negative	QNS	ND	NA	NA
135	M	24	Dark Brown	Newport	20	Negative	QNS	ND	NA	NA
136	F	22	Light Brown	Camel	20	Negative	QNS	ND	20.9	267.5
004	F	30	Brown	Nonsmoker	-	Negative	QNS	ND	<LLOQ	<LLOQ
006	F	32	Light Brown	Nonsmoker	-	Negative	QNS	ND	<LLOQ	<LLOQ
007	M	30	Brown	Nonsmoker	-	**Positive**	QNS	ND	<LLOQ	<LLOQ
008	F	37	Blonde	Nonsmoker	-	Negative	QNS	ND	<LLOQ	<LLOQ
010	M	35	Light Brown	Nonsmoker	-	Negative	QNS	ND	<LLOQ	<LLOQ
011	F	45	Brown	Nonsmoker	-	**Positive**	QNS	ND	<LLOQ	<LLOQ
012	F	33	Dark Brown	Nonsmoker	-	Negative	QNS	ND	<LLOQ	<LLOQ
013	F	25	Light Brown	Nonsmoker	-	Negative	QNS	ND	<LLOQ	<LLOQ
014	F	27	Brown	Nonsmoker	-	Negative	QNS	ND	<LLOQ	<LLOQ
015	F	23	Brown	Nonsmoker	-	Negative	QNS	ND	<LLOQ	<LLOQ

CPD – cigarettes per day; ND – not detected; QNS – quantity not sufficient; NA – not available
[a] – LOD 20 pg/mg; [b] – LOD not established; [c] – LLOQ 1.75 pg/mg; [d] – LLOQ 1 ng/mL; [e] – LLOQ 1 ng/mL

Table 4.4 *(continued)*

SUBJECT	GENDER	AGE	HAIR COLOR	BRAND	CPD	Hair B(a)P[a]	Hair BPDE-protein adducts[b]	Hb BPDE-Hb Adducts[c] (pg/mg)	Plasma Nicotine[e] (ng/mL)	Plasma Cotinine[f] (ng/mL)
016	F	21	Dark Brown	Nonsmoker	-	Negative	QNS	ND	<LLOQ	<LLOQ
017	F	21	Dark Brown	Nonsmoker	-	Negative	QNS	ND	<LLOQ	<LLOQ
018	M	34	Black	Nonsmoker	-	Negative	QNS	ND	<LLOQ	<LLOQ
019	M	21	Brown	Nonsmoker	-	Negative	QNS	ND	<LLOQ	<LLOQ
020	F	34	Black	Nonsmoker	-	Negative	QNS	ND	<LLOQ	<LLOQ
021	M	33	Brown	Nonsmoker	-	Negative	QNS	ND	<LLOQ	<LLOQ
022	M	20	Brown	Nonsmoker	-	Negative	QNS	ND	<LLOQ	<LLOQ
027	F	24	Black	Nonsmoker	-	Negative	QNS	ND	<LLOQ	<LLOQ
028	M	26	Black	Nonsmoker	-	Negative	QNS	ND	<LLOQ	<LLOQ
029	F	32	Dark Brown	Nonsmoker	-	Negative	QNS	ND	<LLOQ	<LLOQ

CPD – cigarettes per day; ND – not detected; QNS – quantity not sufficient; NA – not available
[a] – LOD 20 pg/mg; [b] – LOD not established; [c] – LLOQ 1.75 pg/mg; [d] – LLOQ 1 ng/mL; [e] – LLOQ 1 ng/mL

verified by the presence of measurable plasma concentrations of nicotine and cotinine. (A plasma sample was not available for five of the heavy smoking participants.) Nicotine concentrations ranged from non- detected to 42.7 ng/mL, and cotinine concentrations ranged from 94.9 to 488.0 ng/mL for these participants. The presence of cotinine concentrations at these levels verified the self-reported current smoking status of the participants (typical cotinine concentrations for smokers range from 100 ng/mL to >300 ng/mL [200, 201]). The self-reported nonsmoking status of the nonsmoking participants was also verified by nicotine and cotinine plasma concentrations. Plasma concentrations for both nicotine and cotinine were below their respective LLOQs for all nonsmoking participants, confirming their nonsmoking status at the time of sample collection.

Second, hair samples from study participants were analyzed to determine whether B(a)P was present in the hair of known smokers and absent in the hair of nonsmokers. Clinical hair samples were considered positive for B(a)P if the calculated concentrations were greater than 20 pg/mg, the secondary qualifying ion was present, and the chromatograms showed Gaussian peak shape with S/N ratio $\geq$ 3. Clinical hair samples were considered negative for B(a)P if the calculated concentrations were below 20 pg/mg and S/N ratio was <3. Applying these criteria, B(a)P was only detectable in four (three females, one male) of the 30 heavy smoker hair samples, despite the verified current smoking status via plasma cotinine concentrations of the participant. Additionally, no abnormal non-tobacco related B(a)P exposure was noted on screening questionnaire for any of

these participants. For the nonsmoking participants, B(a)P was detectable in two (both males) of the 20 participants, despite nonsmoking status via plasma cotinine concentrations. No abnormal B(a)P exposed was noted on the screening questionnaire for these nonsmoking participants as well.

Third, we originally proposed to determine the differences in BPDE-protein adducts in the hair of smokers and nonsmokers, however, the quantity of hair received from each participant for analysis was between 34 and 200 mg (average weight collected was 95 mg). Therefore, given the sample amounts required for analysis after initial development and evaluation of analytical methods, we determined that the available quantity was not sufficient enough to perform both B(a)P and BPDE-protein adduct analyses for the study samples. The data for rat hair in Chapter 2, demonstrated that concentrations B(a)P concentrations in rat hair are much higher than concentrations of BPT. We also demonstrated that concentrations of BPT released from rat hair are about 50% lower in hair than released from Hb. With these factors in mind, we thus predicted that there was a greater likelihood to detect B(a)P in human hair, rather than BPT in human hair. Therefore, analysis for B(a)P, rather than BPDE-protein adducts, was performed due to the limited quantity of hair available for testing.

Despite the insufficient weight for the individual clinical hair samples, however, we were able to *pool* five heavy smoker participant's hair samples to obtain a sufficient quantity of hair to attempt BPDE-protein adduct testing using the preparation and extraction detailed in *Materials and Methods* section of this chapter. Since BPT was not detected in an extracted 100 mg of pooled heavy

smoker's hair (data not shown), double the amount of hair was taken through the extraction procedure (200 mg vs. 100 mg) (Figure 4.5, panel A). Despite doubling the amount of hair used in the analysis, BPT was still not detected. Panel B of Figure 4.5 shows a representative chromatogram from an extracted pooled heavy smoker's hair sample using triple the amount of hair (300 mg). The chromatograms from this sample further illustrate that even when tripling the amount of hair for analysis, BPT was still not detected, and this amount of hair greatly reduces the quality of the chromatography. Therefore, increasing the amount of hair analyzed did not improve the ability to detect BPT in human hair.

Fourth, with respect to the detection of BPDE-Hb adducts, only one heavy smoker (female) Hb sample had a concentration above the LLOQ. The measured concentration for BPDE-Hb adducts for this individual was 9.1 pg/mg. This concentration is several fold higher than the average reported concentration for BPDE-Hb adducts in smokers [60, 93, 127]. This individual also had the highest plasma concentration of cotinine of the 30 heavy smoking participants. For the nonsmokers participants, all of the BPDE-Hb results were reported as not detected.

Discussion

In the present study, we proposed to develop analytical methods for the purpose of determining the differences of B(a)P and BPDE-protein adduct incorporation in smokers (those exposed to PTS) and nonsmokers (those with no exposure to PTS or ETS) hair. While no previous studies have examined BPDE-protein adduct concentrations in hair, a single report has been published on a

Figure 4.5 *Ion chromatograms from: A) an extracted 200 mg pooled heavy, and B) an extracted 300 mg pooled heavy smoker's hair sample.* These chromatograms illustrate the reduced sensitivity in the detection of BPT and that increasing the amount of hair reduces the quality of the chromatography. Analyte retention time (RT) is on the x-axis and signal intensity on the y-axis. B(a)P = 252 *m/z* and B(a)P-d_{12} =264 *m/z*

A.

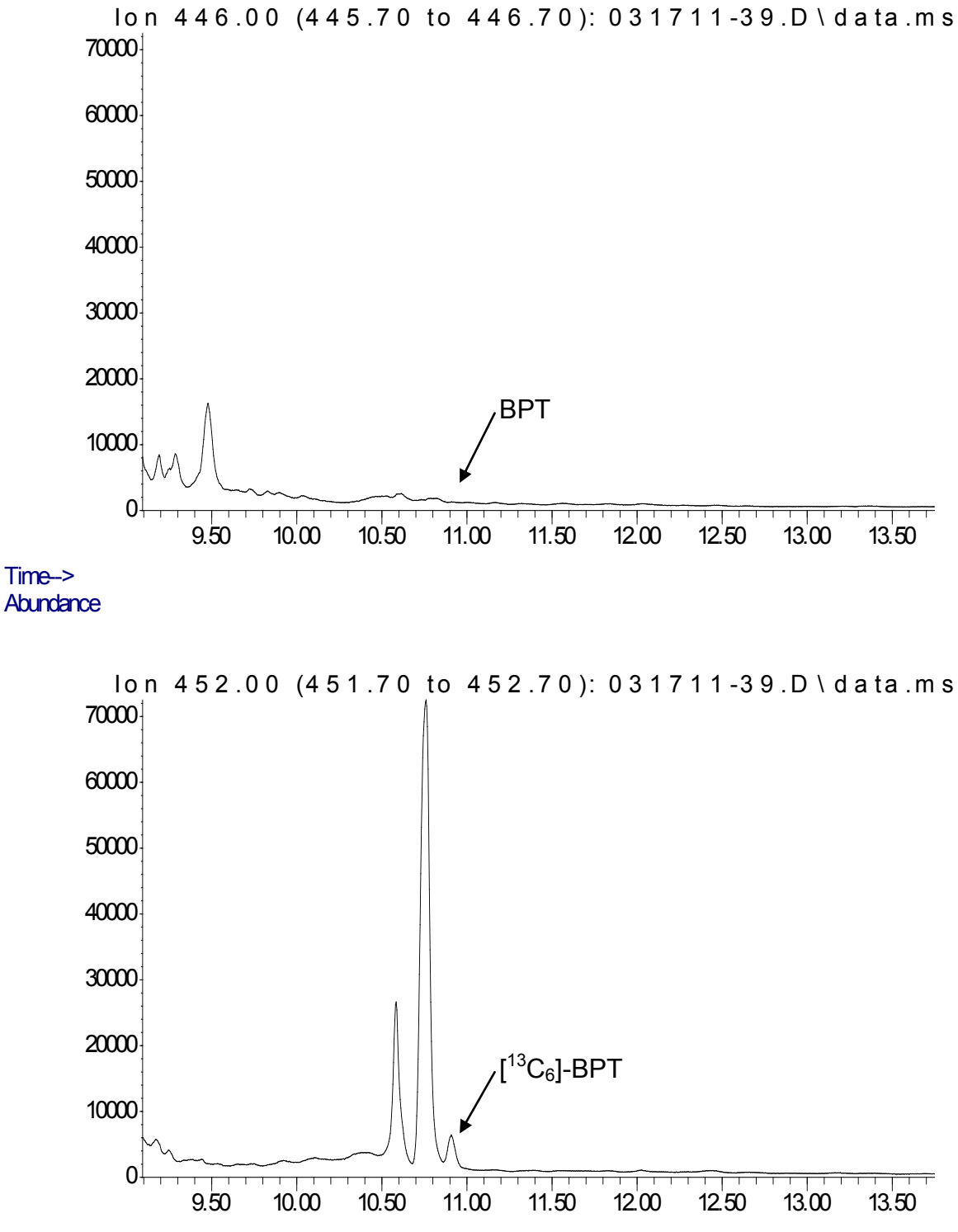
Abundance
Ion 446.00 (445.70 to 446.70): 031711-39.D\data.ms
70000
60000
50000
40000
30000
20000
10000
0
BPT
9.50
10.00
10.50
11.00
11.50
12.00
12.50
13.00
13.50
Time-->
Abundance
Ion 452.00 (451.70 to 452.70): 031711-39.D\data.ms
70000
60000
50000
40000
30000
20000
10000
0
[13C6]-BPT
9.50
10.00
10.50
11.00
11.50
12.00
12.50
13.00
13.50
Time-->

B.

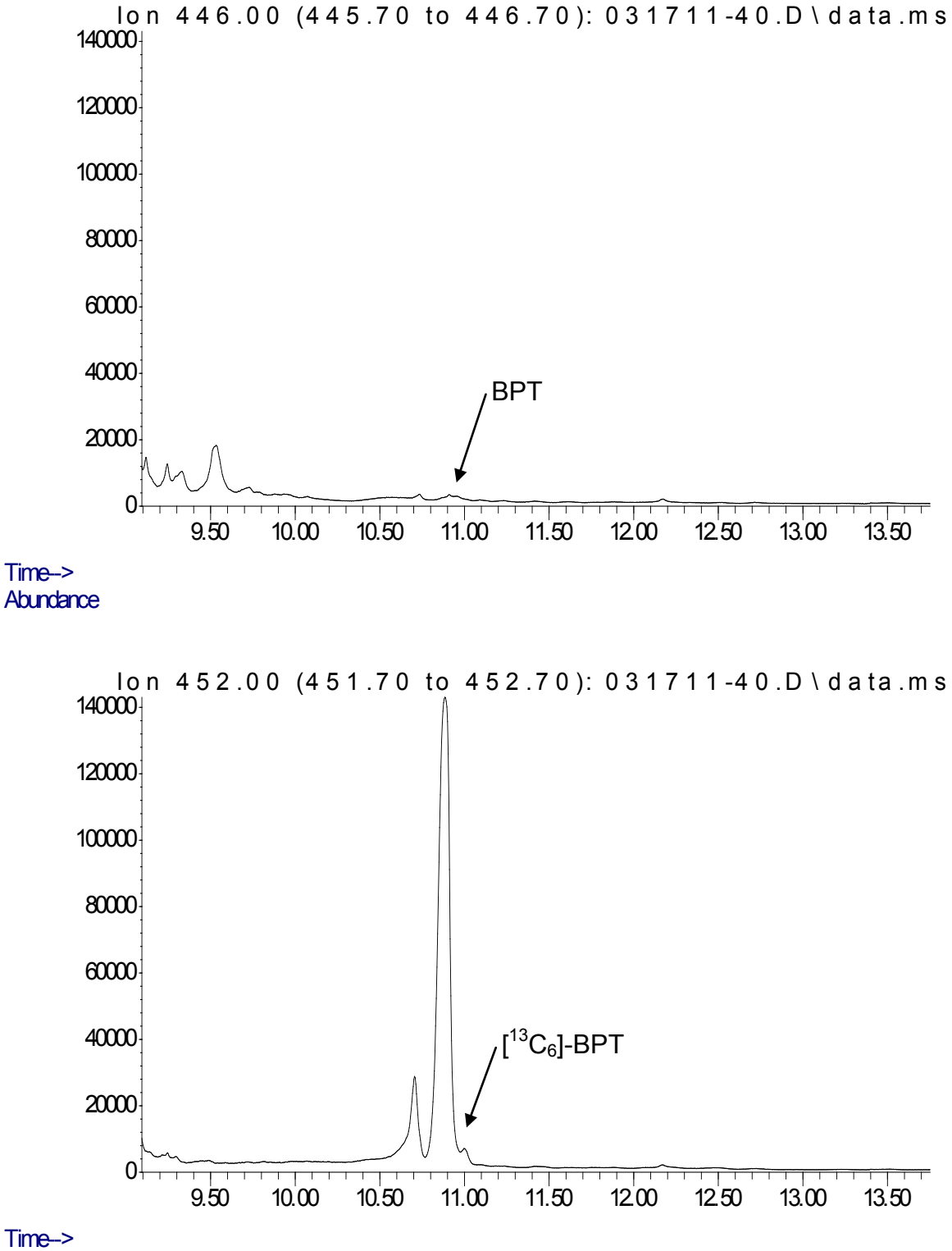
Abundance
Ion 446.00 (445.70 to 446.70): 031711-40.D\data.ms
140000
120000
100000
80000
60000
40000
20000
0
BPT
9.50
10.00
10.50
11.00
11.50
12.00
12.50
13.00
13.50
Time-->
Abundance
Ion 452.00 (451.70 to 452.70): 031711-40.D\data.ms
140000
120000
100000
80000
60000
40000
20000
0
[13C6]-BPT
9.50
10.00
10.50
11.00
11.50
12.00
12.50
13.00
13.50
Time-->

panel of PAHs in human hair. In 2003, Toriba et al. reported an average concentration of B(a)P in smokers hair of 1.1 $\pm$ 0.7 pg/mg and 0.7 $\pm$ 0.3 pg/mg for nonsmokers' hair [59]. Given these available data, we originally planned to validate a quantitative method for detection of B(a)P in human hair with a sensitivity at or below 1 pg/mg. However, we were unable to achieve adequate reproducibility (CV<20%) at concentrations below 20 pg/mg and a qualitative evaluation (positive vs. negative at or above 20 pg/mg) was instead performed for each hair sample in our study.

Using the qualitative method developed for the detection of B(a)P in human hair, we detected B(a)P in four of the 30 heavy smoker hair samples, and two of the 20 nonsmokers hair samples. There are several possible explanations for these findings. First, concentrations of B(a)P in human hair may be extremely low in the group of participants tested, and may be below the LOD of the assay and instrument. Greater sensitivity in the analytical methodology may therefore be necessary in order to determine quantitative concentrations of B(a)P in human clinical hair samples. Second, it is also possible that B(a)P is simply not present in many human hair samples. Third, as mentioned above, B(a)P concentrations in hair have only been reported in one small human study involving 20 participants (6 smokers, 14 nonsmokers) using HPLC with fluorescence detection [59] more than 8 years ago. Although using this HPLC-fluorescence method may have provided greater sensitivity for the detection of B(a)P, it has much lower specificity than GC/MS with selective ion monitoring. In this small study, investigators reported an average hair concentration of B(a)P in smokers

of 1.1 ± 0.7 pg/mg, but evaluation of their blank hair samples (n=4), used for the standard curve and quality control samples, revealed virtually the same concentrations of B(a)P (1.1 + 0.1 pg/mg) as detected in their smokers' hair samples. Also of note, no additional studies reporting B(a)P in hair have been published to date since this paper. This demonstrates that more research is need to evaluate concentrations of B(a)P in human hair, as well as and the factors that contribute to its incorporation and retention in hair. Fourth, the extremely low concentrations of B(a)P in human hair may be due in part by daily hygiene practices. We demonstrated that a 10% shampoo wash of B(a)P incorporated rat hair greatly reduces the detectable amount of B(a)P several fold (Chapter 2, Figure 2.13). Thus the incorporation of B(a)P in hair may not be strong enough to resist the typical hygiene practices of humans. While we do note there are significant structural differences in hair of different species, these effects have yet to be determined experimentally with human hair. Finally, B(a)P is photochemically reactive and it is unknown whether light penetrating the hair shaft reduces the detectable amounts of B(a)P in hair.

In addition to the determination of B(a)P content in human hair, numerous digestion and extraction experiments were performed on human hair that had been fortified with BPT (Table 4.2). These experiments were unsuccessful for the detection of BPT in digested and extracted human hair. There are several possible explanations for these findings: 1) Significant ion suppression is present; 2) There are matrix interferences that were not removed during the extraction of human hair; and 3) We do not have adequate sensitivity for the detection of BPT

in human hair using GC/MS. Given these findings, and the fact that there was an insufficient quantity of human clinical hair samples available for analysis, the development of a validated method for BPDE-protein adducts in human hair was not performed. We were, however, able to evaluate *pooled* heavy smokers' hair samples, to determine whether we could detect BPT using the method detailed in this chapter, and which we validated in Chapter 2 for rat hair. Despite using two and three times the amount of *pooled* heavy smokers' hair for this method, we were unable to detect BPT (Figure 4.5).

BPDE-Hb adducts (from isolated Hb in blood) were selected as our positive control in our both our human studies and animal studies, since they have been well characterized [60, 98] and are known to form after B(a)P exposure, however, we were only able to detect BPDE-Hb adducts from one human participant (in contrast to our rat studies in which we were able to detect BPDE-Hb adducts from all B(a)P dosed rats, see Chapter 2). However, we do note that the doses of B(a)P administered to the rats over seven days was 1000 fold higher than what the approximated human exposure would be in three months (based on the EPA's estimate of 1-3 ug/day for nonsmokers) [202]. Alternatively, the lack of detectable BPT released from Hb, may be due to the increased instrument noise present in human Hb samples that have only had a liquid-liquid extracted performed on them (vs. the rat samples which went through both liquid-liquid and SPE), or that extremely low concentrations of these adducts are present in the current set of participants. It is known that up to 40% of samples tested for BPDE-protein adducts are reported as not detected [60], so

our results were not entirely unexpected. We were unable to determine if the concentration of these biomarkers correlate to the concentration of the positive control (the BPDE-Hb adduct), since virtually all of the samples did not have detectable concentrations of analyte.

The matrix effects/ion suppression observed with in human hair and Hb extracts were much more pronounced than what was seen in rat hair and rat Hb (Chapter 2), and may be due in part to the 10-fold increase in the amount of hair used in the B(a)P assay, and the 2-fold increase in the amount of Hb used in the BPDE-Hb adduct assay. The BPDE-Hb extraction presented in this chapter was also reduced to just a liquid-liquid extraction in order to prevent further loss of BPT through SPE. However, these sample extracts of were very crude (as apparent by the large background signal in the chromatograms, Figure 4.4), and greatly decreased the instrument's signal for BPT over time. Further clean-up of samples by SPE or other techniques will be needed in future studies. In addition to analytical modifications for these extraction methods, different instrumentation may be necessary for determining extremely low concentrations of BPDE adducts in hair and Hb from humans, as discussed below.

GC tandem mass spectrometry (GC-MS/MS) may be able to provide greater sensitivity and improved ability to detect extremely low levels of B(a)P in human hair and BPT released from BPDE-protein adducts. Recently, Simpson *et al.* published a method for the detection of BPT in the urine of smokers using GC/MS-MS) [203]. This instrumentation allowed for detection limits for BPT ("on column") several orders of magnitude lower than our GC/MS. Lower detection

limits for BPT have also been reported with stable isotope dilution high resolution GC [93], liquid chromatography-tandem mass spectrometry (LC-MS/MS) [94], as well as HPLC with laser-induced fluorescence detection [189]. Lower detection limits for B(a)P have also been reported with HPLC using fluorescence detection [204] and HPLC with ultraviolet detection [205], however these studies determined B(a)P concentrations in matrices other than hair.

Some modifications that may prove advantageous for the detection of B(a)P and/or BPDE-protein adducts in hair are: 1) The use of more hair (>100 mg) in the assay if coupled to more stringent sample clean-up methods; 2) Collection of hair that has been plucked instead of cutting close to the scalp, to provide a hair sample that has not been exposed to typical hygiene practices and/or light; 3) Adding a wash procedure before digestion and extraction of human hair to possibly reduce matrix interferences/ion suppression. It is noted however, that washing hair as part of the analytical preparation is contentious and no general consensus has been reached on the topic. 4) The analysis of more abundant PAHs, and their diol expoxide protein adduct forming metabolites, as surrogate analytes for the less abundant B(a)P. Schummer *et al.* have recently demonstrated that mono-hydroxylated PAH metabolites such and hydroxy-napthalene and hydroxyl-phenanthrene can be detected in human hair by GC/MS [206].

In conclusion, B(a)P, but not BPDE-protein adducts can be detected in hair from at least some subjects. Moreover, the data presented in this chapter demonstrate that extremely sensitive analytical methodology may be needed to

evaluate these novel hair biomarkers in humans, and more research involving human clinical samples will be necessary in order to determine if B(a)P and/or BPDE-protein adducts in hair can be a useful tool for assessing B(a)P exposure in humans, particularly smokers.

CHAPTER 5

SUMMARY AND SIGNIFICANCE

Summary

The objective of this research was to investigate whether B(a)P and BPDE-protein adducts can be detected in hair and whether they can be used as novel biomarkers of toxic exposure to B(a)P. The overarching hypothesis for this research was that ***B(a)P and BPDE-protein adducts in hair can be used as biomarkers of toxic exposures to B(a)P.*** To address this hypothesis we conducted the following experiments:

1. Long-Evans rats were exposed to varying doses of B(a)P. Then using liquid-liquid, solid phase, and enzymatic extraction techniques, coupled to our sensitive and specific GC/MS methods, we quantified B(a)P and BPT (released from BPDE- adducts) in biological matrices.

From these analyses we determined:

1a. B(a)P incorporates into rat hair in a dose-dependent manner.

1b. B(a)P concentrations in pigmented and nonpigmented rat hair do not statically differ.

1c. B(a)P concentrations in rat hair correlate with the concentrations of our positive control (the validated BPDE-Hb adduct).

1d. BPT (released from BPDE-protein adducts) can be detected in rat hair, and its concentration is dose-dependent.

1e. BPT concentrations in hair are approximately 1.6 times greater in pigmented vs. nonpigmented hair.

2. A histological approach using a hematoxylin and eosin (H&E) staining was used to detect histopathological events the lung tissue from rats with varying B(a)P exposure. This was completed in order to infer whether B(a)P and BPDE-protein adducts concentrations in hair were associated with the severity ofhistopathologic evidence of lung toxicty. We used subjective and objective measures in an attempt to score the severity of the histopathological events for B(a)P dosed rats. We also employed immunohistochemistry staining directed towards identification of neutrophils.

From these experiments we determined:

2a. Rats exposed to B(a)P in the low, medium, and high dosed groups show alveolar wall thickening, decreased air space, macrophage hyperplasia, and an increased myloperoxidase enzymes.

2b. Subjective measurements of the percentage of alveolar wall thickening of the lung tissue and neutrophil counts did not statistically differ from control rats.

2c. Objective measurement of nuclear space, cellular space, air space and ratios of these items using Image J did not statistically differ from controls.

3. Using samples collected from human clinical trials we sought to investigate the differences of B(a)P and BPDE-protein adducts in the hair of active smokers (those exposed to PTS) and nonsmokers (those with no exposure to PTS or ETS).

From these experiments we determined:

3a. B(a)P, but not BPDE-protein adducts can be detected in hair from at least some human clinical hair samples.

3b. More sensitive analytical methodology is be needed to evaluate concentrations of these novel hair biomarkers in humans, and further research involving human clinical samples will be necessary in order to determine if B(a)P and/or BPDE-protein adducts in hair can be a useful tool for assessing B(a)P exposure in humans, particularly smokers.

Significance

In conclusion, we have developed sensitive and specific quantitative analytical GC/MS methodology to investigate the disposition and concentrations of unique biomarkers in hair from experimental animals exposed to B(a)P and in human subjects enrolled in a smoking clinical trial. To our knowledge, this is the first report of B(a)P and BPDE-protein adducts detection in rat hair, and is only the second report on the detection of B(a)P in human hair. We determined there is a dose-dependent increase of these novel hair biomarkers in rats exposed to B(a)P, as well as insights into the role pigment may be playing on their incorporation into hair. While further studies are needed to elucidate the

underlying mechanisms involving the incorporation of these compounds, the results from this dissertational research show promise for biomonitoring of B(a)P exposure in rats and humans by means of a noninvasive procedure.

APPENDIX

SCREENING QUESTIONNAIRE FOR NONSMOKERS

Date: _____
Study ID: _____
Recorder's Name: _____

1. How old are you? (Criterion: 18 or older)

2. Have you ever smoked a cigarette or used tobacco in any form?

    2 a. When did you smoke your last cigarette or use tobacco?
        - Within the past 12 months
        - More than a year ago (Criterion: More than a year ago)

3. How often are you exposed to other people smoking in the same room as you?
    - Never
    - Once or twice in a month
    - Once or twice in a week
    - Almost every day (Criterion: Once or twice the last 3 months or less)

4. Do you keep your hair cut an inch and a half or longer? (Criterion: Yes)

5. Have you colored your hair with the past 3 months? (Criterion: No)

6. What color is your hair? (Criterion: Dark pigmented preferred, no gray or white)

7. "Since some chemicals found in tobacco smoke can also be present in certain occupational settings, we would like to know – What is your occupation?

8. "Since similar chemicals can also be found in food that has been barbecued or smoked we would like to know – How many times per week do you consume barbecued or smoked food products?

9. Do you drink yerba mate tea (South American smoked tea)?

REFERENCES

1. Boumba, V.A., K.S. Ziavrou, and T. Vougiouklakis, *Hair as a biological indicator of drug use, drug abuse or chronic exposure to environmental toxicants.* Int J Toxicol, 2006. **25**(3): p. 143-63.

2. Harkey, M.R., *Anatomy and physiology of hair.* Forensic Sci Int, 1993. **63**(1-3): p. 9-18.

3. Wix, M.A., P.W. Wertz, and D.T. Downing, *Polar lipid composition of mammalian hair.* Comp Biochem Physiol B, 1987. **86**(4): p. 671-3.

4. Nicolaides, N. and S. Rothman, *Studies on the chemical composition of human hair fat. II. The overall composition with regard to age, sex and race.* J Invest Dermatol, 1953. **21**(1): p. 9-14.

5. Nicolaides, N. and S. Rothman, *Studies on the chemical composition of human hair fat. I. The squalene-cholesterol relationship in children and adults.* J Invest Dermatol, 1952. **19**(6): p. 389-91.

6. Masukawa, Y., H. Narita, and G. Imokawa, *Characterization of the lipid composition at the proximal root regions of human hair.* J Cosmet Sci, 2005. **56**(1): p. 1-16.

7. Wertz, P.W., *Integral lipids of hair and stratum corneum.* EXS, 1997. **78**: p. 227-37.

8. Campbell, J.L., et al., *Determination of trace element profiles and concentrations in human hair by proton-induced X-ray emission spectrometry.* Anal Chem, 1981. **53**(8): p. 1249-53.

9. Harkey, M., *Anatomy and physiology of hair.* Forensic Sci. Int., 1993. **63**: p. 9-18.

10. Krause, K. and K. Foitzik, *Biology of the hair follicle: the basics.* Semin Cutan Med Surg, 2006. **25**(1): p. 2-10.

11. Nakahara, Y., *Hair analysis for abused and therapeutic drugs.* J Chromatogr B Biomed Sci Appl, 1999. **733**(1-2): p. 161-80.

12. Hopps, H.C., *The biologic bases for using hair and nail for analyses of trace elements.* Sci Total Environ, 1977. **7**(1): p. 71-89.

13. Giovanoli-Jakubczak, T. and G.G. Berg, *Measurement of mercury in human hair.* Arch Environ Health, 1974. **28**(3): p. 139-44.

14. Montagna, W., *The biology of hair growth,*, ed. R. Ellis. 1958: New York, Academic Press.

15. Priestley, G.C., *Rates and duration of hair growth in the albino rat.* J Anat, 1966. **100**(Pt 1): p. 147-57.

16. Whiting, D.A., *The Structure of the Human Hair Follicle: Light Microscopy of Vertical and Horizontal Sections of Scalp Biopsies*, in *Canfield Publishing*, Pfizer, Editor. 2004: Fairfield, NJ.

17. Montagna, W.a.V.S., E.J., *The Biology of Hair Growth*. The anatomy of the hair follicle, ed. R.A. Ellis. 1958, New York: Acedemic Press.

18. A.P. Bertolino, L.M.K., and I.M. Freedberg, *Biology of Hair Follicles*. Dermatology in General Medicine, ed. A.Z.E. T.B. Fitzpatrick, K Wolff, I.M Freedberg, K.F. Austen. 1994, New York City: McGraw-Hill, Inc. 289-293.

19. Sanford, D.a.H., F.L., *Determination of Cystine and Cysteine in Altered Human Hair Fibers.* Anal. Chem., 1947. **19**(6): p. 404-406.

20. Pumford, N.R. and N.C. Halmes, *Protein targets of xenobiotic reactive intermediates.* Annu Rev Pharmacol Toxicol, 1997. **37**: p. 91-117.

21. Pumford, N.R., N.C. Halmes, and J.A. Hinson, *Covalent binding of xenobiotics to specific proteins in the liver.* Drug Metab Rev, 1997. **29**(1-2): p. 39-57.

22. Gray, S., *Gray's anatomy*. 1st ed. 1994, New York: Vintage Books. 80 p.

23. Ingold, C.K., *Structure and Mechanism in Organic Chemistry*. 2nd ed. 1969, Ithaca, NY: Cornell University Press.

24. Joseph, R.E., Jr., T.P. Su, and E.J. Cone, *In vitro binding studies of drugs to hair: influence of melanin and lipids on cocaine binding to Caucasoid and Africoid hair.* J Anal Toxicol, 1996. **20**(6): p. 338-44.

25. Wilkins, D.G., et al., *Quantitative analysis of methadone and two major metabolites in hair by positive chemical ionization ion trap mass spectrometry.* J Anal Toxicol, 1996. **20**(6): p. 355-61.

26. Slawson, M.H., et al., *Quantitative determination of phencyclidine in pigmented and nonpigmented hair by ion-trap mass spectrometry.* J Anal Toxicol, 1996. **20**(6): p. 350-4.

27. Hold, K.M., et al., *Detection of stanozolol in hair by negative ion chemical ionization mass spectrometry.* J Anal Toxicol, 1996. **20**(6): p. 345-49.

28. Gygi, S.P., et al., *Incorporation of codeine and metabolites into hair. Role of pigmentation.* Drug Metab Dispos, 1996. **24**(4): p. 495-501.

29. Gygi, S.P., et al., *Dose-related distribution of codeine and its metabolites into rat hair.* Drug Metab Dispos, 1996. **24**(3): p. 282-7.

30. Rollins, D.E., D.G. Wilkins, and G.G. Krueger, *Codeine disposition in human hair after single and multiple doses.* Eur J Clin Pharmacol, 1996. **50**(5): p. 391-7.

31. Wilkins, D.G., et al., *Disposition of codeine in female human hair after multiple-dose administration.* J Anal Toxicol, 1995. **19**(6): p. 492-8.

32. Wilkins, D., et al., *Quantitative analysis of THC, 11-OH-THC, and THCCOOH in human hair by negative ion chemical ionization mass spectrometry.* J Anal Toxicol, 1995. **19**(6): p. 483-91.

33. Gygi, S.P., D.G. Wilkins, and D.E. Rollins, *Distribution of codeine and morphine into rat hair after long-term daily dosing with codeine.* J Anal Toxicol, 1995. **19**(6): p. 387-91.

34. Wilkins, D., et al., *Quantitative determination of codeine and its major metabolites in human hair by gas chromatography-positive ion chemical ionization mass spectrometry: a clinical application.* J Anal Toxicol, 1995. **19**(5): p. 269-74.

35. Rollins, D.E., D.G. Wilkins, and G. Krueger, *Models for studying the cellular processes and barriers to the incorporation of drugs into hair.* NIDA Res Monogr, 1995. **154**: p. 235-44.

36. Henderson, G.L., et al., *Incorporation of isotopically labeled cocaine into human hair: race as a factor.* J Anal Toxicol, 1998. **22**(2): p. 156-65.

37. Hubbard, D.L., D.G. Wilkins, and D.E. Rollins, *The incorporation of cocaine and metabolites into hair: effects of dose and hair pigmentation.* Drug Metab Dispos, 2000. **28**(12): p. 1464-9.

38. Ortonne, J.P. and G. Prota, *Hair melanins and hair color: ultrastructural and biochemical aspects.* J Invest Dermatol, 1993. **101**(1 Suppl): p. 82S-89S.

39. Larsson, B.S., *Interaction between chemicals and melanin.* Pigment Cell Res, 1993. **6**(3): p. 127-33.

40. Ito, S., *Reexamination of the structure of eumelanin.* Biochim Biophys Acta, 1986. **883**(1): p. 155-61.

41. Felix, C.C., et al., *Melanin photoreactions in aerated media: electron spin resonance evidence for production of superoxide and hydrogen peroxide.* Biochem Biophys Res Commun, 1978. **84**(2): p. 335-41.

42. Tjalve, H., M. Nilsson, and B. Larsson, *Binding of 14C-spermidine to melanin in vivo and in vitro.* Acta Physiol Scand, 1981. **112**(2): p. 209-14.

43. Ings, R.M., *The melanin binding of drugs and its implications.* Drug Metab Rev, 1984. **15**(5-6): p. 1183-212.

44. Potts, A.M., *The Reaction of Uveal Pigment in Vitro with Polycyclic Compounds.* Invest Ophthalmol, 1964. **3**: p. 405-16.

45. Roberto, A., B.S. Larsson, and H. Tjalve, *Uptake of 7,12-dimethylbenz(a)anthracene and benzo(a)pyrene in melanin-containing tissues.* Pharmacol Toxicol, 1996. **79**(2): p. 92-9.

46. Dunn, J.E., et al., *Scalp hair and urine mercury content of children in the Northeast United States: the New England Children's Amalgam Trial.* Environ Res, 2008. **107**(1): p. 79-88.

47. Xue, F., et al., *Maternal fish consumption, mercury levels, and risk of preterm delivery.* Environ Health Perspect, 2007. **115**(1): p. 42-7.

48. Barbosa, F., Jr., et al., *A critical review of biomarkers used for monitoring human exposure to lead: advantages, limitations, and future needs.* Environ Health Perspect, 2005. **113**(12): p. 1669-74.

49. Tsatsakis, A.M., et al., *Is hair analysis for dialkyl phosphate metabolites a suitable biomarker for assessing past acute exposure to organophosphate pesticides?* Hum Exp Toxicol, 2011.

50. Jaspers, V.L., et al., *A screening of persistent organohalogenated contaminants in hair of East Greenland polar bears.* Sci Total Environ, 2010. **408**(22): p. 5613-8.

51. Margariti, M.G. and A.M. Tsatsakis, *Analysis of dialkyl phosphate metabolites in hair using gas chromatography-mass spectrometry: a biomarker of chronic exposure to organophosphate pesticides.* Biomarkers, 2009. **14**(3): p. 137-47.

52. Kintz, P., M. Villain, and V. Cirimele, *Hair analysis for drug detection.* Ther Drug Monit, 2006. **28**(3): p. 442-6.

53. Strano-Rossi, S., A. Bermejo-Barrera, and M. Chiarotti, *Segmental hair analysis for cocaine and heroin abuse determination.* Forensic Sci Int, 1995. **70**(1-3): p. 211-6.

54. Uematsu, T., et al., *Human scalp hair as evidence of individual dosage history of haloperidol: a possible linkage of haloperidol excretion into hair with hair pigment.* Arch Dermatol Res, 1990. **282**(2): p. 120-5.

55. Kintz, P., *Segmental hair analysis can demonstrate external contamination in postmortem cases.* Forensic Sci Int, 2011.

56. Eliopoulos, C., J. Klein, and G. Koren, *Validation of self-reported smoking by analysis of hair for nicotine and cotinine.* Ther Drug Monit, 1996. **18**(5): p. 532-6.

57. Florescu, A., et al., *Methods for quantification of exposure to cigarette smoking and environmental tobacco smoke: focus on developmental toxicology.* Ther Drug Monit, 2009. **31**(1): p. 14-30.

58. Yuan, J.M., et al., *Urinary levels of tobacco-specific nitrosamine metabolites in relation to lung cancer development in two prospective cohorts of cigarette smokers.* Cancer Res, 2009. **69**(7): p. 2990-5.

59. Toriba, A., et al., *Quantification of polycyclic aromatic hydrocarbons (PAHs) in human hair by HPLC with fluorescence detection: a biological monitoring method to evaluate the exposure to PAHs.* Biomed Chromatogr, 2003. **17**(2-3): p. 126-32.

60. Skipper, P.L. and S.R. Tannenbaum, *The role of protein adducts in the study of chemical carcinogenesis.* Prog Clin Biol Res, 1990. **340C**: p. 301-10.

61. Brandt, H.C. and W.P. Watson, *Monitoring human occupational and environmental exposures to polycyclic aromatic compounds.* Ann Occup Hyg, 2003. **47**(5): p. 349-78.

62. *Report on Carcinogens*, U.S.D.o.H.a.H. Services, Editor. 2004: Research Triangle Park, NC. p. 220-222.

63. Ding, Y.S., D.L. Ashley, and C.H. Watson, *Determination of 10 carcinogenic polycyclic aromatic hydrocarbons in mainstream cigarette smoke.* J Agric Food Chem, 2007. **55**(15): p. 5966-73.

64. *Tobacco Smoke and Involuntary Smoking: Evaluation of Carcinogenic Risks to Humans*, I.A.f.R.o. Cancer, Editor. 2004, Lyon, France. p. 53-1187.

65. *Polynuclear Aromatic Compounds, Part 1, Chemical, Environmental and Experimental Data*, W.H. Organization, Editor. 1983: Lyon, France. p. 211.

66. Hecht, S.S., W. Grabowski, and K. Groth, *Analysis of faeces for benzo[a]pyrene after consumption of charcoal-broiled beef by rats and humans.* Food Cosmet Toxicol, 1979. **17**(3): p. 223-7.

67. Rihs, H.P., et al., *Occupational exposure to polycyclic aromatic hydrocarbons in German industries: association between exogenous exposure and urinary metabolites and its modulation by enzyme polymorphisms.* Toxicol Lett, 2005. **157**(3): p. 241-55.

68. Lu, P.L., M.L. Chen, and I.F. Mao, *Urinary 1-hydroxypyrene levels in workers exposed to coke oven emissions at various locations in a coke oven plant.* Arch Environ Health, 2002. **57**(3): p. 255-61.

69. Kang, D., et al., *Association of exposure to polycyclic aromatic hydrocarbons (estimated from job category) with concentration of 1-hydroxypyrene glucuronide in urine from workers at a steel plant.* Occup Environ Med, 1995. **52**(9): p. 593-9.

70. Hecht, S.S., *Tobacco smoke carcinogens and lung cancer.* J Natl Cancer Inst, 1999. **91**(14): p. 1194-210.

71. Culp, S.J., et al., *A comparison of the tumors induced by coal tar and benzo[a]pyrene in a 2-year bioassay.* Carcinogenesis, 1998. **19**(1): p. 117-24.

72. *Some Non-Heterocyclic Polycyclic Aromatic Hydrocarbons and Some Related Exposures*, I.A.f.R.o. Cancer, Editor. 2010: Lyon, France. p. 35-818.

73. *Polynuclear Aromatic Compounds, Part 1: Chemical, Environmental, and Experimental Data*, I.A.f.R.o. Cancer, Editor. 1983: Lyon, France. p. 31-91.

74. Sun, J.D., et al., *Lung retention and metabolic fate of inhaled benzo(a)pyrene associated with diesel exhaust particles.* Toxicol Appl Pharmacol, 1984. **73**(1): p. 48-59.

75. Sun, J.D., R.K. Wolff, and G.M. Kanapilly, *Deposition, retention, and biological fate of inhaled benzo(a)pyrene adsorbed onto ultrafine particles and as a pure aerosol.* Toxicol Appl Pharmacol, 1982. **65**(2): p. 231-44.

76. Agency, U.S.E.P. *Benzo(a)pyrene*. Persistent Bioaccumulative and Toxic (PBT) Chemical Program [cited 2011 April, 24]; Available from: http://www.epa.gov/pbt/pubs/benzo.htm.

77. Kummer, V., et al., *Estrogenic activity of environmental polycyclic aromatic hydrocarbons in uterus of immature Wistar rats.* Toxicol Lett, 2008. **180**(3): p. 212-21.

78. Miller, K.P. and K.S. Ramos, *Impact of cellular metabolism on the biological effects of benzo[a]pyrene and related hydrocarbons.* Drug Metab Rev, 2001. **33**(1): p. 1-35.

79. Dostalek, J., et al., *Multichannel SPR biosensor for detection of endocrine-disrupting compounds.* Anal Bioanal Chem, 2007. **389**(6): p. 1841-7.

80. Lu, K.P. and K.S. Ramos, *Identification of genes differentially expressed in vascular smooth muscle cells following benzo[a]pyrene challenge: implications for chemical atherogenesis.* Biochem Biophys Res Commun, 1998. **253**(3): p. 828-33.

81. Hough, J.L., et al., *Benzo(a)pyrene enhances atherosclerosis in White Carneau and Show Racer pigeons.* Arterioscler Thromb, 1993. **13**(12): p. 1721-7.

82. Akpan, V., et al., *High levels of carcinogenic polycyclic aromatic hydrocarbons (PAH) in 20 brands of Chinese cigarettes.* J Appl Toxicol, 2006. **26**(6): p. 480-3.

83. Davis, H.J., *Gas chromatographic determination of benzo(a)pyrene in cigarette smoke.* Anal Chem, 1968. **40**(10): p. 1583-5.

84. Jenkins, R.A. and M.R. Guerin, *Analytical chemical methods for the detection of environmental tobacco smoke constituents.* Eur J Respir Dis Suppl, 1984. **133**: p. 33-46.

85. Sinclair, N.M. and B.E. Frost, *Rapid method for the determination of benzo[a]pyrene in the particulate phase of cigarette smoke by high-performance liquid chromatography with fluorimetric detection.* Analyst, 1978. **103**(1233): p. 1199-203.

86. Pelkonen, O. and D.W. Nebert, *Metabolism of polycyclic aromatic hydrocarbons: etiologic role in carcinogenesis.* Pharmacol Rev, 1982. **34**(2): p. 189-222.

87. Conney, A.H., et al., *Studies on the metabolism of benzo[a]pyrene and dose-dependent differences in the mutagenic profile of its ultimate carcinogenic metabolite.* Drug Metab Rev, 1994. **26**(1-2): p. 125-63.

88. Gelboin, H.V., *Benzo[alpha]pyrene metabolism, activation and carcinogenesis: role and regulation of mixed-function oxidases and related enzymes.* Physiol Rev, 1980. **60**(4): p. 1107-66.

89. Ross, J.A., et al., *Adenomas induced by polycyclic aromatic hydrocarbons in strain A/J mouse lung correlate with time-integrated DNA adduct levels.* Cancer Res, 1995. **55**(5): p. 1039-44.

90. Nesnow, S., et al., *Mechanistic linkage between DNA adducts, mutations in oncogenes and tumorigenesis of carcinogenic environmental polycyclic aromatic hydrocarbons in strain A/J mice.* Toxicology, 1995. **105**(2-3): p. 403-13.

91. Hecht, S.S., *Tobacco carcinogens, their biomarkers and tobacco-induced cancer.* Nat Rev Cancer, 2003. **3**(10): p. 733-44.

92. Lakshman, M.K., et al., *Highly diastereoselective synthesis of nucleoside adducts from the carcinogenic benzo[a]pyrene diol epoxide and a computational analysis.* J Am Chem Soc, 2007. **129**(1): p. 68-76.

93. Ragin, A.D., et al., *A gas chromatography-isotope dilution high-resolution mass spectrometry method for quantification of isomeric benzo[a]pyrene diol epoxide hemoglobin adducts in humans.* J Anal Toxicol, 2008. **39**(9): p. 728-36.

94. Wang, C., et al., *Synthesis and characterization of DNA fluorescent probes containing a single site-specific stereoisomer of anti-benzo[a]pyrene diol epoxide-N2-dG.* Chem Res Toxicol, 2009. **22**(4): p. 676-82.

95. Wang, C., et al., *Quantitative study of stereospecific binding of monoclonal antibody to anti-benzo(a)pyrene diol epoxide-N(2)-dG adducts by capillary electrophoresis immunoassay.* J Chromatogr A, 2010. **1217**(15): p. 2254-61.

96. Luch, A., and Baird, W. M. , *Detoxification of Polycyclic Aromatic Hydrocarbons*. The Carcinogenic Effects of Polycyclic Aromatic Hydrocarbons 2005, London, UK: Imperial College Pres.

97. Shimada, T., et al., *Roles of individual human cytochrome P-450 enzymes in the bioactivation of benzo(a)pyrene, 7,8-dihydroxy-7,8-dihydrobenzo(a)pyrene, and other dihydrodiol derivatives of polycyclic aromatic hydrocarbons.* Cancer Res, 1989. **49**(22): p. 6304-12.

98. Tannenbaum, S.R., et al., *Characterization of various classes of protein adducts.* Environ Health Perspect, 1993. **99**: p. 51-5.

99. Huberman, E., et al., *Identification of mutagenic metabolites of benzo(a)pyrene in mammalian cells.* Proc Natl Acad Sci U S A, 1976. **73**(2): p. 607-11.

100. Darwish, W., et al., *Mutagenic activation and detoxification of benzo[a]pyrene in vitro by hepatic cytochrome P450 1A1 and phase II enzymes in three meat-producing animals.* Food Chem Toxicol, 2010. **48**(8-9): p. 2526-31.

101. Chung, M.K., et al., *A sandwich enzyme-linked immunosorbent assay for adducts of polycyclic aromatic hydrocarbons with human serum albumin.* Anal Biochem, 2010. **400**(1): p. 123-9.

102. Mumford, J.L., et al., *A sensitive color ELISA for detecting polycyclic aromatic hydrocarbon-DNA adducts in human tissues.* Mutat Res, 1996. **359**(3): p. 171-7.

103. Baumgartner WA, H.V., Blahd WH, *Hair Analysis for Drugs of Abuse* Journal of Forensic Sciences, 1989. **34**(6): p. 1433-1453.

104. Gerstenberg, B., et al., *Nicotine and cotinine accumulation in pigmented and unpigmented rat hair.* Drug Metab Dispos, 1995. **23**(1): p. 143-8.

105. Cone, E.J., *Testing human hair for drugs of abuse. I. Individual dose and time profiles of morphine and codeine in plasma, saliva, urine, and beard compared to drug-induced effects on pupils and behavior.* J Anal Toxicol, 1990. **14**(1): p. 1-7.

106. Saisho, K., et al., *Hair analysis for pharmaceutical drugs. II. Effective extraction and determination of sildenafil (Viagra) and its N-desmethyl metabolite in rat and human hair by GC-MS.* Biol Pharm Bull, 2001. **24**(12): p. 1384-8.

107. Uematsu, T., et al., *Possible effect of pigment on the pharmacokinetics of ofloxacin and its excretion in hair.* J Pharm Sci, 1992. **81**(1): p. 45-8.
108. Henderson, G.L., *Mechanisms of drug incorporation into hair.* Forensic Sci Int, 1993. **63**(1-3): p. 19-29.

109. Blank, D.A.K.a.D.L., *Drug Testing in Hair*. 1996, CRC: New York.
110. Nakahara, Y., *The effects of physiochemical factors on incorporation of drugs into hair and behaviour of drugs in hair root*. Drug testing technology: assessment of field applications, ed. Mieczkowski. 1999, Florida: CRC Press.

111. Lindquist, N.G., *Accumulation of drugs on melanin.* Acta Radiol Diagn (Stockh), 1973. **325**: p. 1-92.

112. Rollins, D.E., et al., *The effect of hair color on the incorporation of codeine into human hair.* J Anal Toxicol, 2003. **27**(8): p. 545-51.

113. Borges, C.R., D.G. Wilkins, and D.E. Rollins, *Amphetamine and N-acetylamphetamine incorporation into hair: an investigation of the potential role of drug basicity in hair color bias.* J Anal Toxicol, 2001. **25**(4): p. 221-7.

114. Gygi, S.P., D.G. Wilkins, and D.E. Rollins, *A comparison of phenobarbital and codeine incorporation into pigmented and nonpigmented rat hair.* J Pharm Sci, 1997. **86**(2): p. 209-14.

115. Nakahara, Y. and R. Hanajiri, *Hair analysis for drugs of abuse XXI. Effect of para-substituents on benzene ring of methamphetamine on drug incorporation into rat hair.* Life Sci, 2000. **66**(7): p. 563-74.

116. Han, E., et al., *The dependence of the incorporation of methamphetamine into rat hair on dose, frequency of administration and hair pigmentation.* J Chromatogr B Analyt Technol Biomed Life Sci, 2010. **878**(28): p. 2845-51.

117. Lee, S., et al., *Simultaneous quantification of opiates and effect of pigmentation on its deposition in hair.* Arch Pharm Res, 2010. **33**(11): p. 1805-11.

118. Hold, K.M., et al., *Detection of nandrolone, testosterone, and their esters in rat and human hair samples.* J Anal Toxicol, 1999. **23**(6): p. 416-23.

119. Mieczkowski, T. and M. Kruger, *Interpreting the color effect of melanin on cocaine and benzoylecgonine assays for hair analysis: brown and black samples compared.* J Forensic Leg Med, 2007. **14**(1): p. 7-15.

120. *Guide for the Care and Use of Laboratory Animals*, 8th ed. National Acedemies Press: Washington D.C.

121. Melikian, A.A., et al., *Gas chromatographic-mass spectrometric determination of benzo[a]pyrene and chrysene diol epoxide globin adducts in humans.* Cancer Epidemiol Biomarkers Prev, 1997. **6**(10): p. 833-9.

122. Melikian, A.A., et al., *Detection of DNA and globin adducts of polynuclear aromatic hydrocarbon diol epoxides by gas chromatography-mass spectrometry and -3H-CH3I postlabeling of released tetraols.* Chem Res Toxicol, 1996. **9**(2): p. 508-16.

123. Naylor, S., et al., *Benzo[a]pyrene diol epoxide adduct formation in mouse and human hemoglobin: physicochemical basis for dosimetry.* Chem Res Toxicol, 1990. **3**(2): p. 111-7.

124. Day, B.W., et al., *Enantiospecificity of covalent adduct formation by benzo[a]pyrene anti-diol epoxide with human serum albumin.* Chem Res Toxicol, 1994. **7**(6): p. 829-35.

125. Lee, B.M., S.J. Kwack, and H.S. Kim, *Age-related changes in oxidative DNA damage and benzo(a)pyrene diolepoxide-I (BPDE-I)-DNA adduct levels in human stomach.* J Toxicol Environ Health A, 2005. **68**(19): p. 1599-610.

126. Gyorffy, E., et al., *DNA adducts in tumour, normal peripheral lung and bronchus, and peripheral blood lymphocytes from smoking and non-smoking lung cancer patients: correlations between tissues and detection by 32P-postlabelling and immunoassay.* Carcinogenesis, 2004. **25**(7): p. 1201-9.

127. Boysen, G. and S.S. Hecht, *Analysis of DNA and protein adducts of benzo[a]pyrene in human tissues using structure-specific methods.* Mutat Res, 2003. **543**(1): p. 17-30.

128. Melikian, A.A., et al., *Identification of benzo[a]pyrene metabolites in cervical mucus and DNA adducts in cervical tissues in humans by gas chromatography-mass spectrometry.* Cancer Lett, 1999. **146**(2): p. 127-34.

129. Alexandrov, K., et al., *Evidence of anti-benzo[a]pyrene diolepoxide-DNA adduct formation in human colon mucosa.* Carcinogenesis, 1996. **17**(9): p. 2081-3.

130. Alexandrov, K., et al., *A new sensitive fluorometric assay for the metabolism of (--)-7,8-dihydroxy-7,8-dihydrobenzo[a]pyrene by human hair follicles.* Carcinogenesis, 1990. **11**(12): p. 2157-61.

131. Hukkelhoven, M.W., et al., *Determination of phenolic benzo(a)pyrene metabolites formed by human hair follicles.* Anal Biochem, 1982. **125**(2): p. 370-5.

132. Hukkelhoven, M.W., et al., *Human hair follicles, a convenient tissue for genetic studies on carcinogen metabolism.* Clin Genet, 1982. **21**(1): p. 53-8.

133. Ingold, C.K., *Structure and Mechanism in Organic Chemistry*. 2 ed. 1969, Ithaca, NY: Cornell University Press. 1137-1142, 1157-1163.

134. Morrison, H., V. Hammarskiold, and B. Jernstrom, *Status of reduced glutathione in primary cultures of rat hepatocytes and the effect on conjugation of benzo[a]pyrene-7,8-dihydrodiol-9,10-oxide.* Chem Biol Interact, 1983. **45**(2): p. 235-42.

135. Ritchie, K.J., et al., *Glutathione transferase pi plays a critical role in the development of lung carcinogenesis following exposure to tobacco-related carcinogens and urethane.* Cancer Res, 2007. **67**(19): p. 9248-57.

136. Izzotti, A., et al., *Chemoprevention of smoke-related DNA adduct formation in rat lung and heart.* Carcinogenesis, 1992. **13**(11): p. 2187-90.

137. Pohl, R.J. and J.R. Fouts, *Cytochrome P-450-dependent xenobiotic metabolizing activity in Zymbal's gland, a specialized sebaceous gland of rodents.* Cancer Res, 1983. **43**(8): p. 3660-2.

138. Larsson, B.S., H. Tjiilve, P. Larsson, A. Roberto, I. Brandt, and K. Bergman, F. *Retention of carcinogens in pigmented tissues due to melanin attinity*. in *2nd Meeting of the ESPCR*. 1989. Uppsala, Sweden.

139. Bouchard, M. and C. Viau, *Benzo(a)pyrenediolepoxide-hemoglobin adducts and 3-hydroxy-benzo(a)pyrene urinary excretion profiles in rats subchronically exposed to benzo(a)pyrene.* Arch Toxicol, 1995. **69**(8): p. 540-6.

140. Skipper, P.L., et al., *Origin of tetrahydrotetrols derived from human hemoglobin adducts of benzo[a]pyrene.* Chem Res Toxicol, 1989. **2**(5): p. 280-1.

141. Day, B.W., et al., *Conversion of a hemoglobin alpha chain aspartate(47) ester to N-(2,3-dihydroxypropyl)asparagine as a method for identification of the principal binding site for benzo[a]pyrene anti-diol epoxide.* Chem Res Toxicol, 1991. **4**(3): p. 359-63.

142. Foth, H., *Role of the lung in accumulation and metabolism of xenobiotic compounds--implications for chemically induced toxicity.* Crit Rev Toxicol, 1995. **25**(2): p. 165-205.

143. Perera, F., *Carcinogenicity of airborne fine particulate benzo(a)pyrene: an appraisal of the evidence and the need for control.* Environ Health Perspect, 1981. **42**: p. 163-85.

144. Gram, T.E., *Chemically reactive intermediates and pulmonary xenobiotic toxicity.* Pharmacol Rev, 1997. **49**(4): p. 297-341.

145. Podechard, N., et al., *Interleukin-8 induction by the environmental contaminant benzo(a)pyrene is aryl hydrocarbon receptor-dependent and leads to lung inflammation.* Toxicol Lett, 2008. **177**(2): p. 130-7.

146. Yan, Y., et al., *Efficacy of polyphenon E, red ginseng, and rapamycin on benzo(a)pyrene-induced lung tumorigenesis in A/J mice.* Neoplasia, 2006. **8**(1): p. 52-8.

147. A.M. Roland and G.S, Y., *Comprehensive Toxicology*. 2 ed. Respiratory Toxicology, ed. G.S. Yost. Vol. 8. 2010, Kidlington, UK: ELSEVIER.

148. Baak, J.P., et al., *The molecular genetics and morphometry-based endometrial intraepithelial neoplasia classification system predicts disease progression in endometrial hyperplasia more accurately than the 1994 World Health Organization classification system.* Cancer, 2005. **103**(11): p. 2304-12.

149. Weitzman, S.A. and L.I. Gordon, *Inflammation and cancer: role of phagocyte-generated oxidants in carcinogenesis.* Blood, 1990. **76**(4): p. 655-63.

150. Cerutti, P.A. and B.F. Trump, *Inflammation and oxidative stress in carcinogenesis.* Cancer Cells, 1991. **3**(1): p. 1-7.

151. Lonkar, P. and P.C. Dedon, *Reactive species and DNA damage in chronic inflammation: reconciling chemical mechanisms and biological fates.* Int J Cancer, 2011. **128**(9): p. 1999-2009.

152. Jacobs, L., et al., *Subclinical responses in healthy cyclists briefly exposed to traffic-related air pollution: an intervention study.* Environ Health, 2010. **9**: p. 64.

153. De Larco, J.E., B.R. Wuertz, and L.T. Furcht, *The potential role of neutrophils in promoting the metastatic phenotype of tumors releasing interleukin-8.* Clin Cancer Res, 2004. **10**(15): p. 4895-900.

154. Waugh, D.J. and C. Wilson, *The interleukin-8 pathway in cancer.* Clin Cancer Res, 2008. **14**(21): p. 6735-41.

155. Seekamp, A., et al., *Requirements for neutrophil products and L-arginine in ischemia-reperfusion injury.* Am J Pathol, 1993. **142**(4): p. 1217-26.

156. Smith, C.W., et al., *Recognition of an endothelial determinant for CD 18-dependent human neutrophil adherence and transendothelial migration.* J Clin Invest, 1988. **82**(5): p. 1746-56.

157. Zhang, R., et al., *Association between myeloperoxidase levels and risk of coronary artery disease.* JAMA, 2001. **286**(17): p. 2136-42.

158. Thomas, E.D., et al., *Direct evidence for a bone marrow origin of the alveolar macrophage in man.* Science, 1976. **192**(4243): p. 1016-8.

159. Driscoll, K.E. and J.K. Maurer, *Cytokine and growth factor release by alveolar macrophages: potential biomarkers of pulmonary toxicity.* Toxicol Pathol, 1991. **19**(4 Pt 1): p. 398-405.

160. Holian, C.T.M.a.A., *Comprehensive Toxicology*. 2 ed. Respiratory Toxicology, ed. G.S. Yost. Vol. 8. 2010, Kidlington, UK: ELSEVIER.

161. Standiford, T.J., et al., *TGF-beta-induced IRAK-M expression in tumor-associated macrophages regulates lung tumor growth.* Oncogene, 2011.

162. Stix, G., *A Malignant Flame.* Scientific American, 2007: p. 46-49.

163. Harris, C.C., et al., *Human pulmonary alveolar macrophages metabolise benzo(a)pyrene to proximate and ultimate mutagens.* Nature, 1978. **272**(5654): p. 633-4.

164. Borm, P.J., et al., *Neutrophils amplify the formation of DNA adducts by benzo[a]pyrene in lung target cells.* Environ Health Perspect, 1997. **105 Suppl 5**: p. 1089-93.

165. Petruska, J.M., et al., *Myeloperoxidase-enhanced formation of (+-)-trans-7,8-dihydroxy-7,8-dihydrobenzo[a]pyrene-DNA adducts in lung tissue in vitro: a role of pulmonary inflammation in the bioactivation of a procarcinogen.* Carcinogenesis, 1992. **13**(7): p. 1075-81.

166. Mallet, W.G., D.R. Mosebrook, and M.A. Trush, *Activation of (+-)-trans-7,8-dihydroxy-7,8-dihydrobenzo[a]pyrene to diolepoxides by human polymorphonuclear leukocytes or myeloperoxidase.* Carcinogenesis, 1991. **12**(3): p. 521-4.

167. Knaapen, A.M., et al., *Neutrophils and respiratory tract DNA damage and mutagenesis: a review.* Mutagenesis, 2006. **21**(4): p. 225-36.

168. Rasband, W. *ImageJ*. [cited 2011 April, 25]; Available from: http://imagej.nih.gov/ij/docs/intro.html.

169. Naveenkumar, C., et al., *Potent antitumor and antineoplastic efficacy of baicalein on benzo(a)pyrene-induced experimental pulmonary tumorigenesis.* Fundam Clin Pharmacol, 2011.

170. Zarkovic, M., et al., *Inhibitory effect of probucol on benzo[a]pyrene induced lung tumorigenesis.* Carcinogenesis, 1995. **16**(10): p. 2599-601.

171. Kamaraj, S., et al., *Modulatory effect of hesperidin on benzo(a)pyrene induced experimental lung carcinogenesis with reference to COX-2, MMP-2 and MMP-9.* Eur J Pharmacol, 2010. **649**(1-3): p. 320-7.

172. Hukkanen, J., O. Pelkonen, and H. Raunio, *Expression of xenobiotic-metabolizing enzymes in human pulmonary tissue: possible role in susceptibility for ILD.* Eur Respir J Suppl, 2001. **32**: p. 122s-126s.

173. Simon, R.H. and R. Paine, 3rd, *Participation of pulmonary alveolar epithelial cells in lung inflammation.* J Lab Clin Med, 1995. **126**(2): p. 108-18.

174. Smart, S.J. and T.B. Casale, *Interleukin-8-induced transcellular neutrophil migration is facilitated by endothelial and pulmonary epithelial cells.* Am J Respir Cell Mol Biol, 1993. **9**(5): p. 489-95.

175. L-Y Chang, J.D.C., P Gehr, B Rothen-Rutishauser, C Muhfeld, and F. Blank, *Alveolar Epithelium in Lung Toxicology*. 2 ed. Comprehensive Toxicology, ed. C.A. McQueen. Vol. 8. 2010: Elsevier Ldt.

176. Buckpitt, A. Personal Communications. Nov. 9, 2009: Salt Lake City, Utah.

177. Meuwissen, R. and A. Berns, *Mouse models for human lung cancer.* Genes Dev, 2005. **19**(6): p. 643-64.

178. Calbo, J., et al., *Genotype-phenotype relationships in a mouse model for human small-cell lung cancer.* Cold Spring Harb Symp Quant Biol, 2005. **70**: p. 225-32.

179. Li, L.H., R.F, Jr.; Kirichenko, A.; Holian, A., A. Toxicol. Appl. Pharmacol., 1996. **139**: p. 135-143.

180. Lu, X., et al., *Early whole-genome transcriptional response induced by benzo[a]pyrene diol epoxide in a normal human cell line.* Genomics, 2009. **93**(4): p. 332-42.

181. Tzekova, A., R. Thuot, and C. Viau, *Correlation between biomarkers of polycyclic aromatic hydrocarbon exposure and electrophilic tissue burden in a rat model.* Arch Toxicol, 2004. **78**(6): p. 351-61.

182. Tzekova, A., S. Leroux, and C. Viau, *Electrophilic tissue burden in male Sprague-Dawley rats following repeated exposure to binary mixtures of polycyclic aromatic hydrocarbons.* Arch Toxicol, 2004. **78**(2): p. 106-13.

183. *Annual smoking-attributable mortality, years of potential life lost, and economic costs - United States, 1995-1999*, in *Mortality and Morbidity Weekly Report*. 2002, Centers for Disease Control.

184. Hecht, S.S., et al., *Induction of respiratory tract tumors in Syrian golden hamsters by a single dose of 4-(methylnitrosamino)-1-(3-pyridyl)-1-butanone (NNK) and the effect of smoke inhalation.* Carcinogenesis, 1983. **4**(10): p. 1287-90.

185. Raupach, T., et al., *Secondhand smoke as an acute threat for the cardiovascular system: a change in paradigm.* Eur Heart J, 2006. **27**(4): p. 386-92.

186. Lioy, P.L., et al., *The Total Human Environmental Exposure Study (THEES) to benzo(a)pyrene: comparison of the inhalation and food pathways.* Arch Environ Health, 1988. **43**(4): p. 304-12.

187. Council, N.R., *Environmental Tobacco Smoke: Measuring Exposures and Assessing Health Effects*, C.o.P.S. Board on Environmental Studies and Toxicology, Editor. 1986, National Academy Press: Washington, D.C. p. 63-64.

188. *Benzo(a)pyrene*, I.A.f.R.o.C. IARC, Editor. 1973. p. 3, 91.

189. Ozbal, C.C., et al., *Quantification of (7S,8R)-dihydroxy-(9R,10S)-epoxy-7,8,9,10-tetrahydrobenzo[a]pyrene adducts in human serum albumin by laser-induced fluorescence: implications for the in vivo metabolism of benzo[a]pyrene.* Cancer Epidemiol Biomarkers Prev, 2000. **9**(7): p. 733-9.

190. Thum, T., et al., *Expression of xenobiotic metabolizing enzymes in different lung compartments of smokers and nonsmokers.* Environ Health Perspect, 2006. **114**(11): p. 1655-61.

191. Alexandrov, K., et al., *CYP1A1 and GSTM1 genotypes affect benzo[a]pyrene DNA adducts in smokers' lung: comparison with aromatic/hydrophobic adduct formation.* Carcinogenesis, 2002. **23**(12): p. 1969-77.

192. Rojas, M., et al., *High benzo[a]pyrene diol-epoxide DNA adduct levels in lung and blood cells from individuals with combined CYP1A1 MspI/Msp-GSTM1*0/*0 genotypes.* Pharmacogenetics, 1998. **8**(2): p. 109-18.

193. Rojas, M., et al., *Modulation of benzo[a]pyrene diolepoxide-DNA adduct levels in human white blood cells by CYP1A1, GSTM1 and GSTT1 polymorphism.* Carcinogenesis, 2000. **21**(1): p. 35-41.

194. Al-Delaimy, W.K., J. Crane, and A. Woodward, *Is the hair nicotine level a more accurate biomarker of environmental tobacco smoke exposure than urine cotinine?* J Epidemiol Community Health, 2002. **56**(1): p. 66-71.

195. Lebeau, M.A., M.A. Montgomery, and J.D. Brewer, *The role of variations in growth rate and sample collection on interpreting results of segmental analyses of hair.* Forensic Sci Int, 2011.

196. Miller, E.I., et al., *A novel validated procedure for the determination of nicotine, eight nicotine metabolites and two minor tobacco alkaloids in human plasma or urine by solid-phase extraction coupled with liquid chromatography-electrospray ionization-tandem mass spectrometry.* J Chromatogr B Analyt Technol Biomed Life Sci, 2010. **878**(9-10): p. 725-37.

197. Tolgyesi, A., et al., *Quantification of corticosteroids in bovine urine using selective solid phase extraction and reversed-phase liquid chromatography/tandem mass spectrometry.* J Chromatogr B Analyt Technol Biomed Life Sci, 2010. **878**(19): p. 1471-9.

198. Claffey, D.J., P.R. Stout, and J.A. Ruth, *A comparison of sodium hydroxide and sodium sulfide digestion of mouse hair in the recovery of radioactivity following systemic administration of [3H]-nicotine and [3H]-flunitrazepam.* J Anal Toxicol, 2000. **24**(1): p. 54-8.

199. Harkey, M.R., G.L. Henderson, and C. Zhou, *Simultaneous quantitation of cocaine and its major metabolites in human hair by gas chromatography/chemical ionization mass spectrometry.* J Anal Toxicol, 1991. **15**(5): p. 260-5.

200. *Cotinine Testing - Frequently Asked Questions*. [cited 2011 May 13]; Foundation for Blood Research]. Available from: http://www.fbr.org/publications/pamphlets/cotininefaq.html.

201. Benowitz, N.L., J. Hukkanen, and P. Jacob, 3rd, *Nicotine chemistry, metabolism, kinetics and biomarkers.* Handb Exp Pharmacol, 2009(192): p. 29-60.

202. *Benzo(a)pyrene*. Persistent Bioaccumulative and Toxic (PBT) Chemical Program [cited 2011 April, 24]; Available from: http://www.epa.gov/pbt/pubs/benzo.htm.

203. Zhong, Y., et al., *Analysis of r-7,t-8,9,c-10-tetrahydroxy-7,8,9,10-tetrahydrobenzo[a]pyrene in human urine: a biomarker for directly assessing carcinogenic polycyclic aromatic hydrocarbon exposure plus metabolic activation.* Chem Res Toxicol, 2011. **24**(1): p. 73-80.

204. Lawrence, J.F. and B.S. Das, *Determination of nanogram/kilogram levels of polycyclic aromatic hydrocarbons in foods by HPLC with fluorescence detection.* Int J Environ Anal Chem, 1986. **24**(2): p. 113-31.

205. Karl, H. and M. Leinemann, *Determination of polycyclic aromatic hydrocarbons in smoked fishery products from different smoking kilns.* Z Lebensm Unters Forsch, 1996. **202**(6): p. 458-64.

206. Schummer, C., et al., *Determination of hydroxylated metabolites of polycyclic aromatic hydrocarbons in human hair by gas chromatography-negative chemical ionization mass spectrometry.* J Chromatogr A, 2009. **1216**(32): p. 6012-9.